# The Mechanics and Control of Robotic Locomotion with Applications to Aquatic Vehicles

Thesis by
Scott D. Kelly

In Partial Fulfillment of the Requirements
for the Degree of
Doctor of Philosophy


California Institute of Technology
Pasadena, California

1998

(Defended May 26, 1998)

## Acknowledgements

I'd like to thank Richard Murray for his guidance and indulgence, Nikki Langness for her patience and companionship, and my parents for their love and support. Many friends and colleagues of mine deserve credit for my education; Jim Radford, Jerry Marsden, Francesco Bullo, Jim Ostrowski, Andrew Lewis, Richard Mason, and Joel Burdick are but a few among them. The experimental apparatus described in Chapter 9 was developed with the help of Richard Mason, Fong Liu, Bob Keeney, Carl Anhalt, Seth Lacy, Chris Storey, and Mark Freeman. Ted Wu and Wendong Qu generously provided it with a home.

I dedicate this work, as I dedicate my every undertaking, to my cats.

**The Mechanics and Control of Robotic Locomotion with Applications to Aquatic Vehicles**

by

Scott D. Kelly

In Partial Fulfillment of the
Requirements for the Degree of
Doctor of Philosophy

## Abstract

This work illuminates the utility of a theory of locomotion rooted in geometric mechanics and nonlinear control. We regard the internal configuration of a deformable body, together with its position and orientation in ambient space, as a point in a trivial principal fiber bundle over the manifold of body deformations. We obtain connections on such bundles which describe the nonholonomic constraints, conservation laws, and force balances to which certain propulsors are subject, and contruct and analyze control-affine normal forms for different classes of systems. We examine the applicability of results involving geometric phases to the practical computation of trajectories for systems described by single connections. We propose a model for planar carangiform swimming based on reduced Euler-Lagrange equations for the interaction of a rigid body and an incompressible fluid, accounting for the generation of thrust due to vortex shedding through controlled coupling terms. We investigate the correct form of this coupling experimentally with a robotic propulsor, comparing its observed behavior with that predicted numerically.

# Contents

**1 Prolegomenon** **1**

1.1 Historical perspective . . . . . 1

1.2 Overview of contributions . . . . . 5

**2 Mathematical Preliminaries** **7**

2.1 Notions of differentiation . . . . . 7

2.2 Ideas from differential geometry . . . . . 8

2.2.1 Lie algebras and Lie groups . . . . . 8

2.2.2 Distributions and Frobenius' theorem . . . . . 10

2.2.3 Differential forms and Stokes' theorem . . . . . 11

2.2.4 Actions of Lie groups . . . . . 13

2.2.5 Material, body, and spatial velocity . . . . . 14

2.2.6 Rigid motion in the plane . . . . . 15

2.3 The calculus of variations . . . . . 17

2.4 Principal bundles and related objects . . . . . 18

2.5 Geometric phases . . . . . 25

2.5.1 Holonomy groups and bundles . . . . . 25

2.5.2 Abelian bundles . . . . . 26

**3 Lagrangian Mechanics** **29**

3.1 Fundamentals . . . . . 29

3.1.1 The Euler-Lagrange equations . . . . . 29

3.1.2 Symmetries and momentum maps . . . . . 32

3.1.3 The Lagrange-d'Alembert principle . . . . . 33
3.2 Reduction on Cartesian products . . . . . 34

**4 The Geometry of Locomotion** **37**
4.1 Locomotion and principal bundles . . . . . 37
4.1.1 Connections on configuration bundles . . . . . 37
4.1.2 Kinematic and nonholonomic connections . . . . . 38
4.1.3 The kinematic car . . . . . 39
4.1.4 Mechanical connections . . . . . 41
4.2 Interpolation for Rayleigh systems . . . . . 43
4.2.1 The interpolated equations . . . . . 43
4.2.2 The heavy inchworm . . . . . 46
4.2.3 Extension to more general forces . . . . . 48

**5 Controllability and Related Issues** **51**
5.1 Definitions and tests . . . . . 51
5.2 Controllability for kinematic systems . . . . . 52
5.2.1 Principal connections and Chow's theorem . . . . . 52
5.2.2 Local and global controllability of a wheelchair . . . . . 55
5.3 Accessibility for Rayleigh systems . . . . . 58
5.3.1 Accessibility modulo momentum . . . . . 58
5.3.2 A vehicle with two internal rotors . . . . . 60
5.3.3 The heavy inchworm revisited . . . . . 61

**6 Gaits for Kinematic Systems** **63**
6.1 Definitions . . . . . 63
6.2 Systems on Abelian bundles . . . . . 64
6.3 Inchworm gaits . . . . . 64
6.4 Local expansion of holonomy . . . . . 67
6.5 Two-input systems . . . . . 69

**7 Principal Connections and Swimming** **73**

7.1 Ideal flow and the hydromechanical connection . . . . . 73

7.1.1 Potential flow . . . . . 73

7.1.2 Fluid momentum and Kelvin impluse . . . . . 78

7.1.3 The hydromechanical connection . . . . . 80

7.2 Creeping flow and the Stokes connection . . . . . 82

7.2.1 Stokes flow . . . . . 82

7.2.2 The Stokes connection . . . . . 84

7.3 Squirming circles . . . . . 85

**8 Rigid Bodies in Fluids** **95**

8.1 Modelling assumptions . . . . . 95

8.2 The reduced Lagrangian . . . . . 96

8.3 The reduced equations . . . . . 98

8.4 Special cases . . . . . 106

**9 Planar Carangiform Locomotion** **109**

9.1 The unforced equations . . . . . 109

9.2 The substitution vortex model . . . . . 110

9.3 Planar carangiform accessibility . . . . . 112

9.4 The experiment . . . . . 114

9.5 Modelling and simulation . . . . . 120

9.5.1 The steady flow model . . . . . 120

9.5.2 Simulation and validation . . . . . 126

9.6 The substitution vortex revisited . . . . . 126

9.7 Flow visualization . . . . . 132

9.8 Carangiform gaits . . . . . 134

**10 Future Work** **137**

# List of Figures

2.1 Constructions on a principal bundle. . . . . 20

4.1 The kinematic car on the plane. . . . . 39
4.2 An inchworm robot on a viscous film. . . . . 47

5.1 A wheelchair on the plane. . . . . 55

6.1 Two types of gaits for the inchworm. . . . . 65
6.2 The caterpillar gait. . . . . 65

7.1 Derivation of the potential function. . . . . 75
7.2 A squirming circle. . . . . 86
7.3 Geometric phase for a particular gait. . . . . 92

9.1 Silhouette and cross section of a louvar. . . . . 110
9.2 The apparatus from above. . . . . 115
9.3 The apparatus from the side. . . . . 115
9.4 The apparatus from forward and above. . . . . 116
9.5 The apparatus from the side. . . . . 116
9.6 The Polhemus transmitter. . . . . 117
9.7 Displacement with the peduncle and fin in phase. . . . . 118
9.8 Displacement with the peduncle and fin out of phase. . . . . 119
9.9 The simulated experiment. . . . . 125
9.10 Steady flow model for in-phase gaits. . . . . 127
9.11 Steady flow model for out-of-phase gaits. . . . . 128
9.12 Flow around a flat plate with circulation. . . . . 131

9.13 The characteristic carangiform wake. . . . . 133
9.14 A counter-rotating vortex pair. . . . . 133
9.15 A planar carangiform robot. . . . . 135
9.16 An out-of-phase drive gait. . . . . 136
9.17 An out-of-phase drive-and-rotate gait . . . . . 136

# List of Tables

6.1 Gait table for two-input systems, $T = 2\pi$. . . . . 71

# Chapter 1

# Prolegomenon

Swim. *Fishbone*

## 1.1 Historical perspective

Since

> The way of an eagle in the air,
> the way of a serpent upon a rock,
> The way of a ship on the high seas,
> and the way of a man with a maiden

perplexed the ancient Hebrews [78], locomotion has intrigued the human mind. Leonardo da Vinci's anatomically informed examinations of the human body in motion predated the landmark photographic studies of Eadweard Muybridge [74, 75] by four centuries. According to Sir James Gray [27], however, advancements in the quantitative description of animal locomotion were few until the present. Gray cites Giovanni Borelli's *De motu animalium* (1680), which borrowed its title from a work of Aristotle's, and Étienne-Jules Marey's *Machine Animale* (1873) as works of rare significance.

James Watt's 1769 improvement to the Newcomen atmospheric engine ushered in the age of man-made self-powered vehicles; his flyball governor is often hailed as the first modern control system. Biologists like C. Bernard (*Les phéomenes de*

*la vie*, 1878) and L. Frederick (who coined the term "regulatory agencies" in 1885) were among the first to recognize the similarities between the feedback control of steam engines and fundamental bioregulatory processes [46].

Biomimetic design pervades robotics. As early as 1940, Hutchinson and Smith built a small robot which was able to walk and ascend obstacles on four independently-controlled legs [35]. The General Electric Walking Truck, designed and built in the 1960s, epitomizes large legged vehicles under strictly mechanical control [71]. The last two decades have witnessed the construction of several walking robots with two to six legs, as well as Raibert's hopping machines with as few as one [84, 85]. Tomovic and Karplus [95] first applied mathematical methods, including the theory of finite states, to the analysis of legged locomotion. Hildebrand [32] and McGhee [66] formalized the analysis of perambulatory gaits; the role of central pattern generators in dictating such gaits has been considered by Collins and Stewart [20]. Recent research into the dynamics and control of legged machines has included McGeer's work on passive dynamic walking [65].

Hirose and Umetani began their work with snakelike robots, or "active cord mechanisms," in the 1970s. An early creation of theirs propelled itself in a serpentine fashion but was confined to the plane [33]; a later robot could lift sections of its body for maneuvers which included climbing stairs [34]. The kinematics of "hyper-redundant" robot locomotion have been examined more recently by Chirikjian and Burdick (who coined the term) [16], Krishnaprasad and Tsakiris [47], and Ostrowski [80].

The efficiency, maneuverability, and stealth of marine animals have provided an enticing paradigm for the design of biomimetic robots since Gray's "paradoxical" 1936 study of drag reduction on dolphins. The most celebrated pisciform robots today are arguably the MIT RoboTuna and its siblings [96], which resemble members of the taxonomic family Carangidae in body type. Fukuda and others, however, have developed aquatic microrobots which exploit qualitatively different flow phenomena [25]. Untethered submersible technology currently welcomes cues from many corners of aquatic zoology [94].

The application of gauge theory to the unassisted reorientation of deformable bodies in vacuo began with Marsden, Montgomery, and others [57, 70, 24], inspired in part by conspicuous feline gymnastics [36]. The navigation of deformable bodies undergoing sinusoidal changes in shape was addressed by Murray and Sastry [73]. Lagrangian reduction was developed by Marsden and Scheurle [59, 60] and extended to incorporate systems subject to nonholonomic constraints by Bloch et al. [13]. Kelly and Murray [41] and Ostrowski [80] integrated these ideas into a geometric theory of robotic locomotion.

The evolution of an inviscid, incompressible fluid was first addressed as a problem in geometric mechanics by Arnol'd [6]. Ebin and Marsden probed the manifold structure of certain diffeomorphism groups to realize theorems concerning the existence and uniqueness of solutions to classical equations of fluid flow [22]. Marsden and Weinstein revisited inviscid flow in the context of Hamiltonian reduction [61]. A complete modern exposition of fluid mechanics appears in the recent volume of Arnol'd and Khesin [7].

Benjamin and Ellis [9] and Saffman [87] first demonstrated that a deformable body could accelerate from rest in an ideal fluid; Benjamin introduced Hamiltonian formalism to this problem [8]. Benjamin and Ellis [10] and Miloh and Galper [69] returned to the problem motivated in part by the observed behavior of sonically irradiated air bubbles in water. The Poisson bracket structure underpinning the motion of a finite ideal fluid with a free boundary was clarified by Lewis et al. [52].

The position controllability of a deformable body in an ideal fluid was defined by Mahalov and Nikitin [55]. Kelly and Murray presented the equations governing the rectilinear swimming of a deformable cylinder as a driftless nonlinear control system [42]. Mason [64] and Andreas [4] considered the optimal control of homogeneous and heterogeneous cylinders.

The undulatory swimming of a nearly circular cylinder at low Reynolds number was studied first by Blake [12], anticipating his spherical envelope approach to ciliary propulsion [11]. Shapere and Wilczek addressed the gauge theoretic nature of this problem [90] and examined the efficiency of certain swimming strokes for cylindrical

and spherical bodies [89]. Ehlers [23] and Koiller et al. [46] have applied gauge theoretic techniques to the swimming of a variety of microorganisms; the ability to swim at low Reynolds number on a macroscopic scale boasts arguable advantage as well [28]. Kelly and Murray proposed a simple interpolation between the geometric equations governing inviscid swimming and those governing Stokesian swimming to model the self-propulsion of an inertial body subject to viscous dissipation [42].

The dynamics and stability of a rigid vehicle immersed in an irrotational fluid have been studied, and interpreted in a general Hamiltonian setting, by Leonard and Marsden [51]. Özcazanç examined the dynamical interaction of a finite vortical fluid and a free rigid container [81]. We will see that a piscimimetic vehicle is followed by a wake with a very particular structure, which may be approximated in cross-section by an appropriate arrangement of point vortices. Koiller has studied the coupled motion of vortices and planar rigid bodies [45], and Aref the stability of certain wake-like vortex patterns [5]. Langford and Zhan explored the resonance properties of a model for the vortex-induced vibration of an elastically-mounted cylinder [49].

The biological literature addressing the swimming of fish is considerable. The term "carangiform" was coined by Breder to signify pisciform locomotion of the sort we review; Breder applied the term "anguilliform" to the contrasting swimming of eels [14]. Lighthill has made theoretical contributions across the full spectrum of aquatic locomotion [53], as has Wu [76, 99]. Recent efforts to model carangiform swimming in a fashion amenable to control analysis include those of Harper et al. [29, 30] and Kelly et al. [39, 40].

The most efficient carangiform swimmers sport caudal fins which are lunate in profile; recent refinements to the analysis of their performance include those of Karpouzian et al. [37]. Ahlborn et al. focused on the introduction and extraction of energy to and from a structured wake by a flapping lunate tail with a single rotational degree of freedom [2].

We note, finally, that the computational techniques applied by Martins and Ghoniem to the intake flow in a piston-chamber device [63] seem particularly adaptable to the interaction of a free body and its vortex wake.

## 1.2 Overview of contributions

Problems in the self-propulsion of deformable bodies invite the cooperation of tools from geometric mechanics and nonlinear control theory. The internal configuration of a deformable body, together with its position and orientation in ambient space, constitutes a point in a trivial principal fiber bundle over the manifold of body deformations. A propulsor which controls its own shape navigates this manifold to exploit the conservation laws, nonholonomic constraints, and hydrodynamic effects which allow it to move. Individually, each of these may often be described by a connection on the configuration bundle.

The equivalence of a mechanical connection to the conservation of a deforming body's momentum was described by Marsden et al. [57]. We obtain a mechanical connection which captures the conservation of Kelvin impulse governing the self-propulsion of a deformable surface in an irrotational fluid. The connection underlying swimming at low Reynolds number was recognized by Shapere and Wilczek [90]. We derive this connection from a dissipation function, elucidating its equivalence to the net balance of drag on a Stokesian propulsor. This equivalence of a connection to a force balance is not limited to the aquatic realm; we evince the limits of its extension. We also demonstrate that the equations describing the motion of a Lagrangian system in the presence of quadratic dissipation may, in general, be realized geometrically in terms of two connections and an evolving momentum.

The swimming of fish hinges upon the exchange of fluid vorticity for body momentum. The mechanism by which vorticity is shed gives rise to forces which elude the theory of connections, but we are not at a loss to describe such systems geometrically. Carangiform propulsors resemble, morphologically, certain members of the fish order Percomorphi. In nature, this physical resemblance engenders a similarity in high propulsive efficiency and speed [53]. We propose a planar model for carangiform swimming based on reduced Euler-Lagrange equations for the interaction of a rigid body and an incompressible fluid. We account for the generation of thrust due to vortex shedding through controlled coupling terms. At the heart of this coupling is an abstraction from hydrofoil theory; we investigate its applicability

to real carangiform swimming using an articulated robotic caudal mechanism. We compare the observed behavior of our experimental apparatus to that predicted by steady hydrodynamics.

Ultimately, we view the self-propulsion of any deformable body as a problem in nonlinear control. We realize normal forms for systems described by one or more connections, interpreting established tests for controllability and accessibility in terms of the properties of these connections. Locomotion problems suggest particular nontraditional notions of controllability and accessibility; we define these both intuitively and geometrically.

Related to the constructive demonstration of controllability is the study of gaits. We examine the computation of geometric phases in this context, illuminating the implications of the Ambrose-Singer theorem and an equation for the local expansion of holonomy for certain types of locomotion systems. We explore carangiform gaits experimentally and computationally.

# Chapter 2

# Mathematical Preliminaries

## 2.1 Notions of differentiation

Let $E$ and $F$ be normed spaces, $U$ an open set in $E$, and $u_0$ a point in $U$. If $f : U \to F$, there exists at most one $A \in L(E, F)$ such that

$$g_A : U \to F : u \mapsto f(u_0) + A(u - u_0)$$

is tangent to $f$ at $u_0$, in the sense that

$$\lim_{u \to u_0} \frac{||f(u) - g_A(u)||}{||u - u_0||} = 0.$$

If such an $A$ exists, we say that $f$ is *Fréchet differentiable* at $u_0$, and define its *Fréchet derivative* at $u_0$ to be $Df(u_0) = A$. The evaluation of $Df(u_0)$ on $e \in E$ is denoted $Df(u_0) \cdot e$. If $f$ is Fréchet differentiable at every $u_0 \in U$, the map

$$Df : U \to L(E, F) : u \mapsto Df(u)$$

is said to be the Fréchet derivative of $f$.

The map $f : U \to F$ is said to be differentiable in the direction $e \in E$ at the

point $u_0 \in U$ if the quantity

$$\left.\frac{d}{dt}\right|_{t=0} f(u_0 + te) \tag{2.1}$$

exists. A function $f$ is said to be *Gâteaux differentiable* at the point $u_0$ if it is differentiable in every direction there. If $f$ is Fréchet differentiable at $u_0$, it is Gâteaux differentiable there and its directional derivatives are given by

$$\left.\frac{d}{dt}\right|_{t=0} f(u_0 + te) = Df(u_0) \cdot e.$$

We will sometimes write $D_e f(u_0)$ for the derivative of $f$ in the direction $e$.

## 2.2 Ideas from differential geometry

### 2.2.1 Lie algebras and Lie groups

We denote the space of vectors tangent to the smooth manifold $M$ at the point $x$ by the symbol $T_x M$, the dual space of covectors by $T_x^* M$, and their pairing by

$$\langle \cdot, \cdot \rangle : T_x^* M \times T_x M \to \mathbb{R}.$$

We denote the tangent bundle projection by $\tau_M : TM \to M$. If $f : M \to N : x \mapsto y$ is a smooth map between manifolds, we write $T_x f : T_x M \to T_y N$ to denote its tangent map at the point $x \in M$. We denote the space of smooth vector fields on $M$ by $\mathfrak{X}(M)$. Let $f : M \to \mathbb{R}$ be a smooth function on $M$. The operation $[\cdot, \cdot] : \mathfrak{X}(M) \times \mathfrak{X}(M) \to \mathfrak{X}(M)$ defined by

$$[X, Y]f = XYf - YXf \quad \text{for} \quad X, Y \in \mathfrak{X}(M)$$

is called the *Jacobi-Lie bracket* of vector fields on $M$.

A *Lie algebra* is a vector space $V$ together with an operation $[\cdot, \cdot] : V \times V \to V$ such that

1. $[\cdot,\cdot]$ is bilinear;

2. $[v,v]=0$ for every $v\in V$;

3. $[u,[v,w]]+[v,[w,u]]+[w,[u,v]]=0$ for all $u,v,w\in V$.

The equation specifying the third requirement is called the *Jacobi identity.* A Lie algebra is said to be *Abelian* if the bracket operation is trivial. The Jacobi-Lie bracket endows $\mathfrak{X}(M)$ with the structure of a Lie algebra.

A *Lie group* is a manifold on which a smooth group operation is defined. A Lie group is said to be *Abelian* if this operation is commutative. We denote the identity element of the Lie group $G$ by $e$. If $g,h\in G$, *left translation* by $h$ corresponds to the map

$$L_h : g \mapsto hg$$

and *right translation* by $h$ to the map

$$R_h : g \mapsto gh.$$

If $v\in T_gG$, we will sometimes abuse notation and write

$$hv = T_gL_hv \in T_{hg}G \quad \text{and} \quad vh = T_gR_hv \in T_{gh}G.$$

If $G$ is a Lie group, a vector field $X\in\mathfrak{X}(G)$ is said to be *left invariant* if

$$T_gL_hX(g) = X(hg),$$

and *right invariant* if

$$T_gR_hX(g) = X(gh),$$

for all $g,h\in G$. We denote the set of left invariant vector fields on $G$ by $\mathfrak{X}_L(G)$

and the set of right invariant vector fields on $G$ by $\mathfrak{X}_R(G)$. If $X, Y \in \mathfrak{X}_L(G)$, then

$$\begin{aligned} T_g L_h([X(g), Y(g)]) &= [T_g L_h X(g), T_g L_h Y(g)] \\ &= [X(hg), Y(hg)]; \end{aligned}$$

thus $\mathfrak{X}_L(G)$ constitutes a Lie subalgebra of $\mathfrak{X}(G)$. The left invariance of every $X \in \mathfrak{X}_L(G)$ implies that $\mathfrak{X}_L(G)$ and $T_eG$ are isomorphic as vector spaces. The Jacobi-Lie bracket on $\mathfrak{X}_L(G)$ therefore determines a bracket operation on $T_eG$ given by

$$[\xi, \eta] = [T_e L_g \xi, T_e L_g \eta](e).$$

We denote $T_eG$ together with this bracket operation by $\mathfrak{g}$, and refer to $\mathfrak{g}$ as the Lie algebra corresponding to $G$. We note that Jacobi-Lie bracket on $\mathfrak{X}_R(G)$ also determines a bracket operation $[\cdot, \cdot]_R : T_eG \times T_eG \to T_eG$. Indeed,

$$[\xi, \eta]_R = -[\xi, \eta] \quad \text{for all} \quad \xi, \eta \in \mathfrak{g}.$$

It is proven in [98] that a connected Lie group is Abelian if and only if the corresponding Lie algebra is Abelian.

If $\xi \in \mathfrak{g}$, it is proven in [31] that the differential equation

$$\frac{dg}{dt} = T_e L_g \xi, \qquad g(0) = e$$

has a unique solution $g_\xi(t) \in G$ for all $t$. We define the *exponential map* $\exp : \mathfrak{g} \to G$ such that $\exp \xi = g_\xi(1)$. The exponential map determines a diffeomorphism from a neighborhood of $0 \in \mathfrak{g}$ to a neighborhood of $e \in G$.

### 2.2.2 Distributions and Frobenius' theorem

An $m$-dimensional *distribution* $D$ on $M$ is the smooth assignment of an $m$-dimensional subspace $D(x)$ of $T_xM$ to every $x \in M$. A vector field $X$ on $M$ is said to lie in $D$ if $X(x) \in D(x)$ at every $x \in M$. The distribution $D$ is said to be *involutive* if

$[X, Y] \in D$ for all $X, Y \in D$.

A submanifold $N \subset M$ is an *integral manifold* of $D$ if $D(x) = T_x N$ at every $x \in N$. If $D$ exhibits an integral manifold at every $x \in M$, $D$ is said to be *integrable.* Involutivity and integrability are related by the following result.

**Theorem 2.1 (Frobenius)** *A distribution is integrable if and only if it is involutive.*

Different versions of this theorem are stated and proved in [98]. If $D$ is an $m$-dimensional distribution on an $n$-dimensional manifold $M$, then $M$ is foliated locally by the level surfaces of $(n-m)$ functions $f_1, \ldots, f_{n-m} : M \to \mathbb{R}$.

### 2.2.3 Differential forms and Stokes' theorem

A $(j, k)$ *tensor field* $\alpha$ on a manifold $M$ assigns to each point $x \in M$ a multilinear map (or tensor)

$$\alpha(x) : (T_x^* M)^j \times (T_x M)^k \to \mathbb{R}.$$

The *tensor product* of a $(0, k)$ tensor field $\alpha$ on $M$ and a $(0, l)$ tensor field $\beta$ on $M$ is given by

$$(\alpha \otimes \beta)(x)(v_1, \ldots, v_{k+l}) = \alpha(x)(v_1, \ldots, v_k)\, \beta(x)(v_{k+1}, \ldots, v_{k+l}),$$

where $v_1, \ldots, v_{k+l} \in T_x M$. A $(0, k)$ tensor field $\alpha$ is said to be *skew symmetric* if the value of $\alpha(x)(v_1, \ldots, v_k)$ reverses sign under odd permutations of its arguments. The *alternation operator* acts on a $(0, k)$ tensor field $\alpha$ such that

$$(\mathrm{Alt}\,\alpha)(x)(v_1, \ldots, v_k) = \frac{1}{k!} \sum_{\pi \in S_k} \mathrm{sgn}(\pi)\, \alpha(x)\left(v_{\pi(1)}, \ldots, v_{\pi(k)}\right),$$

where $S_k$ is the group of permutations of the integers $1, \ldots, k$.

A real-valued *differential k form* on the manifold $M$ is a skew symmetric $(0, k)$ tensor field $M$. We denote the set of all $k$ forms on $M$ by $\Lambda^k(M)$, and the set of

all forms on $M$ by $\Lambda(M)$. If $\alpha$ is a $k$ form and $\beta$ an $l$ form on $M$, we define their *wedge product* on $M$ by

$$\alpha \wedge \beta = \frac{(k+l)!}{k!l!} \mathrm{Alt}(\alpha \otimes \beta).$$

We note, in particular, that the wedge product of $\alpha, \beta \in \Lambda(M)$ is given at $x \in M$ by

$$(\alpha \wedge \beta)(v_1, v_2) = \alpha(v_1)\beta(v_2) - \alpha(v_2)\beta(v_1),$$

where $v_1, v_2 \in T_x M$. Endowed with the wedge product, $\Lambda(M)$ forms an associative algebra over $\mathbb{R}$, known as the *exterior algebra* on $M$. If $V$ is a vector space, we define a $V$-valued form on $M$ to be the sum of terms of the form $\alpha \otimes v$, where $\alpha \in \Lambda(M)$ and $v \in V$.

If $\alpha$ is a $k$ form and $X$ a vector field on $M$, we define the *interior product* $\lrcorner : \mathfrak{X}(M) \times \Lambda(M) \to \Lambda(M)$ such that $X \lrcorner \alpha \in \Lambda^{k-1}(M)$ satisfies

$$(X \lrcorner \alpha)(X_1, \ldots, X_{k-1}) = \alpha(X, X_1, \ldots, X_{k-1}).$$

The *exterior derivative* $d\alpha \in \Lambda^{k+1}(M)$ of a differential form $\alpha \in \Lambda^k(M)$ is determined by the unique linear map $d : \Lambda(M) \to \Lambda(M)$ such that

1. $df$ is the differential of $f$ for any function $f \in \Lambda^0(M)$;
2. $d(\alpha \wedge \beta) = d\alpha \wedge \beta + (-1)^k \alpha \wedge d\beta$ for $\alpha \in \Lambda^k(M)$ and $\beta \in \Lambda^l(M)$;
3. $d(d\alpha) = 0$ for any $\alpha \in \Lambda^k(M)$.

If $\alpha$ is a $k$ form on $M$ and $X_0, \ldots, X_k$ vector fields in $\mathfrak{X}(M)$, then

$$\begin{aligned} d\alpha(X_0, \ldots, X_k) = &\sum_{i=0}^{k} (-1)^i X_i \left(\alpha\left(X_0, \ldots, \hat{X}_i, \ldots, X_k\right)\right) \\ &+ \sum_{i<j} (-1)^{i+j} \alpha\left([X_i, X_j], X_0, \ldots, \hat{X}_i, \ldots, \hat{X}_j, \ldots, X_k\right), \end{aligned} \tag{2.2}$$

where $\hat{X}$ indicates that $X$ is omitted from an argument.

An $n$-dimensional manifold $M$ is said to be *orientable* if it admits a nonvanishing $n$ form. Such an $n$ form determines a basis for $\Lambda^n(M)$ and is called a *volume form.*

**Theorem 2.2 (Stokes)** *If $M$ is a compact, oriented, $n$-dimensional manifold with boundary $\partial M$, then*

$$\int_M d\alpha = \int_{\partial M} \alpha$$

*for any $(n-1)$ form on $M$.*

### 2.2.4 Actions of Lie groups

A *left action* of the Lie group $G$ on the manifold $M$ is a smooth map $\Phi : G \times M \to M$ such that

1. $\Phi(e, x) = x$ for all $x \in M$;
2. $\Phi(g, \Phi(h, x)) = \Phi(gh, x)$ for all $x \in M$ and $g, h \in G$.

A *right action* is such that $\Phi(g, \Phi(h, x)) = \Phi(hg, x)$. We consider left actions except as noted. The symbol $\Phi_g(\cdot)$ is often used in place of $\Phi(g, \cdot)$. An action of $G$ on $M$ is said to be *free* if $g \mapsto \Phi_g(x)$ is injective for every $x \in M$. If $M = V$ is a vector space and each $\Phi_g$ a linear transformation, the action $\Phi : G \times V \to V$ is said to be a *representation* of $G$ on $V$. The action defined by

$$\mathrm{Ad} : G \times T_eG \to T_eG : (g, \xi) \mapsto T_gR_{g^{-1}}T_eL_g\xi$$

is called the *adjoint representation* of $G$ on $\mathfrak{g}$. It is sometimes realized as the derivative of the inner automorphism

$$I_g : G \to G : h \mapsto ghg^{-1}.$$

Every representation $\Phi$ of a Lie group $G$ on a vector space $V$ determines a dual *contragredient representation* $\Phi^* : G \times V^* \to V^*$ such that

$$\langle \Phi_g^* z, v \rangle = \langle z, \Phi_g v \rangle$$

for $z \in V^*$ and $v \in V$.

The *infinitesimal generator* of the action $\Phi : G \times M \to M$ corresponding to $\xi \in \mathfrak{g}$ is the vector field on $M$ given by

$$\xi_M(x) = \left. \frac{d}{dt} \right|_{t=0} \Phi(\exp t\xi, x) \quad \text{for} \quad x \in M.$$

The infinitesimal generator of the adjoint representation is given by

$$\mathrm{ad}_\xi \eta = \xi_{\mathfrak{g}} \eta = [\xi, \eta] \quad \text{for} \quad \xi, \eta \in \mathfrak{g}.$$

It is true in general that

$$[\xi_M, \eta_M] = -[\xi, \eta]_M. \tag{2.3}$$

If, in particular, the group $G$ acts on itself by left multiplication

$$\Phi : G \times G \to G : (g, h) \mapsto L_g h,$$

then

$$\xi_G(g) = T_e R_g \xi. \tag{2.4}$$

### 2.2.5 Material, body, and spatial velocity

Let $\gamma : I \to G : t \mapsto g(t)$, where $I \subset \mathbb{R}$, define a curve in the Lie group $G$. The *Lagrangian* or *material velocity* is given by

$$v_{\text{material}}(t) = \dot{g}(t) \in T_{g(t)} G.$$

Left and right translation in $G$ both determine isomorphisms between $T_eG$ and $T_{g(t)}G$. The *convective* or *body velocity* is given by

$$v_{\text{body}}(t) = T_{g(t)}L_{g^{-1}(t)}\dot{g}(t) \in T_eG,$$

and the *Eulerian* or *spatial velocity* by

$$v_{\text{spatial}}(t) = T_{g(t)}R_{g^{-1}(t)}\dot{g}(t) \in T_eG.$$

It follows that

$$\begin{aligned} v_{\text{spatial}}(t) &= T_{g(t)}R_{g^{-1}(t)}T_eL_{g(t)}v_{\text{body}}(t) \\ &= \text{Ad}_{g(t)}\, v_{\text{body}}(t) \end{aligned}$$

and

$$\begin{aligned} v_{\text{body}}(t) &= T_{g(t)}L_{g^{-1}(t)}T_eR_{g(t)}v_{\text{spatial}}(t) \\ &= T_{g^{-1}(t)}R_{g(t)}T_eL_{g^{-1}(t)}v_{\text{spatial}}(t) \\ &= \text{Ad}_{g^{-1}(t)}\, v_{\text{spatial}}(t). \end{aligned}$$

It is demonstrated in [1] that if $\xi(t) \in \mathfrak{g}$, then

$$\frac{d}{dt}\left(\text{Ad}_{g(t)}\,\xi(t)\right) = \text{Ad}_{g(t)}\,\dot{\xi}(t) + \text{Ad}_{g(t)}\,\text{ad}_{T_{g(t)}L_{g^{-1}(t)}\dot{g}(t)}\,\xi(t).$$

If $\mu(t) \in \mathfrak{g}^*$, it is furthermore the case that

$$\frac{d}{dt}\left(\text{Ad}^*_{g(t)}\,\mu(t)\right) = \text{Ad}^*_{g(t)}\,\dot{\mu}(t) + \text{ad}^*_{T_{g(t)}L_{g^{-1}(t)}\dot{g}(t)}\,\text{Ad}^*_{g(t)}\,\mu(t), \tag{2.5}$$

where $\text{Ad}^* : \mathfrak{g}^* \to \mathfrak{g}^*$ denotes the contragredient *coadjoint representation.*

### 2.2.6 Rigid motion in the plane

We often work explicitly with $SE(2)$ and its associated Lie algebra, $\mathfrak{se}(2)$. Their properties, as detailed below, may be derived from the properties of $SE(3)$ and

$\mathfrak{se}(3)$ detailed in [72].

We may regard elements of $SE(2)$ as matrices of the form

$$g = \begin{bmatrix} \cos\theta & -\sin\theta & x \\ \sin\theta & \cos\theta & y \\ 0 & 0 & 1 \end{bmatrix},$$

so that the group operation corresponds to matrix multiplication. We will sometimes denote the corresponding elements of $SE(2)$ by triplets $(x, y, \theta)$. If $g_1 = (x_1, y_1, \theta_1)$ , $g_2 = (x_2, y_2, \theta_2) \in SE(2)$, then

$$g_1 \cdot g_2 = (x_1 + x_2 \cos\theta_1 - y_2 \sin\theta_1, y_1 + x_2 \sin\theta_1 + y_2 \cos\theta_1, \theta_1 + \theta_2) .$$

We may regard elements of $\mathfrak{se}(2)$ as matrices of the form

$$g = \begin{bmatrix} 0 & -\xi_\theta & \xi_x \\ \xi_\theta & 0 & \xi_y \\ 0 & 0 & 0 \end{bmatrix},$$

so that the bracket operation corresponds to matrix commutation. We will sometimes denote the corresponding elements of $\mathfrak{se}(2)$ by triplets $(\xi_x, \xi_y, \xi_\theta)$. If $\xi = (\xi_x, \xi_y, \xi_\theta)$ , $\eta = (\eta_x, \eta_y, \eta_\theta) \in \mathfrak{se}(2)$, then

$$[\xi, \eta] = (\xi_y \eta_\theta - \xi_\theta \eta_y, \xi_\theta \eta_x - \xi_x \eta_\theta, 0) . \tag{2.6}$$

The exponential map $\exp : \mathfrak{se}(2) \to SE(2)$ is given by

$$\exp\xi = \left( \frac{1}{\xi_\theta} (-\xi_y + \xi_y \cos\xi_\theta + \xi_x \sin\xi_\theta) , \frac{1}{\xi_\theta} (\xi_x - \xi_x \cos\xi_\theta + \xi_y \sin\xi_\theta) , \xi_\theta \right)$$

if $\xi_\theta \neq 0$, and by the Abelian exponential map $(\xi_x, \xi_y, 0) \mapsto (\xi_x, \xi_y, 0)$ if $\xi_\theta = 0$. It follows that the infinitesimal generator of left translation corresponding to $\xi \in \mathfrak{se}(2)$

is given by

$$\xi_{SE(2)} = (\xi_x - y\xi_\theta, \xi_y + x\xi_\theta, \xi_\theta)\,. \tag{2.7}$$

The adjoint action of $SE(2)$ on $\mathfrak{se}(2)$ is given by

$$\mathrm{Ad}_g\,\xi = (\xi_x \cos\theta - \xi_y \sin\theta + \xi_\theta y, \xi_x \sin\theta + \xi_y \cos\theta - \xi_\theta x, \xi_\theta)\,. \tag{2.8}$$

If $g(t) = (x(t), y(t), \theta(t))$ is a curve in $SE(2)$, then

$$g^{-1}\dot{g} = \left(\dot{x}\cos\theta + \dot{y}\sin\theta, \dot{y}\cos\theta - \dot{x}\sin\theta, \dot{\theta}\right). \tag{2.9}$$

## 2.3 The calculus of variations

The calculus of variations characterizes the extremals of real-valued functions on infinite-dimensional domains. Functions of this sort are sometimes called *functionals*. Of particular interest are functionals on manifolds of curves joining points in other manifolds. Let $\Omega(q_1, q_2, [a,b])$ denote the manifold of curves $c : [a,b] \to Q : t \mapsto c(t)$ such that $c(a) = q_1$ and $c(b) = q_2$. The tangent space $T_c\Omega(q_1, q_2, [a,b])$ may be thought of to comprise the restrictions to the curve $c \subset Q$ of vector fields on $Q$ which vanish at $q_1$ and $q_2$.

Consider a curve $c_s : \mathbb{R} \to \Omega(q_1, q_2, [a,b])$. Each point along $c_s$ is, itself, a curve in $Q$. We refer to any such one-parameter family of curves in $Q$ as a *variation* of the curve $c = c_0 \subset Q$. For any variation $c_s$, we define

$$\delta c = \left.\frac{dc_s}{ds}\right|_{s=0} \in T_c\Omega(q_1, q_2, [a,b])\,.$$

We refer to $\delta c$ as an *infinitesimal variation* of $c$.

A functional $\mathbb{J} : \Omega(q_1, q_2, [a,b]) \to \mathbb{R}$ has a critical point at $c \in \Omega(q_1, q_2, [a,b])$ if

and only if

$$d\mathbb{J}(c) \cdot \delta c = \left. \frac{d\mathbb{J}(c_s)}{ds} \right|_{s=0} = 0$$

for all variations $c_s$ of the curve $c = c_0$. We abbreviate this requirement as $\delta\mathbb{J} = 0$.

## 2.4 Principal bundles and related objects

Let $M$ be a manifold and $G$ a Lie group. A (left) *principal fiber bundle* with *base space* $M$ and *structure group* $G$ comprises a manifold $Q$ and a free (left) action $\Phi$ of $G$ on $Q$ such that

1. $M = Q/G$;
2. The canonical projection $\pi_M : Q \to M$ is differentiable;
3. $Q = M \times G$ locally.

We denote the image of the point $q$ under the action of $h \in G$ by $hq$. If $Q = M \times G$ globally, the bundle is said to be *trivial*, and the action in question corresponds to left translation in $G$. We denote the image of the point $(r, g) \in M \times G$ under the action of $h \in G$ by $(r, hg)$. We use the symbol $Q$ to denote both the *bundle space* or *total space* and the bundle itself.

The point $q \in Q$ is said to lie in the *fiber* over $\pi_M(q) \in M$. A vector $v_q \in T_qQ$ tangent to the fiber through $q$ is said to be *vertical*; we denote the space of all such vectors by $V_qQ$. A *connection* on the principal bundle $Q$ is an assignment of a complement $H_qQ$ to $V_qQ \subset T_qQ$ at each $q \in Q$ such that

1. $H_{hq}Q = T_q\Phi_h H_qQ$;
2. $H_qQ$ depends differentiably on $q \in Q$.

Vectors in $H_qQ$ are said to be *horizontal*. Given a connection on $Q$, any tangent vector $v_q \in T_qQ$ may be uniquely decomposed into its corresponding horizontal and

vertical components

$$v_q = \text{hor}\, v_q + \text{ver}\, v_q,$$

where $\text{hor}\, v_q \in H_q Q$ and $\text{ver}\, v_q \in V_q Q$.

A connection may be specified on the principal bundle $Q$ by its unique *connection one form* $\Gamma : TQ \to \mathfrak{g}$, where $\mathfrak{g}$ is the Lie algebra corresponding to the structure group $G$. The connection one form satisfies

1. $\Gamma(\xi_Q) = \xi$;
2. $\Gamma(T_q \Phi_g(v_q)) = \text{Ad}_g \Gamma(v_q)$;

and operates on generic vectors tangent to $Q$ such that

$$(\Gamma(v_q))_Q(q) = \text{ver}\, v_q. \tag{2.10}$$

The one form $\Gamma : TQ \to \mathfrak{g}$ thus specifies the horizontal subspace of $T_q Q$ to comprise those vectors which it annihilates.

Given a connection on the bundle $Q$, the tangent map $T_q \pi_M : T_q Q \to T_{\pi_M(q)} M$ maps the horizontal subspace at each $q \in Q$ isomorphically onto $T_{\pi_M(q)} M$. Given a vector $u_r \in T_r M$ and a point $q$ in the fiber over $r$, there is a unique vector in $H_q Q$ which projects via $T_q \pi_M$ onto $u_r$. Given a vector field $X$ on $M$, there is a unique horizontal vector field $X^h$ on $Q$ which projects via $T\pi_M$ onto $X$. We refer to $X^h$ as the *horizontal lift* of $X$. If $Y$ and $Z$ are two vector fields on $M$, it is straightforward to show that

$$\text{hor}[Y^h, Z^h] = [Y, Z]^h, \tag{2.11}$$

where $[\cdot, \cdot]$ denotes the Jacobi-Lie bracket on the appropriate manifold in each case.

The following result is proven in [44] from the equivalence of the Jacobi-Lie bracket to a Lie derivative.

**Lemma 2.3** *If $Z$ is a horizontal vector field on $Q$ and $\xi \in \mathfrak{g}$, then $[Z, \xi_Q]$ is a*

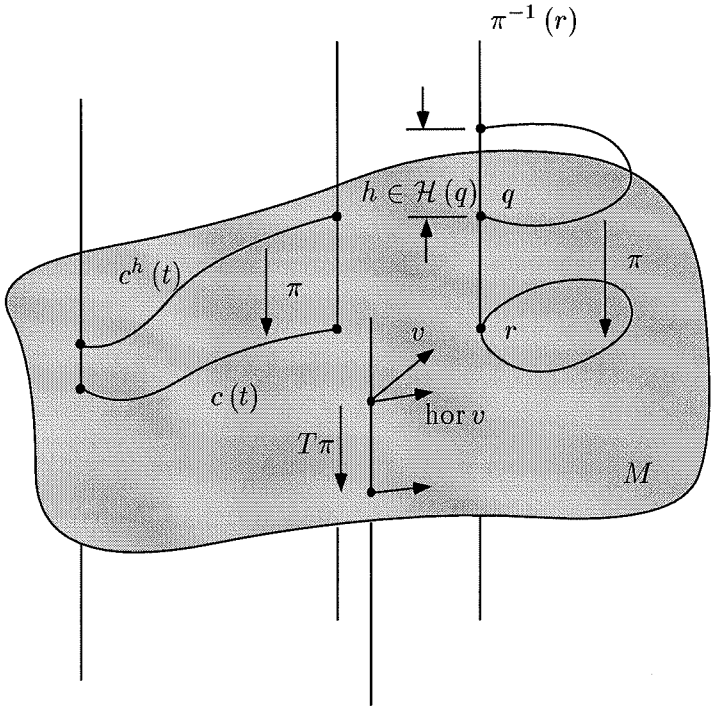


**Figure 2.1** Constructions on a principal bundle.

*horizontal vector field on* $Q$.

Now consider a curve $c(t)$ in $M$ passing through $c(0) = r \in M$. For each point $q$ in the fiber over $r$, there is a unique curve $c^h(t)$ in $Q$, called the *horizontal lift* of $c$, which passes through $q$, projects to $c(t)$, and satisfies $\frac{d}{dt}c^h(t) \in H_qQ$ for all $q = c^h(t)$. If $c(t_1) = r_1$ and $c(t_2) = r_2$, each point $q_1$ in the fiber over $r_1$ is connected by a unique horizontal lift of $c(t)$ to a point $q_2$ in the fiber over $r_2$. We refer to this map from $q_1$ to $q_2$ as *parallel translation* along $c(t)$.

Given a differential form $\alpha : (TQ)^n \to \mathfrak{g}$, we define its *covariant exterior derivative* $D\alpha : (TQ)^{n+1} \to \mathfrak{g}$ with respect to a connection such that

$$D\alpha(X_1, \ldots, X_{n+1}) = d\alpha(\text{hor}\, X_1, \ldots, \text{hor}\, X_{n+1}).$$

The *curvature form* $D\Gamma : TQ \times TQ \to \mathfrak{g}$ corresponding to the connection form $\Gamma$ is given by its covariant exterior derivative

$$D\Gamma(X,Y) = d\Gamma(\operatorname{hor} X, \operatorname{hor} Y). \tag{2.12}$$

Note that (2.2) applied to the connection form $\Gamma$ implies that

$$\Gamma([Y,Z]) = Y\Gamma(Z) - Z\Gamma(Y) - d\Gamma(Y,Z). \tag{2.13}$$

In practice, we often compute the curvature of a connection using the following result, known as Cartan's structure equation.

**Theorem 2.4** *If $\Gamma : TQ \to \mathfrak{g}$ is a connection form and $D\Gamma : TQ \times TQ \to \mathfrak{g}$ the corresponding curvature form, then*

$$D\Gamma(X,Y) = d\Gamma(X,Y) - [\Gamma(X), \Gamma(Y)]. \tag{2.14}$$

*Proof:* We prove the structure equation at an arbitrary point $q \in Q$. We define $\zeta, \lambda \in \mathfrak{g}$ such that $\zeta = \Gamma(X)$ and $\lambda = \Gamma(Y)$ at $q$; then $\zeta_Q = \operatorname{ver} X$ and $\lambda_Q = \operatorname{ver} Y$ at $q$. Since $d\Gamma$ is linear,

$$\begin{aligned} d\Gamma(X,Y) &= d\Gamma(\operatorname{hor} X + \operatorname{ver} X, \operatorname{hor} Y + \operatorname{ver} Y) \\ &= d\Gamma(\operatorname{hor} X, \operatorname{hor} Y) + d\Gamma(\operatorname{hor} X, \operatorname{ver} Y) + d\Gamma(\operatorname{ver} X, \operatorname{hor} Y) \\ &\quad + d\Gamma(\operatorname{ver} X, \operatorname{ver} Y) \\ &= d\Gamma(\operatorname{hor} X, \operatorname{hor} Y) + d\Gamma(\operatorname{hor} X, \eta_Q) + d\Gamma(\zeta_Q, \operatorname{hor} Y) + d\Gamma(\zeta_Q, \eta_Q). \end{aligned}$$

Using (2.13), the fact that $\Gamma(\text{hor}\cdot) = 0$, and (2.3), then

$$\begin{aligned} d\Gamma(X,Y) &= -\Gamma([\text{hor}\,X, \text{hor}\,Y]) + \text{hor}\,X\Gamma(\lambda_Q) - \Gamma([\text{hor}\,X, \lambda_Q]) - \text{hor}\,Y\Gamma(\zeta_Q) \\ &\quad - \Gamma([\zeta_Q, \text{hor}\,Y]) + \zeta_Q\Gamma(\lambda_Q) - \lambda_Q\Gamma(\zeta_Q) - \Gamma([\zeta_Q, \lambda_Q]) \\ &= -\Gamma([\text{hor}\,X, \text{hor}\,Y]) + \text{hor}\,X\lambda - \Gamma([\text{hor}\,X, \lambda_Q]) - \text{hor}\,Y\zeta \\ &\quad - \Gamma(-[\text{hor}\,Y, \zeta_Q]) + \zeta_Q\lambda - \lambda_Q\zeta - \Gamma(-[\zeta,\lambda]_Q) \\ &= -\Gamma([\text{hor}\,X, \text{hor}\,Y]) - \Gamma([\text{hor}\,X, \lambda_Q]) + \Gamma([\text{hor}\,Y, \zeta_Q]) + \Gamma([\zeta,\lambda]_Q). \end{aligned}$$

Applying (2.13) and $\Gamma(\text{hor}\cdot) = 0$ together with (2.12),

$$\begin{aligned} D\Gamma(X,Y) &= d\Gamma(\text{hor}\,X, \text{hor}\,Y) \\ &= -\Gamma([\text{hor}\,X, \text{hor}\,Y]) \\ &= d\Gamma(X,Y) + \Gamma([\text{hor}\,X, \lambda_Q]) - \Gamma([\text{hor}\,Y, \zeta_Q]) - \Gamma([\zeta,\lambda]_Q). \end{aligned}$$

From the definition of the connection form,

$$\Gamma([\zeta,\lambda]_Q) = [\zeta,\lambda] = [\Gamma(X), \Gamma(Y)];$$

from Lemma 2.3,

$$\Gamma([\text{hor}\,X, \lambda_Q]) = \Gamma([\text{hor}\,Y, \zeta_Q]) = 0.$$

Thus

$$D\Gamma(X,Y) = d\Gamma(X,Y) - [\Gamma(X), \Gamma(Y)].$$

■

The preceding result is often written in terms of a multiplicative operation defined for $\mathfrak{g}$-valued forms in the following way. If $\alpha, \beta : TQ \to \mathbb{R}$ and $\xi, \eta \in \mathfrak{g}$,

then

$$[\alpha \otimes \xi, \beta \otimes \eta] = \alpha \wedge \beta \otimes [\xi, \eta].$$

Using this notation, we may write (2.14) as

$$D\Gamma(X,Y) = d\Gamma(X,Y) - \frac{1}{2}[\Gamma,\Gamma](X,Y).$$

Indeed, Cartan's structure equation is a consequence of the more general result

$$D\rho = d\rho - \frac{1}{2}[\Gamma,\rho],$$

where $\rho$ is any equivariant $\mathfrak{g}$-valued one form. With the distinction between $[\Gamma,\Gamma](\cdot,\cdot)$ and $[\Gamma(\cdot),\Gamma(\cdot)]$ in mind, we note that differences among authors' definitions of the wedge product add variety to the appearance of (2.14) in the literature.

A local trivialization $Q = M \times G$ allows us to express the connection form $\Gamma : TQ \to \mathfrak{g}$ in terms of coordinates around $r \in M$ and $g \in G$. Since $(0,v) \in T_rM \times T_gG$ is vertical,

$$\Gamma(r,g)(0,v) = vg^{-1}$$

so that

$$\begin{aligned}(\Gamma(r,g)(0,v))_Q(r,g) &= \left(vg^{-1}\right)_Q(r,g)\\ &= \left(0,\left(vg^{-1}\right)g\right)\\ &= (0,v).\end{aligned}$$

Thus

$$\begin{aligned}\Gamma(r,g)(u,v) &= \Gamma(r,g)((0,v)+(u,0))\\ &= \Gamma(r,g)(0,v) + \Gamma(r,g)(u,0)\\ &= vg^{-1} + \Delta(r,g)(u).\end{aligned}$$

Similarly,

$$\Gamma(r, hg)(u, hv) = hvg^{-1}h^{-1} + \Delta(r, hg)(u).$$

But

$$\begin{aligned}\Gamma(r, hg)(u, hv) &= \mathrm{Ad}_h \Gamma(r, g)(u, v) \\ &= \mathrm{Ad}_h \left(vg^{-1} + \Delta(r, g)(u)\right) \\ &= h\left(vg^{-1} + \Delta(r, g)(u)\right) h^{-1} \\ &= hvg^{-1}h^{-1} + h\Delta(r, g)(u) h^{-1},\end{aligned}$$

so

$$\begin{aligned}\Delta(r, hg)(u) &= h\Delta(r, g)(u) h^{-1} \\ &= \mathrm{Ad}_h \Delta(r, g)(u).\end{aligned}$$

Setting $h = g^{-1}$, we obtain

$$\Delta(r, e)(u) = \mathrm{Ad}_{g^{-1}} \Delta(r, g)(u).$$

Setting $A(r) = \Delta(r, e)$, then

$$\begin{aligned}\Gamma(r, g)(u, v) &= vg^{-1} + \mathrm{Ad}_g A(r)(u) \\ &= \mathrm{Ad}_g \left(g^{-1}v + A(r)(u)\right).\end{aligned}$$

We call the map $A : TM \to \mathfrak{g}$ the *local connection one form.* If $(r(t), g(t))$ determines a curve in $Q$ locally, it follows that

$$\Gamma(\dot{r}, \dot{g}) = \mathrm{Ad}_g \left(g^{-1}\dot{g} + A(r)\dot{r}\right). \tag{2.15}$$

We define $DA : TM \times TM \to \mathfrak{g}$ to be the *local curvature form* which satisfies

$$D\Gamma(r, g)\left(X^h, Y^h\right) = \mathrm{Ad}_g DA(r)(X, Y) \tag{2.16}$$

for $X, Y \in \mathfrak{X}(M)$. Note that $DA$ isn't really a covariant exterior derivative. In terms of the Lie bracket on $\mathfrak{g}$,

$$DA(X,Y) = dA(X,Y) - [A(X), A(Y)] \tag{2.17}$$

for $X, Y \in \mathfrak{X}(M)$.

## 2.5 Geometric phases

### 2.5.1 Holonomy groups and bundles

Let $c(t)$ be an oriented closed curve in $M$ passing through the point $r = \pi_M(q)$. Parallel translation along $c(t)$ maps the point $q \in \pi_M^{-1}(r)$ to some (possibly different) point $p \in \pi_M^{-1}(r)$. Since $q$ and $p$ lie along the same fiber over $M$, there exists some $g \in G$ such that $p = gq$. We refer to $g$ as the *geometric phase*, or *holonomy*, associated with the curve $c(t)$. The *holonomy group* with reference point $q$ contains all $g \in G$ such that $gq$ is reachable from $q$ via parallel translation along a closed curve in $M$, and is denoted by $\mathcal{H}(q)$. The *holonomy bundle* with reference point $q$ comprises the points in $Q$ which are joined to $q$ by horizontal curves, and is denoted by $Q_{\mathcal{H}}(q)$.

If we restrict the construction of $\mathcal{H}(q)$ to permit parallel translation only along contractible closed curves in $M$, we obtain the *restricted holonomy group* $\mathcal{H}_{\text{rest}}(q)$. If we further confine this construction to consider only closed curves lying entirely within some neighborhood $U \subset M$ of $r = \pi_M(q)$, and denote the resulting subgroup of $\mathcal{H}(q)$ by $\mathcal{H}_U(q)$, we define the *local holonomy group* $\mathcal{H}_{\text{loc}}(q)$ to be the intersection of all such $\mathcal{H}_U(q)$.

The Lie algebra associated with $\mathcal{H}(q)$ is related to $\Gamma$ and $Q_{\mathcal{H}}(q)$ as follows.

**Theorem 2.5 (Ambrose-Singer)** *Let $Q$ be a principal bundle with structure group $G$ over a connected manifold $M$. Let $\Gamma$ be a connection form on $Q$, $D\Gamma$ its curvature, $\mathcal{H}(q)$ the holonomy group with reference point $q \in Q$, and $Q_{\mathcal{H}}(q)$ the holonomy bundle with reference point $q$. Then the Lie algebra $\mathfrak{h}(q)$ associated with $\mathcal{H}(q)$ is*

*equal to the subalgebra of* $\mathfrak{g}$*, the Lie algebra associated with* $G$*, spanned by elements of the form* $D\Gamma(p)(u,v)$*, where* $u, v \in H_pQ$ *and* $p \in Q_{\mathcal{H}}(q)$.

Let $m_k(q)$, $k = 0, 1, \ldots$, be the subspace of $\mathfrak{g}$ spanned by elements of the form

$$Z_1 \cdots Z_k \, D\Gamma(q)(X, Y), \tag{2.18}$$

where $X, Y, Z_1, \ldots, Z_k$ are horizontal vector fields on $Q$. The *infinitesimal holonomy group* $\mathcal{H}_{\text{inf}}(q)$ with reference point $q$ is generated by the union $\mathfrak{h}_{\text{inf}}(q)$ of all $m_k(q)$. The infinitesimal holonomy group $\mathcal{H}_{\text{inf}}(q)$ is a subgroup of the local holonomy group $\mathcal{H}_{\text{loc}}(q)$ at any $q \in Q$. If the dimension of $\mathcal{H}_{\text{inf}}(q)$ is constant throughout a neighborhood of $q \in Q$, then $\mathcal{H}_{\text{inf}}(q)$ and $\mathcal{H}_{\text{loc}}(q)$ are equal; if the dimension of $\mathcal{H}_{\text{inf}}(q)$ is constant throughout $Q$, then $\mathcal{H}_{\text{inf}}(q) = \mathcal{H}_{\text{loc}}(q) = \mathcal{H}_{\text{rest}}(q)$ for all $q \in Q$. These facts are proven in [44].

### 2.5.2 Abelian bundles

Along a curve in $Q$ which is everywhere horizontal, (2.15) implies that

$$\dot{g} = -gA(r)\,\dot{r}$$

in local coordinates. In general, the geometric phase associated with a closed curve $c : [0, T] \to M$ is given by

$$g(T) = g(0) \exp \xi(c),$$

where

$$\xi(c) = -\overline{A} + \frac{1}{2}\overline{[A, A]} - \frac{1}{3}\overline{[[A, A], A]} - \frac{1}{12}\overline{[A, [A, A]]} + \ldots \tag{2.19}$$

and

$$\begin{aligned}\overline{A} &= \int_0^T A\left(c\left(t\right)\right)\dot{c}\left(t\right)dt,\\ \overline{\left[\overline{A},A\right]} &= \int_0^T \left[\int_0^t A\left(c\left(\tau\right)\right)\dot{c}\left(\tau\right)d\tau, A\left(c\left(t\right)\right)\dot{c}\left(t\right)\right]dt,\\ &\vdots\end{aligned}$$

This formula appears in modified form in [54]. If $G$ is Abelian, only the first term in this expansion is nonzero, so that

$$g\left(T\right) = g\left(0\right)\exp\left(-\int_0^T A\left(c\left(t\right)\right)\dot{c}\left(t\right)dt\right).$$

By Stokes' theorem, then

$$\begin{aligned}g\left(T\right) &= g\left(0\right)\exp\left(-\int_S dA\left(r\right)\right)\\ &= \exp\left(-\int_S dA\left(r\right)\right)g\left(0\right),\end{aligned}$$

where S is any oriented submanifold of $M$ whose boundary is traced by $c\left(t\right)$ as $t$ increases from 0 to $T$. This result is the *area rule* for Abelian bundles.

If $G$ is Abelian, then the local curvature form satisfies

$$DA\left(X,Y\right) = D\Gamma\left(X^h, Y^h\right)$$

for $X, Y \in \mathfrak{X}\left(M\right)$ by (2.16). But

$$DA\left(X,Y\right) = dA\left(X,Y\right)$$

by (2.17). Thus we have

**Corollary 2.6 (Abelian Ambrose-Singer)** *If $G$ is Abelian, the Lie algebra $\mathfrak{h}\left(q\right)$ is equal to the subalgebra of $\mathfrak{g}$ spanned by elements of the form $dA\left(u,v\right)$, where*

$u, v \in T_r M$ *for any* $r \in M$.

# Chapter 3

# Lagrangian Mechanics

## 3.1 Fundamentals

### 3.1.1 The Euler-Lagrange equations

The Lagrangian description of a mechanical system whose configuration is specified by a point $q \in Q$ begins with a function $L : TQ \to \mathbb{R}$. This function, termed the *Lagrangian*, represents the difference between the system's kinetic energy and its potential energy. We define the *fiber derivative* $\mathbb{F}L : TQ \to T^*Q$ of the Lagrangian $L : TQ \to \mathbb{R}$ such that

$$\langle \mathbb{F}L(u), v \rangle = \left. \frac{d}{dt} \right|_{t=0} L(u + tv) \quad \text{for} \quad u, v \in T_qQ$$

at every $q \in Q$. Thus $\langle \mathbb{F}L(u), v \rangle$ is the derivative of $L$ at the point $u \in T_qQ$ in the direction $v$. The Lagrangian $L$ is said to be *regular*, or *nondegenerate*, if $\mathbb{F}L$ is regular at all $(q, u) \in TQ$. It is proven in [1] that $L$ is regular if and only if $\mathbb{F}L : TQ \to T^*Q$ is a local diffeomorphism. The Lagrangian $L$ is said to be *hyperregular* if $\mathbb{F}L : TQ \to T^*Q$ is a global diffeomorphism.

We define the one form $\theta_L : T(TQ) \to \mathbb{R}$ such that

$$\theta_L(w) = \langle \mathbb{F}L(\tau_{TQ}w), T\tau_Q(w) \rangle,$$

and the two form $\omega_L : T(TQ) \times T(TQ) \to \mathbb{R}$ such that

$$\omega_L = -d\theta_L.$$

We refer to $\omega_L$ as the *Lagrange two form.* We define the *action* $\mathrm{A} : TQ \to \mathbb{R}$ such that

$$\mathrm{A}(u) = \langle \mathbb{F}L(u), u \rangle \quad \text{for} \quad u \in T_qQ,$$

and refer to the difference $E = \mathrm{A} - L$ as the *energy.* A *Lagrangian vector field* $X_E$ on $TQ$ satisfies

$$X_E \lrcorner \omega_L = dE.$$

A *second order equation* on $Q$ is a vector field $X$ on $TQ$ such that $T\tau_Q \circ X$ is the identity map on $TQ$. If $L : TQ \to \mathbb{R}$ is regular, then $X_E$ exists and is second order.

History instructs us to regard Newton's law $F = d(mv)/dt$ as axiomatic in the study of mechanical systems. For conservative, unconstrained systems, this relation is rooted in the extremization of the functional

$$\mathbb{J} = \int L dt.$$

For finite dimensional systems, we may therefore realize equations of motion according to the following result.

**Theorem 3.1 (Hamilton's Principle)** *Let $L : TQ \to \mathbb{R}$ be a regular Lagrangian, and let $q_1$ and $q_2$ be points fixed in $Q$. Then the curve $c : [a, b] \to Q$ represents a critical point of the functional*

$$\mathbb{J} : \Omega(q_1, q_2, [a, b]) \to \mathbb{R} : c \mapsto \int_a^b L(c(t), c'(t))\, dt$$

*if and only if*

$$\frac{d}{dt}\frac{\partial L}{\partial \dot{q}^i} - \frac{\partial L}{\partial q^i} = 0,$$

*where $q^i$ are local coordinates on $Q$.*

*Proof:* Recall that $\mathbb{J}$ has a critical point at $c$ if and only if

$$d\mathbb{J}(c) \cdot \delta c = \left.\frac{d\mathbb{J}(c_s)}{ds}\right|_{s=0} = 0$$

for all variations $c_s$ of $c = c_0$. Since

$$\begin{aligned}
\left.\frac{d}{ds}\right|_{s=0} \int_a^b L\left(c_s(t), c_s'(t)\right) dt &= \int_a^b \left(\frac{\partial L}{\partial q^i}\frac{\partial}{\partial s}q^i(s,t) + \frac{\partial L}{\partial \dot{q}^i}\frac{\partial}{\partial s}\dot{q}^i(s,t)\right)\Bigg|_{s=0} dt \\
&= \int_a^b \frac{\partial L}{\partial q^i}\delta q^i dt + \left.\frac{\partial L}{\partial \dot{q}^i}\delta q^i\right|_{t=a}^{t=b} - \int_a^b \delta q^i \frac{d}{dt}\frac{\partial L}{\partial \dot{q}^i} dt \\
&= -\int_a^b \left(\frac{d}{dt}\frac{\partial L}{\partial \dot{q}^i} - \frac{\partial L}{\partial q^i}\right)\delta q^i dt,
\end{aligned}$$

$d\mathbb{J}(c) \cdot \delta c$ vanishes for all variations of $c$ if and only if

$$\int_a^b \left(\frac{d}{dt}\frac{\partial L}{\partial \dot{q}^i} - \frac{\partial L}{\partial q^i}\right)\delta q^i dt$$

vanishes for all $\delta q^i$. Thus $\mathbb{J}$ has a critical point at $c$ if and only if

$$\frac{d}{dt}\frac{\partial L}{\partial \dot{q}^i} - \frac{\partial L}{\partial q^i} = 0 \tag{3.1}$$

along $c$. ■

Equations (3.1) are the classical *Euler-Lagrange equations* in coordinate form. Their generalization to infinite dimensions is presented in [1] as follows.

**Theorem 3.2** *Let $X_E$ be a second order Lagrangian vector field on $TQ$ corresponding to $L : TQ \to \mathbb{R}$. If $(q(t), \dot{q}(t))$ represents an integral curve of $X_E$ in a local*

*chart, then*

$$\frac{d}{dt}D_2L\left(q\left(t\right),\dot{q}\left(t\right)\right)-D_1L\left(q\left(t\right),\dot{q}\left(t\right)\right)=0.$$

Here $D_iL\left(\cdot,\cdot\right)$ refers to the Gâteaux derivative of $L$ with respect to its $i$th argument.

### 3.1.2 Symmetries and momentum maps

The Lagrangian $L:TQ\rightarrow\mathbb{R}$ determines a *kinetic energy metric* $\langle\!\langle\cdot,\cdot\rangle\!\rangle_{\mathrm{KE}}:T_qQ\times T_qQ\rightarrow\mathbb{R}$ at each $q\in Q$ such that

$$\langle\!\langle u,v\rangle\!\rangle_{\mathrm{KE}}=\langle\mathbb{F}L\left(u\right),v\rangle.$$

Let $\Phi:G\times Q\rightarrow Q$ be an action of the Lie group $G$ on the manifold $Q$. The Lagrangian $L:TQ\rightarrow\mathbb{R}$ is said to be $G$ *invariant* if

$$L\left(\Phi_g q,T_q\Phi_g v_q\right)=L\left(q,v_q\right)$$

for all $q\in Q$, $v_q\in T_qQ$, and $g\in G$. Given such a Lagrangian, we define the *momentum map* $J:TQ\rightarrow\mathfrak{g}^*$ such that

$$\begin{aligned}\langle J\left(v_q\right),\eta\rangle&=\langle\mathbb{F}L\left(v_q\right),\eta_Q\left(q\right)\rangle\\&=\langle\!\langle v_q,\eta_Q\left(q\right)\rangle\!\rangle_{\mathrm{KE}}\end{aligned}$$

for $v_q\in T_qQ$ and $\eta\in\mathfrak{g}$. If $L$ is $G$ invariant, then $G$ is said to determine a *symmetry* of the system given by the Euler-Lagrange equations. The relationship between symmetries and conservation laws is specified by the following result, proven in [13].

**Theorem 3.3 (Noether)** *If $L:TQ\rightarrow\mathbb{R}$ is $G$ invariant, then the momentum $J:TQ\rightarrow\mathfrak{g}^*$ is conserved along integral curves of the Euler-Lagrange equations corresponding to $L$.*

### 3.1.3 The Lagrange-d'Alembert principle

We refer to a fiber preserving map $F : TQ \to T^*Q$ over the identity as a *force field.* In the presence of a force field $F : TQ \to T^*Q$, the *integral Lagrange-d'Alembert principle* for a curve $q(t)$ in $Q$ states that

$$\delta \int_a^b L(q(t), \dot{q}(t))\, dt + \int_a^b F(q(t), \dot{q}(t)) \cdot \delta q\, dt = 0, \tag{3.2}$$

where

$$\begin{aligned} \delta \int_a^b L(q(t), \dot{q}(t))\, dt &= \int_a^b \left( \frac{\partial L}{\partial q^i} \delta q^i + \frac{\partial L}{\partial \dot{q}^i} \frac{d}{dt} \delta q^i \right) dt \\ &= \int_a^b \left( \frac{\partial L}{\partial q^i} - \frac{d}{dt} \frac{\partial L}{\partial \dot{q}^i} \right) \delta q^i dt. \end{aligned}$$

A force field $F : TQ \to T^*Q$ determines a one form $\tilde{F} : T(TQ) \to \mathbb{R}$ such that

$$\tilde{F}(v) W = \langle F(v), T_v \tau_Q W \rangle$$

for $v \in TQ$ and $W \in T_v(TQ)$. If $L$ is regular, this one form determines a vector field $Y_F$ on $TQ$ such that

$$T\tau_Q Y_F = 0$$

and

$$\tilde{F} = -Y_F \lrcorner \omega_L.$$

The vector field $Y_F$ is said to be *weakly dissipative* if

$$\langle dE, Y_F \rangle \leq 0$$

throughout $TQ$, and *dissipative* if

$$\langle dE, Y_F \rangle < 0$$

off the zero section $Q \times \{0\}$. The force field $F$ is dissipative if and only if

$$\langle F(v), v \rangle < 0$$

for all nonzero $v \in TQ$. In Chapter 4, we will encounter dissipative force fields of the form $F = \mathbb{F}(-R)$, where $R : TQ \to \mathbb{R}$. A function $R$ which generates a dissipative force field in this way is called a *Rayleigh dissipation function.*

## 3.2 Reduction on Cartesian products

In Chapter 8, we will appeal to the following result regarding Lagrangian reduction on the Cartesian product of two Lie groups. The proposition and its proof mimic those appearing in [60].

**Proposition 3.4** *Let $G$ and $\Psi$ be Lie groups and $Q = G \times \Psi$ their Cartesian product. Let $L : TQ \to \mathbb{R}$ be invariant with respect to both the left action $(g, \eta) \mapsto (hg, \eta)$ of $G$ on $Q$ and the right action $(g, \eta) \mapsto (g, \eta\zeta)$ of $\Psi$ on $Q$. Let $l : \mathfrak{g} \times \psi \to \mathbb{R}$ be the restriction of $L$ to the space tangent to $Q$ at the identity $(e, e) \in G \times \Psi$. For a curve $q(t) = (g(t), \eta(t))$ in $Q$, let $\xi(t) = g^{-1}\dot{g}$ and $u(t) = \dot{\eta} \circ \eta^{-1}$. Then the following four statements are equivalent:*

*(i) The curve $q(t)$ satisfies the Euler-Lagrange equations for $L$ on $Q$;*

*(ii) The variational principle $\delta \int_a^b L(q(t), \dot{q}(t))\, dt = 0$ holds for variations with fixed endpoints;*

*(iii) The* reduced Euler-Lagrange equations

$$\begin{aligned} \frac{d}{dt}\frac{\partial l}{\partial \xi} &= \mathrm{ad}^*_\xi \frac{\partial l}{\partial \xi} \\ \frac{d}{dt}\frac{\partial l}{\partial u} &= \mathrm{ad}^*_u \frac{\partial l}{\partial u} \end{aligned} \tag{3.3}$$

*hold;*

*(iv) The variational principle* $\delta \int l(\xi(t), u(t))\, dt = 0$ *holds on* $\mathfrak{g} \times \psi$ *for variations of the form* $\delta q = \delta g + \delta u = \left(\dot{\zeta} + [\xi, \zeta]\right) + (\dot{w} + [u, w])$.

*Proof:* We will apply this theorem to the case in which $G$ is a matrix Lie group but $\Psi$ is not; the proof presented here makes these assumptions. We acknowledge, furthermore, that different Lie brackets in (iv) can give rise to different signs in (3.3); we have stated the result in a manner consistent with its application in Chapter 8.

We addressed the equivalence of (i) and (ii) in Section 3.1. To demonstrate the equivalence of (ii) and (iv), we compute the infinitesimal variation $\delta\xi + \delta u$ induced by an infinitesimal variation $\delta q$, beginning with the variation $\delta u$ alone. From the definitions above,

$$\begin{aligned} \delta u &= \left.\frac{\partial}{\partial \epsilon}\right|_{\epsilon=0} \left(\dot{\eta}(\epsilon, t) \circ \eta^{-1}(\epsilon, t)\right) \\ &= \left(\left.\frac{\partial}{\partial \epsilon}\right|_{\epsilon=0} \dot{\eta}(\epsilon, t)\right) \circ \eta^{-1}(\epsilon, t) + \left(\frac{\partial}{\partial t} T\eta(\epsilon, t)\right) \left.\frac{\partial}{\partial \epsilon}\right|_{\epsilon=0} \eta^{-1}(\epsilon, t) \\ &= \left(\frac{\partial}{\partial t}\delta\eta\right) \circ \eta^{-1}(\epsilon, t) - \left(\frac{\partial}{\partial t} T\eta(\epsilon, t)\right) \left(T\eta^{-1}(\epsilon, t)\right) \delta\eta \circ \eta^{-1}(\epsilon, t). \end{aligned}$$

We define

$$w(\epsilon, t) = \delta\eta \circ \eta^{-1}(\epsilon, t);$$

then

$$\begin{aligned} &\frac{\partial}{\partial t} w(\epsilon, t) \\ &= \left(\frac{\partial}{\partial t}\delta\eta\right) \circ \eta^{-1}(\epsilon, t) - \left(\left.\frac{\partial}{\partial \epsilon}\right|_{\epsilon=0} T\eta(\epsilon, t)\right) \left(T\eta^{-1}(\epsilon, t)\right) \left(\frac{\partial}{\partial t}\eta(\epsilon, t)\right) \circ \eta^{-1}(\epsilon, t). \end{aligned}$$

It follows that

$$\begin{aligned}\delta u - \dot{w} &= \left(\left.\frac{\partial}{\partial \epsilon}\right|_{\epsilon=0} T\eta(\epsilon,t)\right)\left(T\eta^{-1}(\epsilon,t)\right)\left(\frac{\partial}{\partial t}\eta(\epsilon,t)\right)\circ\eta^{-1}(\epsilon,t) \\ &\quad - \left(\frac{\partial}{\partial t}T\eta(\epsilon,t)\right)\left(T\eta^{-1}(\epsilon,t)\right)\delta\eta\circ\eta^{-1}(\epsilon,t) \\ &= \left[\dot{\eta}(\epsilon,t)\circ\eta^{-1}(\epsilon,t), \delta\eta\circ\eta^{-1}(\epsilon,t)\right] \\ &= [u,w],\end{aligned}$$

so

$$\delta u = \dot{w} + [u,w].$$

The determination of $\delta\xi$ proceeds analogously, and appears explicitly in [58]. Since $\zeta$ and $w$ vanish at the endpoints $a$ and $b$ but are otherwise arbitrary,

$$\begin{aligned}\delta\int_a^b l\left(\xi(\epsilon,t), u(\epsilon,t)\right)dt &= \left.\frac{\partial}{\partial\epsilon}\right|_{\epsilon=0}\int_a^b l\left(\xi(\epsilon,t), u(\epsilon,t)\right)dt \\ &= \int_a^b\left(\frac{\partial l}{\partial\xi}\delta\xi + \frac{\partial l}{\partial u}\delta u\right)dt \\ &= \int_a^b\left(\frac{\partial l}{\partial\xi}\left(\dot{\zeta} + \mathrm{ad}_\xi\,\zeta\right) + \frac{\partial l}{\partial u}\left(\dot{w} + \mathrm{ad}_u\, w\right)\right)dt \\ &= \int_a^b\left(\left(-\frac{d}{dt}\frac{\partial l}{\partial\xi} + \mathrm{ad}^*_\xi\frac{\partial l}{\partial\xi}\right)\zeta + \left(-\frac{d}{dt}\frac{\partial l}{\partial u} + \mathrm{ad}^*_u\frac{\partial l}{\partial u}\right)w\right)dt.\end{aligned}$$

Thus

$$\delta\int_a^b l\left(\xi(\epsilon,t), u(\epsilon,t)\right)dt = 0$$

if and only if 3.3 holds, and (iii) and (iv) are equivalent. ■

# Chapter 4

# The Geometry of Locomotion

## 4.1 Locomotion and principal bundles

### 4.1.1 Connections on configuration bundles

In the context of locomotion, we regard the shape of a deformable body as a point in a *shape manifold* $M$. A point in the configuration manifold $Q = M \times G$ represents this shape together with the body's position and orientation in ambient space. The Lie group $G$ corresponds, for a particular fixed shape, to the space of rigid motions of the body with respect to a reference position. We think of $Q = M \times G$ as a trivial principal bundle over $M$ with structure group $G$; the action of $G$ on $Q$ is given by $\Phi_h(r, g) = (r, hg)$ for $(r, g) \in Q$ and $h \in G$.

A connection on the configuration bundle $Q$ over $M$ provides a unique correspondence between sequential changes in shape, represented by curves in $M$ which begin at $r \in M$, and trajectories of the system in $Q$ which begin at a configuration $q \in \pi_M^{-1}(r)$. We are particularly interested in the self-propulsion of deformable bodies undergoing *cyclic* changes in shape, represented by closed loops in $M$. Parallel translation along a closed curve in $M$ which begins and ends at $r$ maps each point $q \in \pi_M^{-1}(r)$ to another point $p \in \pi_M^{-1}(r)$. In other words, a cyclic change in shape may result in the net displacement or reorientation of a deforming body in space. The element of $G$ representing this net motion is the geometric phase corresponding to the closed curve in $M$.

It should be clear that if the self-propulsion of a deformable body is governed by a single principal connection, at least two modes of deformation are needed to effect fiberwise motion. To negotiate a closed loop in a one-dimensional shape space, a propulsor must undo any sequence of deformations it has completed, thereby generating zero geometric phase. This fact constitutes the *scallop theorem*, so named in [82] for a biomimetic propulsor with a single internal degree of freedom.

In Section 4.2, we will encounter systems for which single connections cannot provide accurate models. It will prove to be the case, however, that the notion of a connection can still contribute to the geometrization of the equations governing such systems. In Chapters 8 and 9, we will model a class of systems for which the relevance of principal connections has yet to be established.

### 4.1.2 Kinematic and nonholonomic connections

Much terrestrial locomotion is essentially tractional. In order to pull itself along, a propulsor must establish contact with the ground in a manner which can support shear. The robot to be considered in Section 4.2.2 exemplifies systems for which this contact is viscous. In many instances, however, it is reasonable to assume that a foot or wheel makes slipless contact with the ground. A wheel which cannot slip may still roll freely; from this idealization we distill nonholonomic constraints which govern the motion of wheeled vehicles.

We realize a set of rolling constraints as the distribution on $Q$ comprising allowable velocities $\dot{q} = (\dot{r}, \dot{g})$. If such a distribution coincides with the horizontal subbundle of $TQ$ determined by a connection $\Gamma$, we refer to this connection as *kinematic*. We will construct a kinematic connection explicitly in Section 4.1.3. In general, we refer to a system which evolves along curves which are horizontal with respect to any connection as kinematic. This semiotic subtlety is intended to acknowledge the geometric equivalence of all such systems.

It need not be the case that a set of nonholonomic constraints determines a connection in the sense of Section 2.4. For certain systems, constraints break the symmetries which foster traditional conservation laws without proscribing fiberwise

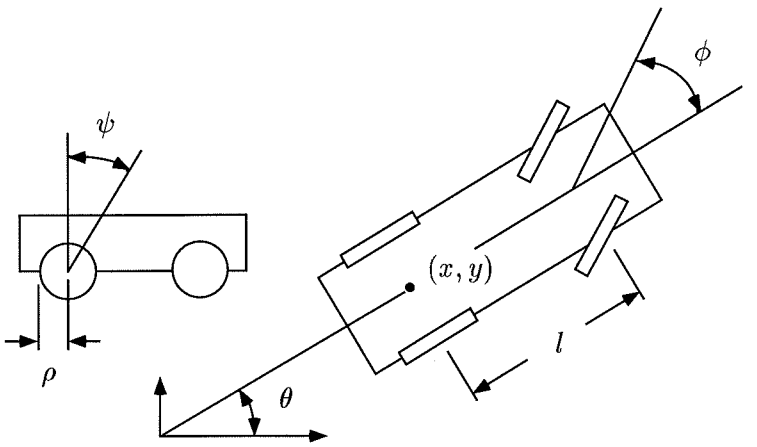


**Figure 4.1** The kinematic car on the plane.

drift. Given a $G$ invariant distribution of constraints, one may study the evolution of a $G$ invariant *generalized momentum* in terms of a *nonholonomic connection.* This perspective is explored in [80] and [13].

### 4.1.3 The kinematic car

The equations governing the planar motion of the simplified automobile depicted in Figure 4.1 are equivalent to a kinematic connection on the configuration bundle $Q = M \times G = \mathbb{T}^2 \times SE(2)$. We treat the front and rear wheel pairs as single wheels affixed at the midpoints of their respective axles, and parametrize the shape space $M = \mathbb{T}^2 = \mathbb{S}^1 \times \mathbb{S}^1$ by the steering angle $\phi$ and the angle of rotation $\psi$ of the rear wheel. The car's trajectory in the plane is determined by the variation of these angles with time; we need not consider the angle of rotation of the front wheel. We define $\psi$ to increase as the car moves forward. We denote the radius of the wheels by $\rho$ and the distance between their centers by $l$.

The car's movement is restricted at any moment by the specification that the wheels can roll but not slip on the plane. Since neither wheel can slip transverse to its rolling direction,

$$\dot{x} \sin\theta - \dot{y} \cos\theta = 0$$

and

$$\dot{x}\sin(\theta+\phi)-\dot{y}\cos(\theta+\phi)-l\dot{\theta}\cos\phi=0.$$

Since the rear wheel cannot slip along its rolling direction,

$$\dot{x}\cos\theta+\dot{y}\sin\theta-\rho\dot{\psi}=0.$$

We decompose the arbitrary velocity vector

$$v_q=\begin{bmatrix}\dot{\phi}\\ \dot{\psi}\\ \dot{x}\\ \dot{y}\\ \dot{\theta}\end{bmatrix}=\begin{bmatrix}\dot{\phi}\\ \dot{\psi}\\ \rho\dot{\psi}\cos\theta\\ \rho\dot{\psi}\sin\theta\\ (\rho/l)\,\dot{\psi}\tan\phi\end{bmatrix}+\begin{bmatrix}0\\ 0\\ \dot{x}-\rho\dot{\psi}\cos\theta\\ \dot{y}-\rho\dot{\psi}\sin\theta\\ \dot{\theta}-(\rho/l)\,\dot{\psi}\tan\phi\end{bmatrix}=\operatorname{hor}v_q+\operatorname{ver}v_q$$

such that the component termed horizontal satisfies the constraints and that termed vertical lies in the fiber direction. Since

$$\left(\Gamma\left(v_q\right)\right)_Q\left(q\right)=\operatorname{ver}\left(v_q\right)=\begin{bmatrix}0\\ 0\\ \dot{x}-\rho\dot{\psi}\cos\theta\\ \dot{y}-\rho\dot{\psi}\sin\theta\\ \dot{\theta}-(\rho/l)\,\dot{\psi}\tan\phi\end{bmatrix},$$

(2.7) implies that the connection one-form $\Gamma$ returns

$$\Gamma\left(v_q\right)=\begin{bmatrix}\dot{x}-(\rho\cos\theta+(\rho/l)\,y\tan\phi)\,\dot{\psi}+y\dot{\theta}\\ \dot{y}+((\rho/l)\,x\tan\phi-\rho\sin\theta)\,\dot{\psi}-x\dot{\theta}\\ \dot{\theta}-(\rho/l)\,\dot{\psi}\tan\phi\end{bmatrix},$$

or, using (2.8) and (2.9),

$$\begin{aligned}\Gamma(\dot{r},\dot{g}) &= \begin{bmatrix}\cos\theta & -\sin\theta & y\\ \sin\theta & \cos\theta & -x\\ 0 & 0 & 1\end{bmatrix}\begin{bmatrix}\dot{x}\cos\theta+\dot{y}\sin\theta-\rho\dot{\psi}\\ \dot{y}\cos\theta-\dot{x}\sin\theta\\ \dot{\theta}-(\rho/l)\,\dot{\psi}\tan\phi\end{bmatrix}\\ &= \begin{bmatrix}\cos\theta & -\sin\theta & y\\ \sin\theta & \cos\theta & -x\\ 0 & 0 & 1\end{bmatrix}\left(\begin{bmatrix}\dot{x}\cos\theta+\dot{y}\sin\theta\\ \dot{y}\cos\theta-\dot{x}\sin\theta\\ \dot{\theta}\end{bmatrix}+\begin{bmatrix}-\rho\dot{\psi}\\ 0\\ -(\rho/l)\,\dot{\psi}\tan\phi\end{bmatrix}\right)\\ &= \mathrm{Ad}_g\left(g^{-1}\dot{g}+A(r)\,\dot{r}\right).\end{aligned}$$

The local connection form is therefore given by

$$A(r) = A(\phi,\psi) = \begin{bmatrix}-\rho d\psi\\ 0\\ -(\rho/l)\tan\phi d\psi\end{bmatrix}.$$

### 4.1.4 Mechanical connections

Principal connections may also be defined to represent conservation laws and force balances. Suppose that $G$ acts on $Q$ to define a principal bundle over $M$. If $L : TQ \to \mathbb{R}$ is $G$ invariant, we define the *locked inertia tensor* $\mathbb{I} : \mathfrak{g} \to \mathfrak{g}^*$ at each $q \in Q$ such that

$$\langle \mathbb{I}(q)\,\xi, \eta\rangle = \langle\!\langle \xi_Q(q), \eta_Q(q)\rangle\!\rangle_{\mathrm{KE}}. \tag{4.1}$$

The locked inertia tensor may be written locally as

$$\mathbb{I}(r,g) = \mathrm{Ad}^*_{g^{-1}}\,\mathbb{I}_{\mathrm{loc}}(r)\,\mathrm{Ad}_{g^{-1}}. \tag{4.2}$$

The *mechanical connection* $\Gamma_{\mathrm{mech}} : TQ \to \mathfrak{g}$ is given by

$$\Gamma_{\mathrm{mech}} : (q,\dot{q}) \mapsto \mathbb{I}^{-1}(q)\,J(q,\dot{q}), \tag{4.3}$$

where $J : TQ \to \mathfrak{g}^*$ is the momentum map from Section 3.1.2. As a system evolves along a trajectory in $Q$ which is horizontal with respect to a mechanical connection, the momentum

$$J(q, \dot{q}) = 0$$

is conserved.

We defined a principal connection in terms of a choice of horizontal subbundle $HQ$ to complement the vertical subbundle $VQ$ of $TQ$. A connection derived from a $G$ invariant Lagrangian determines $H_qQ$ to be orthogonal to $V_qQ$ with respect to $\langle\!\langle \cdot, \cdot \rangle\!\rangle_{\mathrm{KE}}$ at each $q \in Q$.

The definition of the mechanical connection supposes the Lagrangian in question to correspond to kinetic energy [56], but neither (4.1) nor (4.3) restricts the physical significance of $L$. Given a dissipative force field $F : TQ \to T^*Q$, the equation

$$\langle F(q, \dot{q}), \xi_Q(q) \rangle = 0 \qquad \forall \xi \in \mathfrak{g} \tag{4.4}$$

represents a balance of fiberwise dissipative forces. The $G$ invariance of a Rayleigh dissipation function $R$ such that $F = \mathbb{F}(-R)$ allows us to define a momentum map $K : TQ \to \mathfrak{g}^*$ such that

$$\langle K(q, \dot{q}), \xi \rangle = \langle F(q, \dot{q}), \xi_Q(q) \rangle$$

and a *viscosity tensor* $\mathbb{V} : \mathfrak{g} \to \mathfrak{g}^*$ such that

$$\langle \mathbb{V}(q)\xi, \eta \rangle = \langle F(\xi_Q(q)), \eta_Q(q) \rangle$$

and

$$\mathbb{V}(r, g) = \mathrm{Ad}^*_{g^{-1}} \mathbb{V}_{\mathrm{loc}}(r) \mathrm{Ad}_{g^{-1}} . \tag{4.5}$$

A trajectory in $Q$ which is horizontal with respect to the *Stokes connection*

$$\Gamma_{\text{Stokes}} : (q, \dot{q}) \mapsto \mathbb{V}^{-1}(q)\, K(q, \dot{q})$$

is a trajectory which observes the force balance (4.4).

## 4.2 Interpolation for Rayleigh systems

### 4.2.1 The interpolated equations

From (2.15), (4.2), and (4.5), we obtain the local expressions

$$\begin{aligned}\Gamma_{\text{mech}} &= \mathbb{I}^{-1} J \\ &= \text{Ad}_g\, \mathbb{I}_{\text{loc}}^{-1} \text{Ad}_g^* J \\ &= \text{Ad}_g \left(g^{-1}\dot{g} + A_{\text{mech}}\dot{r}\right)\end{aligned}$$

and

$$\begin{aligned}\Gamma_{\text{Stokes}} &= \mathbb{V}^{-1} K \\ &= \text{Ad}_g\, \mathbb{V}_{\text{loc}}^{-1} \text{Ad}_g^* K \\ &= \text{Ad}_g \left(g^{-1}\dot{g} + A_{\text{Stokes}}\dot{r}\right).\end{aligned}$$

Thus

$$g^{-1}\dot{g} + A_{\text{mech}}\dot{r} = \mathbb{I}_{\text{loc}}^{-1} p,$$

where

$$p = \text{Ad}_g^* J$$

is the *body momentum*, and

$$g^{-1}\dot{g} + A_{\text{Stokes}}\dot{r} = \mathbb{V}_{\text{loc}}^{-1} \text{Ad}_g^* K.$$

Recall the integral Lagrange-d'Alembert principle from Section 3.1.3. Choose a function $\phi(t,s)$ such that $\phi(a,s) = \phi(b,s) = \phi(t,0) = 0$, and consider the variation

$$q(t,s) = \exp(\phi(t,s)\,\xi)\,q(t),$$

where $\xi \in \mathfrak{g}$. Substituting the corresponding infinitesimal variation

$$\delta q(t) = \left.\frac{\partial \phi}{\partial s}\right|_{s=0} \xi_Q(q(t))$$

into (3.2), we obtain

$$\begin{aligned}\langle F(q,\dot{q}), \xi_Q(q)\rangle &= \frac{d}{dt}\langle \mathbb{F}L(q,\dot{q}), \xi_Q(q)\rangle \\ &= \frac{d}{dt}\langle J(q,\dot{q}), \xi\rangle \\ &= \langle \frac{d}{dt} J(q,\dot{q}), \xi\rangle.\end{aligned}$$

Thus $K(q,\dot{q}) = \dot{J}(q,\dot{q})$ under the natural identification of $\mathfrak{g}^*$ with $T_J\mathfrak{g}^*$, and

$$g^{-1}\dot{g} + A_{\text{Stokes}}\dot{r} = \mathbb{V}_{\text{loc}}^{-1}\,\text{Ad}_g^*\,\dot{J}.$$

It follows from (2.5) that

$$\begin{aligned}\text{Ad}_g^*\,\dot{J} &= \text{Ad}_g^*\,\frac{d}{dt}\left(\text{Ad}_{g^{-1}}^*\,p\right) \\ &= \text{Ad}_g^*\left(\text{Ad}_{g^{-1}}^*\,\dot{p} + \text{ad}_{g\frac{d}{dt}(g^{-1})}^*\,\text{Ad}_{g^{-1}}^*\,p\right) \\ &= \dot{p} + \text{Ad}_g^*\,\text{ad}_{g(-g^{-1}\dot{g}g^{-1})}^*\,\text{Ad}_{g^{-1}}^*\,p \\ &= \dot{p} + \text{Ad}_g^*\,\text{ad}_{-\dot{g}g^{-1}}^*\,\text{Ad}_{g^{-1}}^*\,p.\end{aligned}$$

Since

$$\begin{aligned}
\langle \mathrm{Ad}_g^* \, \mathrm{ad}^*_{-\dot{g}g^{-1}} \, \mathrm{Ad}^*_{g^{-1}} \, p, \xi \rangle &= \langle \mathrm{ad}^*_{-\dot{g}g^{-1}} \, \mathrm{Ad}^*_{g^{-1}} \, p, \mathrm{Ad}_g \, \xi \rangle \\
&= \langle \mathrm{Ad}^*_{g^{-1}} \, p, \mathrm{ad}_{-\dot{g}g^{-1}} \, \mathrm{Ad}_g \, \xi \rangle \\
&= \langle \mathrm{Ad}^*_{g^{-1}} \, p, [-\dot{g}g^{-1}, g\xi g^{-1}] \rangle \\
&= \langle \mathrm{Ad}^*_{g^{-1}} \, p, [-\dot{g}, g\xi] g^{-1} \rangle \\
&= -\langle \mathrm{Ad}^*_{g^{-1}} \, p, [\dot{g}, g\xi] g^{-1} \rangle \\
&= -\langle p, \mathrm{Ad}_{g^{-1}} \left( [\dot{g}, g\xi] g^{-1} \right) \rangle \\
&= -\langle p, g^{-1} [\dot{g}, g\xi] g^{-1} g \rangle \\
&= -\langle p, [g^{-1}\dot{g}, \xi] \rangle \\
&= -\langle p, \mathrm{ad}_{g^{-1}\dot{g}} \, \xi \rangle \\
&= -\langle \mathrm{ad}^*_{g^{-1}\dot{g}} \, p, \xi \rangle
\end{aligned}$$

for any $\xi \in \mathfrak{g}$,

$$\mathrm{Ad}_g^* \, \mathrm{ad}^*_{-\dot{g}g^{-1}} \, \mathrm{Ad}^*_{g^{-1}} \, p = - \, \mathrm{ad}^*_{g^{-1}\dot{g}} \, p$$

and

$$\begin{aligned}
\mathrm{Ad}_g^* \, \dot{J} &= \dot{p} - \mathrm{ad}^*_{g^{-1}\dot{g}} \, p \\
&= \mathbb{V}_{\mathrm{loc}} \left( g^{-1}\dot{g} + A_{\mathrm{Stokes}} \dot{r} \right).
\end{aligned}$$

Rearranging terms, we obtain

$$\begin{aligned}
g^{-1}\dot{g} &= -A_{\mathrm{mech}} \dot{r} + \mathbb{I}_{\mathrm{loc}}^{-1} p, \\
\dot{p} &= \mathbb{V}_{\mathrm{loc}} \left( A_{\mathrm{Stokes}} - A_{\mathrm{mech}} \right) \dot{r} + \mathbb{V}_{\mathrm{loc}} \, \mathbb{I}_{\mathrm{loc}}^{-1} p + \mathrm{ad}^*_{g^{-1}\dot{g}} \, p.
\end{aligned} \tag{4.6}$$

These equations describe the evolution of a system to which inertial effects and dissipative effects both pertain. We refer to such systems as *Rayleigh systems* to distinguish them from Lagrangian systems, which are conservative, and Stokesian systems, for which inertial effects are completely overwhelmed by dissipative forces.

In the inviscid limit, $\mathbb{V} \to 0$ above and (4.6) reduces to

$$g^{-1}\dot{g} = -A_{\text{mech}}\dot{r} + \mathbb{I}_{\text{loc}}^{-1} p,$$
$$\dot{p} = \text{ad}^*_{g^{-1}\dot{g}}\, p.$$

The latter equality is simply the conservation law $\dot{J} = 0$; if the momentum is zero initially it remains zero and the mechanical connection completely describes the evolution of the system

$$g^{-1}\dot{g} = -A_{\text{mech}}\dot{r}.$$

Premultiply the latter equality in (4.6) by $\mathbb{I}_{\text{loc}}\mathbb{V}_{\text{loc}}^{-1}$. The classical *Reynolds number* represents the ratio of inertial forces to viscous forces in a fluid system; the tensor $\mathbb{I}_{\text{loc}}\mathbb{V}_{\text{loc}}^{-1}$ extends this notion to the present situation. In the low Reynolds number limit, then, we allow $\mathbb{I}_{\text{loc}}\mathbb{V}_{\text{loc}}^{-1} \to 0$ to obtain

$$g^{-1}\dot{g} = -A_{\text{mech}}\dot{r} + \mathbb{I}_{\text{loc}}^{-1} p,$$
$$0 = \mathbb{I}_{\text{loc}} \left(A_{\text{Stokes}} - A_{\text{mech}}\right) \dot{r} + p,$$

or

$$g^{-1}\dot{g} = -A_{\text{Stokes}}\dot{r}.$$

The Stokes connection completely describes the evolution of the system.

### 4.2.2 The heavy inchworm

Consider the rectilinear motion of the inchworm-like robot depicted in Figure 4.2. The variables $l_r$, $l_h$, and $s_h$ denote the lengths of the rear segment of the robot in contact with the ground, the longitudinal span of the raised hump, and the arclength of the hump, resprectively. We assume the robot to have unit length overall. The variable $x$ denotes the displacement of the trailing edge with respect to a point fixed on the ground. The configuration of the system is specified as a point in a trivial

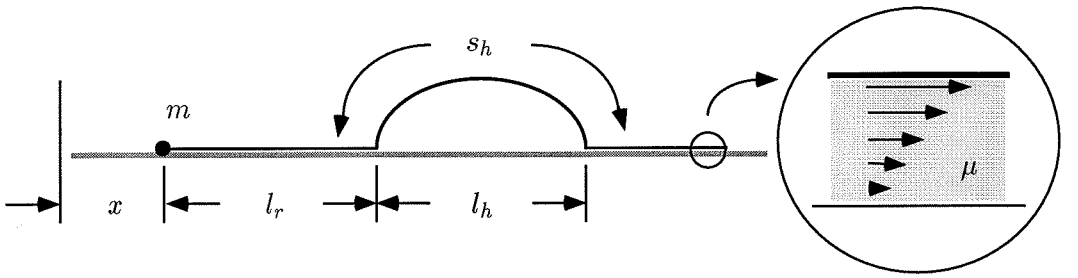


**Figure 4.2** An inchworm robot on a viscous film.

$(\mathbb{R}, +)$ bundle over the space of shapes $(l_r, l_h, s_h) \in U \subset \mathbb{R}^3$.

If we assume the mass $m$ of the robot to be concentrated at its trailing edge, its kinetic energy is given by

$$L = \frac{1}{2} m \dot{x}^2.$$

The locked inertia tensor is constant and the local mechanical connection null; the shape parameters $(l_r, l_h, s_h)$ may vary freely in the absence of dissipation with no effect on the displacement $x$. If we assume a uniformly thin, laminar, Newtonian fluid film between the robot and the ground, the horizontal sliding of a contact segment will be opposed by a force proportional to both the sliding velocity and the segment's length. The associated dissipation is captured (for a particular set of film parameters) by the Rayleigh dissipation function

$$R = \frac{1}{2} l_r \dot{x}^2 + \frac{1}{2} (1 - l_r - s_h) \left( \dot{x} + \dot{l}_h - \dot{s}_h \right)^2.$$

Thus

$$F = \mathbb{F}(-R) = -(1 - s_h)\, \dot{x} - (1 - l_r - s_h) \left( \dot{l}_h - \dot{s}_h \right)$$

and

$$\mathbb{V} = -(1 - s_h),$$

where each map from $\mathbb{R}$ to $\mathbb{R}$ is given by multiplication with the quantity shown. It follows that the local Stokes connection form is

$$A_{\text{Stokes}} = \frac{(1 - l_r - s_h)}{(1 - s_h)} (dl_h - ds_h) .$$

For this system, (4.6) assumes the form

$$\begin{aligned} \dot{x} &= \frac{p}{m}, \\ \dot{p} &= (1 - l_r - s_h) \left( \dot{s}_h - \dot{l}_h \right) - (1 - s_h) \frac{p}{m}, \end{aligned}$$

or

$$m\ddot{x} = (1 - l_r - s_h) \left( \dot{s}_h - \dot{l}_h \right) - (1 - s_h) \dot{x}.$$

This is precisely the statement that the robot's momentum changes at a rate equal to the sum of the viscous drag forces acting upon it. We note that the viscous interface between the robot and the ground could represent a set of wheels or tracks exhibiting viscous damping.

### 4.2.3 Extension to more general forces

Given any force field $F : TQ \to T^*Q$, we may define a map $\mathbb{V} : \mathfrak{g} \to \mathfrak{g}^*$ by

$$\langle \mathbb{V}(\xi), \eta \rangle = \langle F(\xi_Q), \eta_Q \rangle. \tag{4.7}$$

The addition of this force field to a system governed by a mechanical connection leads to equations of the form

$$\begin{aligned} g^{-1}\dot{g} &= -A_{\text{mech}}\, \dot{r} + \mathbb{I}_{\text{loc}}^{-1} p, \\ \dot{p} &= \Xi + \mathbb{V}_{\text{loc}} \mathbb{I}_{\text{loc}}^{-1} p + \text{ad}^*_{g^{-1}\dot{g}}\, p. \end{aligned}$$

If $F$ is not the derivative of a Rayleigh dissipation function, however, then (4.7) need not determine a tensorial map. The definition of the Stokes connection requires the

invertibility of this map. It is not clear that a system which evolves according to a general force balance may be described by a principal connection.

In Section 9.5.1, our model for the generation of lift on a moving hydrofoil will yield a force field $F : T\left(\mathbb{T}^2 \times \mathbb{R}\right) \to T^*\left(\mathbb{T}^2 \times \mathbb{R}\right)$ of the form

$$F\left(\phi, \psi, \dot{\phi}, \dot{\psi}, \dot{x}_m\right) = C\left(4B\dot{\phi}\cos\phi + D\dot{\psi}\cos\psi\right)\left(D\dot{\psi} + 4B\dot{\phi}\cos\left(\phi - \psi\right) - 4\dot{x}_m \sin\psi\right).$$

Here $B$, $C$, and $D$ are constants, $(\phi, \psi) \in \mathbb{T}^2$ parametrizes the shape of a propulsor, and $F$ is invariant with respect to translation in the fiber variable $x_m \in (\mathbb{R}, +)$. The system's kinetic energy

$$L\left(\dot{x}_m\right) = \frac{1}{2} m \dot{x}_m^2$$

is also invariant with respect to translations in $x_m$. The map $\mathbb{V} : \mathbb{R} \to \mathbb{R}$ given by

$$\mathbb{V}\left(\xi\right) = 0 \qquad \forall \xi \in \mathbb{R}$$

is clearly not invertible. The term in which the local Stokes connection appears in (4.6) is replaced, uninformatively, by $F$.

# Chapter 5

# Controllability and Related Issues

## 5.1 Definitions and tests

Given a finite-dimensional control system

$$\dot{x} = f(x, u^1, \ldots, u^m), \quad x \in M, \tag{5.1}$$

and a particular point $x_0 \in M$, we define $\mathcal{R}_T^V(x_0)$ to be the set of points in $M$ which are reachable from $x_0$ in time $t \leq T$ along trajectories which remain in the neighborhood $V \subset M$ of $x_0$. The system (5.1) is said to be *locally accessible* if, for all $x_0 \in M$, $\mathcal{R}_T^V(x_0)$ contains a non-empty open subset of $M$ for every choice of $T > 0$ and $V$. The system (5.1) is said to be *locally controllable* if, for all $x_0 \in M$, $x_0$ is interior to $\mathcal{R}_T^V(x_0)$ for every choice of $T > 0$ and $V$.

Given a control-affine system with drift

$$\dot{x} = f(x) + h_1(x)u^1 + \cdots + h_m(x)u^m, \tag{5.2}$$

we define the accessibility algebra $\mathfrak{C}$ to be the smallest subalgebra of $\mathfrak{X}(M)$ containing $f, h_1, \ldots, h_m$. The accessibility distribution $C$ on $M$ is then defined by

$$C(x) = \operatorname{span}\{X(x) | X \in \mathfrak{C}\}, \quad x \in M.$$

**Theorem 5.1** *If* $\dim C(x) = \dim T_xM$ *for all* $x \in M$, *then the system* (5.2) *is*

*locally accessible.*

This result, a consequence of Frobenius' theorem, is proved in [77] as the *Lie algebra rank condition* for accessibility.

Now suppose that $M = M_1 \times M_2$, and let $\pi : M \to M_1$ and $T\pi : TM \to TM_1$ denote the projection onto the first component of $M$ and its tangent map, respectively. Define the *restricted accessibility distribution* $T\pi C$ at $x_1 \in M_1$ by

$$T\pi C(x_1) = \text{span}\{T\pi X(x) | X \in \mathfrak{C}, x_1 = \pi(x)\}.$$

If $\dim T\pi C(x_1) = \dim T_{x_1} M_1$ for all $x_1 \in M$, we will refer to (5.2) as *locally* $M_1$ *accessible.* Loosely speaking, this property corresponds to accessibility of the system on $M_1$ without regard for the evolution of the system on $M_2$. Clearly, if the system on $M_1 \times M_2$ is locally accessible, it is locally $M_1$ accessible.

If $f = 0$ in (5.2), we are left with the *driftless* system

$$\dot{x} = h_1(x)u^1 + \cdots + h_m(x)u^m. \tag{5.3}$$

Local controllability and local accessibility are equivalent notions in the absence of drift, in which case Theorem 5.1 is equivalent to *Chow's theorem* [18]. A driftless system on $M = M_1 \times M_2$ which is locally $M_1$ accessible is said to be *locally* $M_1$ *controllable.*

## 5.2 Controllability for kinematic systems

### 5.2.1 Principal connections and Chow's theorem

Suppose that the locomotion of a robotic propulsor is governed by a single principal connection on the finite-dimensional trivial principal bundle $Q = M \times G$, and that this propulsor has complete authority over the rate at which it deforms. We may

then write the equations of motion as the driftless control system

$$\dot{q} = X_i^h u^i, \quad X_i = \frac{\partial}{\partial r^i}, \quad i = 1, \ldots, m. \tag{5.4}$$

In practice, we are often concerned with a robot's ability to position some end effector in its environment without regard for its internal configuration. We refer to a system on $Q = M \times G$ as *totally controllable* if it is locally $Q$ controllable, and *fiber controllable* if it is locally $G$ controllable. The special form of (5.4) allows us to restate Chow's theorem in terms of the local connection form $A$ and its curvature. Thus we define

$$\begin{aligned}
\mathfrak{h}_1 &= \text{span}\{A(X_i)\}, \\
\mathfrak{h}_2 &= \text{span}\{DA(X_i, X_j)\}, \\
\mathfrak{h}_3 &= \text{span}\{X_k DA(X_i, X_j) - [A(X_k), DA(X_i, X_j)]\}, \\
&\vdots \\
\mathfrak{h}_k &= \text{span}\{X_i \xi - [A(X_i), \xi], [\xi, \eta], \xi \in \mathfrak{h}_{k-1}, \eta \in \mathfrak{h}_2 + \cdots + \mathfrak{h}_{k-1}\}
\end{aligned} \tag{5.5}$$

and realize the following result.

**Proposition 5.2** *The driftless system* (5.4) *is fiber controllable near* $q = (r, g) \in Q$ *if and only if*

$$\mathfrak{g} = \mathfrak{h}_1 + \mathfrak{h}_2 + \ldots$$

*there, and totally controllable near* $q \in Q$ *if and only if*

$$\mathfrak{g} = \mathfrak{h}_2 + \mathfrak{h}_3 + \ldots$$

*there.*

*Proof:* The proof amounts to computing the fiber components of the elements of $\mathfrak{C}$ at each level of Jacobi-Lie bracketing. If the projections onto $T_g G$ of the elements of $C(q)$ span $T_g G$, the system is fiber controllable. The base components of

the input vector fields $X_i$ will not survive the first level of bracketing. Total controllability therefore requires fiber controllability in the absence of the unbracketed contributions to $C(q)$.

Note, first of all, that the Jacobi-Lie bracket

$$[X_i, X_j] = \left[\frac{\partial}{\partial x_i}, \frac{\partial}{\partial x_j}\right]$$

of any two input vector fields on $M$ is null. By (2.11), then

$$\mathrm{hor}[X_i^h, X_j^h] = [X_i, X_j]^h = 0,$$

so $[X_i^h, X_j^h]$ is vertical. By (2.10), then

$$[X_i^h, X_j^h] = \Gamma_Q\left([X_i^h, X_j^h]\right);$$

it follows from (2.4), (2.13), (2.12), and (2.16) that

$$\begin{aligned}
T\pi_G[X_i^h, X_j^h] &= \left(\Gamma[X_i^h, X_j^h]\right) g \\
&= \left(X_i^h\Gamma(X_j^h) - X_j^h\Gamma(X_i^h) - d\Gamma(X_i^h, X_j^h)\right) g \\
&= -\left(d\Gamma(X_i^h, X_j^h)\right) g \\
&= -g\,\mathrm{Ad}_{g^{-1}}\, d\Gamma(X_i^h, X_j^h) \\
&= -g\,\mathrm{Ad}_{g^{-1}}\, D\Gamma(X_i^h, X_j^h) \\
&= -g\,\mathrm{Ad}_{g^{-1}}\,\mathrm{Ad}_g\, DA(X_i, X_j) \\
&= -gDA(X_i, X_j).
\end{aligned}$$

The Jacobi-Lie brackets of control vector fields $X_i^h$ with one another thus contribute vertical vector fields to the accessibility algebra $\mathfrak{C}$ whose fiber projections correspond to elements in the range of the local curvature form.

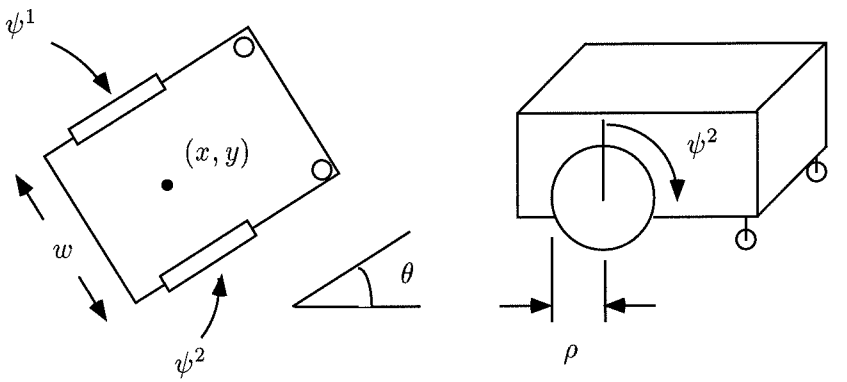


**Figure 5.1** A wheelchair on the plane.

If $Z$ is a vertical vector field such that $T\pi_G Z = -g\xi$ for some $\xi = \xi(r) \in \mathfrak{g}$, then

$$\begin{aligned} T\pi_G[X_i^h, Z] &= X_i(-g\xi) + [gAX_i, g\xi]_{JLG} \\ &= -g(X_i\xi - [AX_i, \xi]), \end{aligned}$$

where $[\cdot, \cdot]_{JLG}$ denotes the Jacobi-Lie bracket on $\mathfrak{X}(G)$. If $W$ is also a vertical vector field such that $T\pi_G W = -g\eta$ for $\eta = \eta(r) \in \mathfrak{g}$, then

$$T\pi_G[Z, W] = [g\xi, g\eta]_{JLG} = g[\xi, \eta].$$

We invoke the group invariance underlying (5.4) by assuming, without loss of generality, that $g = e$. Thus $T\pi G$ maps elements of $T_{(r,e)}Q$ to $\mathfrak{g}$, and the $i$th level of Jacobi-Lie bracketing in the construction of $C(r, e)$ amounts to the construction of $\mathfrak{h}_{i+1} \subset \mathfrak{g}$. ■

### 5.2.2 Local and global controllability of a wheelchair

Figure 5.1 depicts a wheelchair on a flat surface. The two wheels of radius $\rho$ are separated by a distance $w$ and rotate independently through angles $\psi^1$ and $\psi^2$. The midpoint of the axle connecting the wheels defines the point $(x, y)$ in the plane; the angle $\theta$ measures the net rotation of the wheelchair with respect to a fixed axis. The castors which support a real wheelchair contribute nothing to our planar model.

This system is referred to in [41] and elsewhere as the Hilare robot.

We assume the wheels to roll on the plane without slipping. Since the velocity of the point $(x, y)$ must remain parallel to the wheels,

$$\dot{x}\sin\theta - \dot{y}\cos\theta = 0.$$

Since neither wheel slips as it rotates,

$$\dot{x}\cos\theta + \dot{y}\sin\theta = \frac{\rho}{2}(\dot{\psi}^1 + \dot{\psi}^2)$$

and

$$\rho(\dot{\psi}^2 - \dot{\psi}^1) = w\dot{\theta}.$$

We derive a connection from these constraints as we derived the connection governing the motion of the car in Section 4.1.3. The local connection form $A : TM \to \mathfrak{se}(3) \approx \mathbb{R}^3$ is given by

$$A = \begin{bmatrix} -\frac{\rho}{2}(d\psi^1 + d\psi^2) \\ 0 \\ \frac{\rho}{w}(d\psi^1 - d\psi^2) \end{bmatrix},$$

where $M = \mathbb{T}^2$ is covered globally by coordinate pairs $(\psi^1, \psi^2)$. Its range is

$$\mathfrak{h}_1 = \text{span}\left\{ A_1 = \begin{bmatrix} -\frac{\rho}{2} \\ 0 \\ \frac{\rho}{w} \end{bmatrix}, A_2 = \begin{bmatrix} -\frac{\rho}{2} \\ 0 \\ -\frac{\rho}{w} \end{bmatrix} \right\}.$$

The range of the local curvature form

$$DA = \begin{bmatrix} 0 \\ \frac{\rho^2}{w} d\psi^1 \wedge d\psi^2 \\ 0 \end{bmatrix}$$

is

$$\mathfrak{h}_2 = \text{span}\left\{ DA_{12} = \begin{bmatrix} 0 \\ \frac{\rho^2}{w} \\ 0 \end{bmatrix} \right\}.$$

Since $\mathfrak{h}_1 + \mathfrak{h}_2 = \mathbb{R}^3$, the wheelchair is fiber controllable by Proposition 5.2. Since $A_1$, $A_2$, and $DA_{12}$ are all constant, (2.6) implies that no element of $\mathfrak{h}_2 + \mathfrak{h}_3 + \mathfrak{h}_4 + \ldots$ can have a nonzero third component. The wheelchair cannot, therefore, be totally controllable. Suppose that the wheelchair were to describe a circle in the plane such that the point $(x, y)$ travelled a distance $2\pi\varrho$. We define $\varrho$ to assume positive values for clockwise rotation. Such a maneuver would rotate the wheels through angles

$$\Delta\psi^1 = \frac{2\pi}{\rho}\left(\varrho + \frac{w}{2}\right), \qquad \Delta\psi^2 = \frac{2\pi}{\rho}\left(\varrho - \frac{w}{2}\right).$$

It is tempting to think that one could reorient the wheels arbitrarily using a sequence of similar motions. At the completion of $n$ such maneuvers, however, it will always be the case that

$$\Delta\psi^1 - \Delta\psi^2 = \frac{2\pi}{\rho} nw.$$

We shall see in Chapter 6 that noncontractible loops in shape space can make only limited contributions to locomotion on an Abelian bundle.

## 5.3 Accessibility for Rayleigh systems

### 5.3.1 Accessibility modulo momentum

The introduction of viscous dissipation to (5.4) yields the control-affine system with drift

$$\begin{bmatrix} \dot{r} \\ \ddot{r} \\ \dot{g} \\ \dot{p} \end{bmatrix} = \begin{bmatrix} 0 \\ e_1 \\ 0 \\ 0 \end{bmatrix} u^1 + \cdots + \begin{bmatrix} 0 \\ e_m \\ 0 \\ 0 \end{bmatrix} u^m$$

$$+ \begin{bmatrix} \dot{r} \\ 0 \\ g(-A_{\text{mech}}\dot{r} + \mathbb{I}_{\text{loc}}^{-1} p) \\ \mathbb{V}_{\text{loc}}(A_{\text{Stokes}} - A_{\text{mech}})\dot{r} + \mathbb{V}_{\text{loc}}\mathbb{I}_{\text{loc}}^{-1} p + \text{ad}^*_{g^{-1}\dot{g}}\, p \end{bmatrix}$$

$$= h_1 u^1 + \cdots + h_m u^m + f(r, \dot{r}, g, p). \tag{5.6}$$

The expression $e_i$ refers to the $i$th vector in the standard basis for $\mathbb{R}^m$. The inputs $u^i$ to the system are accelerations in the shape variables; we assume sufficient control of any base dynamics through internal forces to justify this model.

In the absence of dissipation, this system reduces to the driftless system

$$\begin{bmatrix} \dot{r} \\ g^{-1}\dot{g} \end{bmatrix} = \begin{bmatrix} e_1\, v^1 \\ -A_{\text{mech}} e_1 v^1 \end{bmatrix} + \cdots + \begin{bmatrix} e_m\, v^m \\ -A_{\text{mech}} e_m v^m \end{bmatrix} \tag{5.7}$$

as described in Section 4.2. Here we view the controls $v^i$ as entering at the level of velocities in the shape variables, integrating the controls $u^i$ once with respect to time.

**Proposition 5.3** *If the system without dissipation* (5.7) *on* $M \times G$ *is totally con-*

*trollable, the system with dissipation* (5.6) *on* $TM \times G \times \mathfrak{g}^*$ *is locally* $TM \times G$ *accessible, or* accessible modulo momentum.

*Proof:* This result follows from direct examination of the algebra generated by the vectors $f, h_1, \ldots, h_m$ in (5.6) and the projections of its elements from $T(TM \times G \times \mathfrak{g}^*)$ to $T(TM \times G)$. Note, first of all, that the $h_i$ have nonzero components only in the $\ddot{r}^i$ directions. The $m$ vectors $\alpha_i = [f, h_i]$ take the form

$$\alpha_i = [f, h_i] = \begin{bmatrix} e_i \\ 0 \\ -gA_{\text{mech}}\frac{\partial}{\partial r^i} \\ * \end{bmatrix}.$$

All additional elements of the subalgebra generated by the $\alpha_i$, furthermore, take the form

$$\begin{bmatrix} 0 \\ 0 \\ \zeta \\ ** \end{bmatrix},$$

where the group velocities $\zeta$ are precisely those corresponding to the Lie algebra elements in $\mathfrak{h}_2 + \mathfrak{h}_3 + \ldots$. Let $\mathfrak{C}$ be the accessibility algebra for the system (5.6). We define $\mathfrak{C}_{\text{mech}}$ to be the subalgebra of $\mathfrak{C}$ spanned by $f$, $h_1, \ldots, h_m$, and the algebra generated by $\alpha_1, \ldots, \alpha_m$; we define $C_{\text{mech}}(r, \dot{r}, g, p)$ by

$$C_{\text{mech}}(r, \dot{r}, g, p) = \text{span}\{X(r, \dot{r}, g, p) | X \in \mathfrak{C}_{\text{mech}}\}.$$

If $\pi : M \times G \times \mathfrak{g}^* \to M \times G$, clearly $T\pi C_{\text{mech}}(r, \dot{r}, g) \subset T\pi C(r, \dot{r}, g)$ for all $(r, \dot{r}, g) \in TM \times G$. If (5.7) is totally controllable, $\mathfrak{g} = \mathfrak{h}_2 + \mathfrak{h}_3 + \ldots$ and

$$\dim T\pi C_{\text{mech}}(r, \dot{r}, g) = \dim T_{(r,\dot{r},g)}(TM \times G).$$

Then

$$\dim T\pi C(r,\dot{r},g) = \dim T_{(r,\dot{r},g)}(TM \times G)$$

and (5.6) is locally $TM \times G$ accessible. ■

### 5.3.2 A vehicle with two internal rotors

Consider a rigid satellite in space with internal rotors about two of its principal axes. The orientations of the rotors with respect to the satellite body may be taken together as a pair $(\phi^1, \phi^2) \in \mathbb{T}^2$; the full configuration of the satellite is specified as a point in a trivial $SO(3)$ bundle over the torus. We think of this as a locomotion system in which the angular velocities of the rotors relative to the satellite are specified to effect desired satellite reorientations. The angular momentum of the system is invariant under reorientation; conservation of momentum provides a mechanical connection on the configuration bundle. This system is considered in this context in [60].

Identifying $\mathfrak{so}(3)$ with $\mathbb{R}^3$ in the usual way, we may represent the span of the range of the local connection form $A_{\text{mech}} : T(\mathbb{T}^2) \to \mathbb{R}^3$ as

$$\mathfrak{h}_1 = \text{span}\{e_1, e_2\},$$

where $\{e_1, e_2, e_3\}$ is the standard basis for $\mathbb{R}^3$. The range of $A$ is independent of $\phi^1$ and $\phi^2$ because the satellite's inertia is unchanged by the motion of the rotors. The Lie bracket on $\mathfrak{so}(3)$ is equivalent to the cross product on $\mathbb{R}^3$, and the range of the local curvature form is given by

$$\mathfrak{h}_2 = \text{span}\{e_1 \times e_2\} = \text{span}\{e_3\};$$

similarly

$$\begin{aligned}\mathfrak{h}_3 &= \text{span}\{e_1 \times e_3, e_2 \times e_3\} \\ &= \text{span}\{e_2, e_1\}.\end{aligned}$$

Since $\mathfrak{g} = \mathfrak{h}_2 + \mathfrak{h}_3$, the system is totally controllable according to Proposition 5.2.

A device similar to this satellite might be implemented as an underwater vehicle with torque control of the rotors. It follows from Proposition 5.3 that any model for its behavior which assumes linear drag will be accessible modulo momentum. Standard models for underwater vehicles incorporate drag of this sort. Note also that the attitude of an underwater vehicle has been adjusted about one principal axis experimentally using thrusters to provide torque about the other two [50].

### 5.3.3 The heavy inchworm revisited

In order to emphasize that the conditions of Proposition 5.3 are sufficient but not necessary for accessibility modulo momentum, we return to the inchworm robot from Section 4.2.2. Since $A_{\text{mech}} = 0$, this system clearly fails to satisfy the conditions of Propositions 5.2 and 5.3. Straightforward application of Theorem 5.1, however, reveals that the system is actually locally accessible, and thus accessible modulo momentum, near any configuration for which $(1 - l_r - s_h) \neq 0$.

# Chapter 6

# Gaits for Kinematic Systems

## 6.1 Definitions

Propulsors which deform themselves in order to move often do so cyclically. Indeed, it is dubious motile progress which requires a permanent change in body shape. We define a *gait* to be a time-parametrized cyclic shape change, or a map $\gamma : I \to M : t \mapsto r(t)$ from some interval $I \subset \mathbb{R}$ into a shape manifold $M$. Reparametrization with respect to time constitutes an equivalence relation on a set of gaits; a gait class $[\gamma]$ contains all gaits which determine the same loop in $M$.

In Chapter 2 we observed the parametrization invariance of the geometric phase associated with a closed loop in the base space of a principal bundle. We use the terms "gait" and "gait class" interchangeably in discussing kinematic systems.

Two gaits $\gamma_1, \gamma_2 : I \to M$ are said to be *homotopic* if there exists a smooth map $H : I \times [0,1] \to M$ such that $H(t,0) = \gamma_1(t)$ and $H(t,1) = \gamma_2(t)$ for all $t \in I$. Homotopy determines an equivalence relation [62]; the set of equivalence classes of loops passing through $r \in M$ constitutes the *fundamental group* of $M$ with respect to $r$ under composition. A gait $\gamma$ is said to be *null homotopic* if it is homotopic to a *null gait* $g_0 : I \to M : t \mapsto r_0$, where $r_0 \in M$ is fixed.

## 6.2 Systems on Abelian bundles

Recall from Section 2.5.1 that if the dimension of the infinitesimal holonomy group $\mathcal{H}_{\text{inf}}(q)$ corresponding to a connection on a principal bundle is constant throughout the total space $Q$, then the holonomy groups $\mathcal{H}_{\text{inf}}(q)$, $\mathcal{H}_{\text{loc}}(q)$, and $\mathcal{H}_{\text{rest}}(q)$ are equal throughout $Q$. Comparing (2.18) to (5.5), we see that

$$\mathfrak{h}_{\text{inf}} = \mathfrak{h}_2 + \mathfrak{h}_3 + \dots$$

if $\mathfrak{g}$ is Abelian, and we recognize the following.

**Corollary 6.1** *If the infinitesimal holonomy group $\mathcal{H}_{inf}(q)$ corresponding to a connection on a principal bundle has constant dimension throughout the total space $Q = M \times G$, and the Lie algebra $\mathfrak{g}$ is Abelian, then the associated locomotion system* (5.4) *is totally controllable near $q = (r, g)$ if and only if $\mathfrak{h}_{rest}(r, e) = \mathfrak{g}$.*

In other words, we need only consider null homotopic gaits in steering a system on an Abelian bundle.

## 6.3 Inchworm gaits

We now return to the inchworm robot from Section 4.2.2. If we assume $m$ to be zero, self-propulsion of the robot in the $x$ direction is governed by the Stokes connection

$$\begin{aligned}\Gamma_{\text{Stokes}} &= dx + A_{\text{Stokes}} \\ &= dx + \frac{(1 - l_r - s_h)}{(1 - s_h)}(dl_h - ds_h).\end{aligned}$$

Three qualitatively distinct families of gaits for this robot correspond to holding fixed each of the shape parameters $l_r$, $l_h$, and $s_h$. Figure 6.1 depicts gaits corresponding to constant $l_r$ and constant $l_h$.

Figure 6.2 depicts a "caterpillar" gait corresponding to constant $s_h$. The robot lifts and buckles its trailing end, replacing its hind tip with some forward displacement. The arched segment then passes the length of the robot's body to its forward

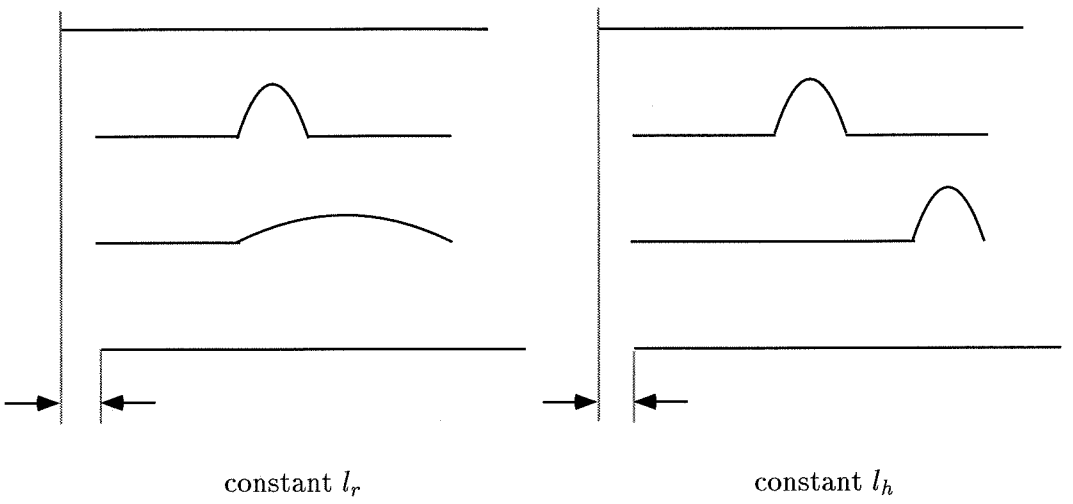


**Figure 6.1** Two types of gaits for the inchworm.

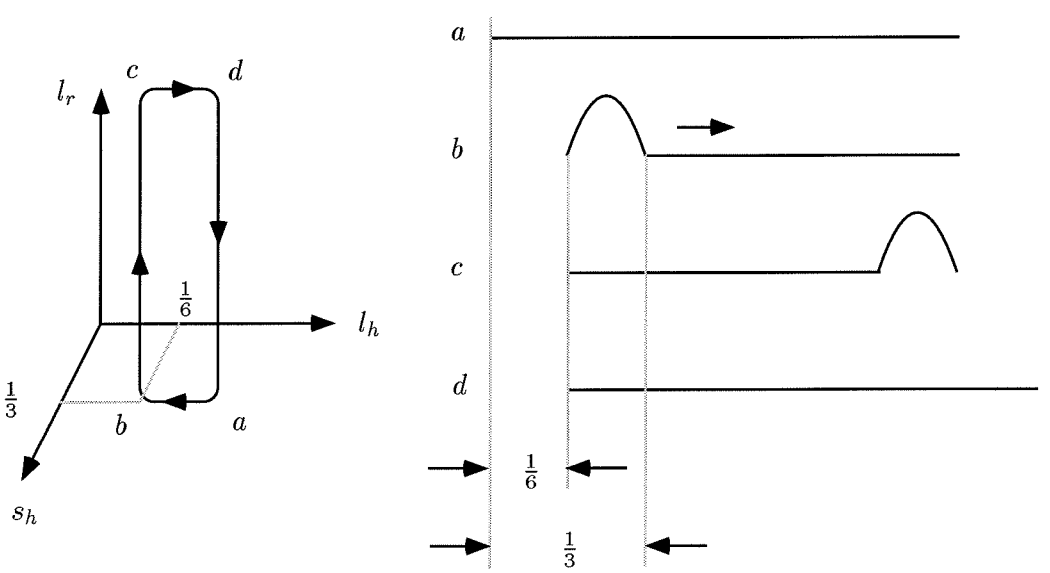


**Figure 6.2** The caterpillar gait.

tip, and the robot re-extends in its new location. At no point does any portion of the robot drag along or exert a tangential force upon the ground. Because our parametrization of the robot's shape suggests constant contact with the ground at both ends, we regard the lifted buckling and unbuckling motions as if segments of zero length were being dragged. We demonstrate the utility of the area rule from Section 2.5.2 in computing the associated geometric phase.

If $x(0) = 0$ and the robot assumes the sequence of configurations represented in Figure 6.2 in time $T$, the net linear displacement of its rearmost point is

$$x(T) = \exp\left(-\int_\gamma A_{\text{Stokes}}\right).$$

Since

$$\begin{aligned}\int_\gamma A_{\text{Stokes}} &= \int_\gamma \frac{(1 - l_r - s_h)}{(1 - s_h)}(dl_h - ds_h) \\ &= \int_{1/3}^{1/6} dl_h \\ &= -\frac{1}{6}\end{aligned}$$

and the exponential map on $(\mathbb{R}, +)$ is the identity,

$$x(T) = \frac{1}{6}.$$

Since we measure the robot's progress in terms of the displacement of its hind tip, the integrals corresponding to three of this maneuver's four stages evaluate to zero identically.

Since $(\mathbb{R}, +)$ is Abelian, the local curvature form is equal to the exterior derivative

$$\begin{aligned}dA_{\text{Stokes}} &= d\left(\frac{(1 - l_r - s_h)}{(1 - s_h)}\right) \wedge (dl_h - ds_h) \\ &= \frac{1}{1 - s_h}\left(-dl_r \wedge dl_h + dl_r \wedge ds_h + \frac{l_r}{1 - s_h} dl_h \wedge ds_h\right),\end{aligned}$$

and the geometric phase corresponding to the path shown in Figure 6.2 is indeed

$$\begin{aligned} x(T) &= \exp\left(\int_S \frac{1}{1-s_h}\, dl_r \wedge dl_h\right) \\ &= \exp\left(\int_{1/6}^{1/3}\int_0^{2/3} \frac{3}{2}\, dl_r dl_h\right) \\ &= \exp\left(\frac{1}{6}\right) \\ &= \frac{1}{6}. \end{aligned}$$

## 6.4 Local expansion of holonomy

If $\gamma : [0,T] \to M$, the corresponding geometric phase may be approximated by

$$g(T) = g(0)\exp\xi(\gamma),$$

where

$$\xi(\gamma) = -\frac{1}{2}DA_{ij}\int_\gamma dr^i dr^j + \frac{1}{3}(DA_{ij,k} + [DA_{ij}, A_k])\int_\gamma dr^i dr^j dr^k. \tag{6.1}$$

This formula is developed from (2.19) in [83]. Here

$$\int_\gamma dr^i dr^j = \int_0^T \left(\int_0^{t_j} \dot{r}^i(t_i)dt_i\right) \dot{r}^j(t_j)dt_j \tag{6.2}$$

and

$$\int_\gamma dr^i dr^j dr^k = \int_0^T \left(\int_0^{t_k} \left(\int_0^{t_j} \dot{r}^i(t_i)dt_i\right) \dot{r}^j(t_j)dt_j\right) \dot{r}^k(t_k)dt_k. \tag{6.3}$$

A system's full complement of gaits is often well represented, at least qualitatively, by those gaits which correspond to Lissajous figures in shape space. Such a figure may be characterized by its number of lobes. This number corresponds loosely to the degree of the Lie bracket of input vector fields capturing the gait's infinitesmal character.

If we confine ourselves to shape changes of the form

$$\begin{aligned} r^i(t) &= r^i(0) + R^i \sin n_i t \\ r^j(t) &= r^j(0) + R^j \sin n_j t \\ r^k(t) &= r^k(0) + R^k \sin n_k t \end{aligned}$$

and set $T = 2\pi$, we compute the integrals in (6.2) and (6.3) to be

$$\int_\gamma dr^i dr^j = 0$$

and

$$\int_\gamma dr^i dr^j dr^k = \begin{cases} -R^i R^j R^k \frac{\pi n_i}{2} & (n_i \neq n_j, n_i = n_j + n_k \text{ or } n_k = n_i + n_j) \\ R^i R^j R^k \frac{\pi n_j}{2} & (n_i \neq n_j, n_j = n_k + n_i) \\ -R^i R^j R^k \frac{\pi n_i}{2} & (n_i = n_j, n_k = 2n_i) \\ 0 & \text{otherwise} \end{cases} .$$

If, instead,

$$\begin{aligned} r^i(t) &= r^i(0) + R^i \cos n_i t - R^i \\ r^j(t) &= r^j(0) + R^j \sin n_j t \\ r^k(t) &= r^k(0) + R^k \sin n_k t \end{aligned} ,$$

we obtain

$$\int_\gamma dr^i dr^j = \begin{cases} 0 & n_i \neq n_j \\ R^i R^j n_i \pi & n_i = n_j \end{cases}$$

and

$$\int_\gamma dr^i dr^j dr^k = 0.$$

We compute the remaining possibilities for the case $n_i = n_j = n_k$ to be

$$SS = 0 \qquad CS = R^i R^j \pi$$
$$SC = -R^i R^j \pi \qquad CC = 0$$

and

$$SSS = 0 \qquad CSS = 0$$
$$SSC = 0 \qquad CSC = 2R^i R^j R^k \pi$$
$$SCS = 0 \qquad CCS = -R^i R^j R^k \pi$$
$$SCC = -R^i R^j R^k \pi \qquad CCC = 0 \quad .$$

Here the acronyms are constructed such that $SS$, $SSS$, $CS$, and $CSS$ refer to the cases already addressed.

## 6.5 Two-input systems

If we restrict ourselves to systems with only two shape variables, the effects of sinusoidal shape changes on $\xi(\gamma)$ may be elucidated by a *gait table.* The six columns on the right of Table 6.1 present data generic to two-input systems; the leftmost column specifies the terms appearing in $\xi(\gamma)$ for the wheelchair introduced in Section 5.2.2. We note that the top two rows in the table do not really correspond to terms appearing in $\xi(\gamma)$, but their inclusion completes the utility of the table for

approximating the effects of noncyclic deformations.

We illustrate the use of Table 6.1 by estimating the holonomy associated with two wheelchair gaits. Suppose the system satisfies $(x, y, \theta) = (0, 0, 0)$ initially, and assume the wheels of radius $\rho = 1/2$ to be separated by a distance $w = 1$. If the wheel angles vary as

$$\begin{bmatrix} \psi^1(t) \\ \psi^2(t) \end{bmatrix} = \begin{bmatrix} 0 \\ \frac{1}{5}t \end{bmatrix} + \text{constant terms},$$

Table 6.1 predicts a net motion in the plane

$$\begin{aligned} \begin{bmatrix} x(2\pi) \\ y(2\pi) \\ \theta(2\pi) \end{bmatrix} &= \exp\left( 2 \cdot \frac{1}{5} \cdot \pi \cdot \begin{bmatrix} 1/4 \\ 0 \\ 1/2 \end{bmatrix} \right) \\ &= \begin{bmatrix} \frac{1}{2}\sin\frac{\pi}{5} \\ \frac{1}{2}(1 - \cos\frac{\pi}{5}) \\ \pi/5 \end{bmatrix} \\ &\approx \begin{bmatrix} .2939 \\ .09549 \\ .6283 \end{bmatrix}. \end{aligned}$$

If we simulate the evolution of the system numerically, we obtain these same results with the precision shown. If, instead,

$$\begin{bmatrix} \psi^1(t) \\ \psi^2(t) \end{bmatrix} = \begin{bmatrix} \frac{1}{10}\sin 2t \\ \frac{7}{100}(\cos 2t - 1) \end{bmatrix},$$

| wheelchair example | terms in $\xi(\gamma)$ | $R^1 t$ <br> 0 | 0 <br> $R^2 t$ | $R^1 \sin nt$ <br> $R^2 \cos nt$ | $R^1 \cos nt$ <br> $R^2 \sin nt$ | $R^1 \cos nt$ <br> $R^2 \sin 2nt$ |
|---|---|---|---|---|---|---|
| $\begin{bmatrix} \rho/2 \\ 0 \\ -\rho/w \end{bmatrix}$ | $-A_1$ | $2R^1\pi$ | 0 | 0 | 0 | 0 |
| $\begin{bmatrix} \rho/2 \\ 0 \\ \rho/w \end{bmatrix}$ | $-A_2$ | 0 | $2R^2\pi$ | 0 | 0 | 0 |
| $\begin{bmatrix} 0 \\ -\rho^2/2w \\ 0 \end{bmatrix}$ | $-\frac{1}{2}DA_{12}$ | 0 | 0 | $-R^1R^2n\pi$ | $R^1R^2n\pi$ | 0 |
| $\begin{bmatrix} 0 \\ \rho^2/2w \\ 0 \end{bmatrix}$ | $-\frac{1}{2}DA_{21}$ | 0 | 0 | $R^2R^1n\pi$ | $-R^2R^1n\pi$ | 0 |
| $\begin{bmatrix} \rho^3/3w^2 \\ 0 \\ 0 \end{bmatrix}$ | $\frac{1}{3}(DA_{12,1}+$ <br> $[DA_{12}, A_1])$ | 0 | 0 | 0 | $2R^1R^2R^1n\pi$ | $-R^1R^2R^1n\pi$ |
| $\begin{bmatrix} -\rho^3/3w^2 \\ 0 \\ 0 \end{bmatrix}$ | $\frac{1}{3}(DA_{12,2}+$ <br> $[DA_{12}, A_2])$ | 0 | 0 | $-R^1R^2R^2n\pi$ | 0 | 0 |
| $\begin{bmatrix} -\rho^3/3w^2 \\ 0 \\ 0 \end{bmatrix}$ | $\frac{1}{3}(DA_{21,1}+$ <br> $[DA_{21}, A_1])$ | 0 | 0 | 0 | $-R^2R^1R^1n\pi$ | 0 |
| $\begin{bmatrix} \rho^3/3w^2 \\ 0 \\ 0 \end{bmatrix}$ | $\frac{1}{3}(DA_{21,2}+$ <br> $[DA_{21}, A_2])$ | 0 | 0 | $2R^2R^1R^2n\pi$ | 0 | 0 |

**Table 6.1** Gait table for two-input systems, $T = 2\pi$.

Table 6.1 predicts a net motion

$$\begin{bmatrix} x(2\pi) \\ y(2\pi) \\ \theta(2\pi) \end{bmatrix} = \exp\left( -\frac{1}{10}\cdot\frac{7}{100}\cdot 2\cdot\pi\cdot\begin{bmatrix} 0 \\ -1/8 \\ 0 \end{bmatrix} + \frac{7}{100}\cdot\frac{1}{10}\cdot 2\cdot\pi\cdot\begin{bmatrix} 0 \\ 1/8 \\ 0 \end{bmatrix} \right.$$
$$\left. -\frac{1}{10}\cdot\frac{7}{100}\cdot\frac{7}{100}\cdot 2\cdot\pi\cdot\begin{bmatrix} -1/24 \\ 0 \\ 0 \end{bmatrix} + 2\cdot\frac{7}{100}\cdot\frac{1}{10}\cdot\frac{7}{100}\cdot 2\cdot\pi\cdot\begin{bmatrix} 1/24 \\ 0 \\ 0 \end{bmatrix} \right)$$
$$= \exp\begin{bmatrix} 147\pi/120000 \\ 7\pi/2000 \\ 0 \end{bmatrix}$$
$$\approx \begin{bmatrix} .003848 \\ .01010 \\ .0000 \end{bmatrix},$$

while simulation returns

$$\begin{bmatrix} x(2\pi) \\ y(2\pi) \\ \theta(2\pi) \end{bmatrix} = \begin{bmatrix} .003846 \\ .01098 \\ .0000 \end{bmatrix}.$$

# Chapter 7

# Principal Connections and Swimming

## 7.1 Ideal flow and the hydromechanical connection

### 7.1.1 Potential flow

Though we deviate from certain sign conventions therein, we are guided by the development of potential flow theory in [68]. We realize the equations for potential flow as a simplification of Euler's equations for the motion of an inviscid fluid. We will derive Euler's equations in a moving frame as reduced Euler-Lagrange equations in Chapter 8.

Suppose a fluid with density $\rho(x,t)$ to occupy a region F. We denote the spatial velocity field describing the fluid's instantaneous motion by $u(x,t)$. Continuity of the fluid requires that

$$\frac{\partial \rho}{\partial t} + \nabla \cdot (\rho\, u) = 0 \tag{7.1}$$

at every point $x \in \mathrm{F}$. Equation (7.1) is often derived from the balance of mass flux through an arbitrary control volume. We consider only fluids of constant density. It is worth noting that the term *incompressible* is applied to any fluid which satisfies

$$\frac{\partial \rho}{\partial t} + u \cdot \nabla \rho = 0.$$

This is true identically if $\rho$ is constant. The operator

$$\frac{\partial}{\partial t} + u \cdot \nabla$$

is called the *Lagrangian derivative* or *material derivative* in the classical fluids literature. Intuitively, it returns the rate at which a particular fluid element (rather than a spatial point) experiences a change in some property. The classical shift from a Lagrangian perspective to an Eulerian perspective corresponds, in the setting of Chapter 8, to reduction with respect to a particle-relabelling symmetry.

For an incompressible fluid, continuity implies that

$$\begin{aligned} \frac{\partial \rho}{\partial t} + \nabla \cdot (\rho\, u) &= \frac{\partial \rho}{\partial t} + \rho\, \nabla \cdot u + u \cdot \nabla \rho \\ &= \rho\, \nabla \cdot u \\ &= 0. \end{aligned} \tag{7.2}$$

Thus $u$ is divergence free, or *solenoidal.* In a region occupied by an inviscid, incompressible fluid, the net force on an arbitrary control volume must equal the rate of change of the linear momentum contained therein. In the absence of external forces, this requires that

$$\frac{\partial u}{\partial t} + u \cdot \nabla u = -\frac{1}{\rho} \nabla p; \tag{7.3}$$

here $p(x,t)$ is the scalar *pressure.* We refer to (7.2) and (7.3) together as *Euler's equations* for inviscid flow.

A velocity field is said to be *irrotational* if

$$\nabla \times u = 0.$$

Using the vector identity

$$u \cdot \nabla u = \frac{1}{2} \nabla (u \cdot u) - u \times (\nabla \times u),$$

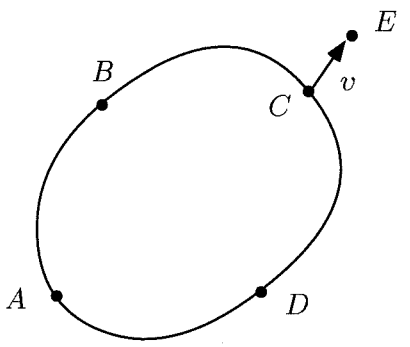


**Figure 7.1** Derivation of the potential function.

we may rewrite (7.3) as

$$\begin{aligned}\frac{\partial u}{\partial t} &= -u\cdot\nabla u - \frac{1}{\rho}\nabla p \\ &= -\frac{1}{2}\nabla(u\cdot u) + u\times(\nabla\times u) - \frac{1}{\rho}\nabla p \\ &= -\frac{1}{2}\nabla(u\cdot u) - \frac{1}{\rho}\nabla p \\ &= -\nabla\left(\frac{1}{2}u\cdot u + \frac{1}{\rho}p\right)\end{aligned} \tag{7.4}$$

in the case of irrotational flow.

Let $A$ be a fixed point, and $C$ an arbitrary point, in a simply connected region F containing an irrotational fluid. Join $A$ to $C$ along two different paths in F, as shown in Figure 7.1. At any point in time, by Stokes' Theorem,

$$\int_{ABC} u\,ds + \int_{CDA} u\,ds = \int_{\mathrm{S}} (\nabla\times u)\,n\,dS,$$

where S is any surface in F with $ABCDA$ as its rim and $n$ as its unit normal. If the motion of the fluid is irrotational, then

$$\int_{ABC} u\,ds = \int_{ADC} u\,ds = \phi_C(t),$$

where $\phi_C(t)$ is a function of the position of $C$ but not of the choice of path from $A$ to $C$. Now consider a point $E$ whose position relative to $C$ is given by the vector

$v$. In the limit as $E$ approaches $C$,

$$v\,\nabla\phi_C(t) = \int_{CE} u\,ds = vu.$$

The velocity field may therefore be written at any point in time as

$$u = \nabla\phi(x,t), \tag{7.5}$$

where $\phi(x,t)$ is called the *velocity potential.* Conversely, any velocity field which is the gradient of a potential function must be irrotational, since

$$\nabla \times (\nabla f) = 0$$

for any function $f : \mathrm{F} \to \mathbb{R}$.

We combine (7.4) and (7.5) to obtain

$$\nabla\left(\frac{\partial\phi}{\partial t} + \frac{1}{2}\,u\cdot u + \frac{1}{\rho}\,p\right) = 0,$$

or

$$\frac{\partial\phi}{\partial t} + \frac{1}{2}\,u\cdot u + \frac{1}{\rho}\,p = C(t). \tag{7.6}$$

This is called the *pressure equation. Bernoulli's theorem* [68] requires this relation to hold along each streamline in an inviscid flow; we have shown that it holds throughout an irrotational flow.

Equations (7.2) and (7.5) combine to recover *Laplace's equation*

$$\nabla^2\phi = 0. \tag{7.7}$$

Thus, plausable instantaneous irrotational motions of an inviscid fluid correspond to harmonic potential functions. If the fluid evolves in the presence of solid boundaries, it is furthermore the case that the velocity normal to any boundary must coincide

with the normal velocity of the boundary itself. In this way we rule out cavitation in potential flow, although the theory may be adjusted to accommodate such phenomena. We allow an inviscid fluid to slip along a solid boundary; in Section 7.2.1 we will impose an adherence condition upon the flow of a viscous fluid.

So far, we have considered irrotational flow in simply connected domains. Simple connectedness guarantees the uniqueness of the velocity potential $\phi$; when $\phi$ is unique the corresponding potential flow is said to be *acyclic*. Though a flow field $u$ must itself be single-valued in a multiply connected domain, the corresponding potential function satisfying (7.5) need be unique only up to an additive scalar $\kappa$ satisfying $\nabla\kappa = 0$. Multiple connectedness of a domain F corresponds to the existence of closed paths within F which are not null homotopic. The scalar $\kappa$ corresponding to a particular cyclic flow in a multiply connected domain may be identified with the circulation $\Gamma$ along any of a family of mutually homotopic closed paths in F which are not null homotopic. The circulation along an oriented closed path $\vartheta$ is defined to be

$$\Gamma = \int_{\vartheta} u\, ds.$$

In considering the self-propulsion of deformable bodies in planar irrotational flow, we often encounter *periphractic* regions, so called because they are bounded internally by closed surfaces. We restrict our discussion to acyclic flow in such regions by specifying the circulation to be zero around any contour which is not null homotopic. In Chapter 9 we will discuss the forces experienced by a hydrofoil about which the circulation changes with time.

The total kinetic energy of the fluid with constant density $\rho$ and velocity $u$ in a domain F is given by

$$\mathrm{KE} = \frac{1}{2}\rho \int_{\mathrm{F}} u \cdot u\, dx$$

when this integral converges. If the domain F is bounded by a surface S and the

fluid moves irrotationally and acyclicly, Stokes' theorem implies that

$$\begin{aligned} \mathrm{KE} &= \frac{1}{2}\rho \int_{\mathrm{F}} \nabla\phi \cdot \nabla\phi \, dx \\ &= -\frac{1}{2}\rho \int_{\mathrm{S}} \phi \frac{\partial \phi}{\partial n} \, dS, \end{aligned} \tag{7.8}$$

where $\partial\phi/\partial n$ is the velocity of the fluid normal to S on S. Several consequences of this result are outlined in [68]. We note, in particular, that the acyclic irrotational motion of a fluid which is bounded internally by an immersed solid and quiescent at infinity is determined uniquely by the motion of the solid. The motion of the fluid will cease instantly if the solid ceases to move, and is unchanged by reparametrizations of time.

### 7.1.2 Fluid momentum and Kelvin impluse

Suppose that a finite body with surface S moves through a fluid such that $u = \nabla\phi$ is acyclic. We define the *Kelvin impulse* of the fluid to be the vector quantity

$$I = \int_{\mathrm{S}} \phi \, n \, dS,$$

where $n$ is the outward unit vector normal to S on S. This quantity is often described as the impulsive force which would set the surface from rest into its present motion [43, 48]. We will see that it behaves as the effective momentum of the surface.

It is tempting to assume that the total fluid momentum

$$\rho \int_{\mathrm{F}} u \, dx$$

would serve as the effective momentum of a translating surface. This momentum is ill-defined, however, when the fluid fills a region of infinite extent. Consider the fluid occupying a region $\mathrm{V} \subset \mathrm{F}$ bounded by a surface $\Sigma$ with outward unit normal

$\varsigma$. In three dimensions, we may invoke the vector identity

$$\int_{\mathrm{V}} u\,dx = \frac{1}{2}\int_{\mathrm{V}} x \times \omega\,dx + \frac{1}{2}\int_{\Sigma} (u(\varsigma \cdot x) - \varsigma(u \cdot x))\,dS.$$

The surface integral is bounded generically as $\Sigma$ becomes infinitely large, but continues in this limit to depend upon the shape of $\Sigma$.

Using (7.6) and an identity from [88], however, we see that

$$\begin{aligned}
\frac{dI}{dt} &= \frac{d}{dt}\int_{\mathrm{S}} \phi\, n\,dS \\
&= \int_{\mathrm{S}} \frac{\partial \phi}{\partial t}\, n\,dS + \int_{\mathrm{S}} (u \cdot n)\nabla\phi\,dS \\
&= \int_{\mathrm{S}} \left( C(t) - \frac{1}{2}\, u \cdot u - \frac{1}{\rho} p \right) n\,dS + \int_{\mathrm{S}} (u \cdot n)\, u\,dS \\
&= \int_{\mathrm{S}} C(t)\, n\,dS - \frac{1}{\rho}\int_{\mathrm{S}} p\, n\,dS + \int_{\mathrm{S}} \left( (u \cdot n)\, u - (\frac{1}{2}\, u \cdot u)\, n \right) dS \\
&= 0 - \frac{1}{\rho}\int_{\mathrm{S}} p\, n\,dS - \int_{\mathrm{F}} u \times \omega\,dx \\
&= -\frac{1}{\rho}\int_{\mathrm{S}} p\, n\,dS
\end{aligned}$$

for irrotational flow. The integral on the right side of this equality represents the total force applied to the surface S by the fluid.

The *Kelvin impulse couple* is given by

$$I_C = \int_S \phi\, x \times n\,dS,$$

and behaves as the apparent angular momentum of the surface S. The Kelvin impulse and impulse couple are conserved as a closed surface moves through an irrotational fluid in the absence of external forces [69]. We note that certain authors define $I$ and $I_C$ to differ in sign from the integrals above. We will use the symbol $I$ below to denote the impulse and impulse couple together.

### 7.1.3 The hydromechanical connection

Suppose that the points in an $n$-dimensional manifold $M$ correspond to deformations of a closed flexible surface, and that this surface is immersed in an inviscid fluid which is initially at rest. As the surface deforms, tracing a path in $M$, it may displace and reorient itself with respect to its initial situation in the fluid. By affixing a frame of reference to each deformation represented in $M$, we identify the motion of the surface through its environment with a trajectory in $SE(3)$.

If we suppose the interior of the swimming surface to be evacuated, the kinetic energy shared by the swimmer and its environment is entirely contained in the fluid. We make this assumption for simplicity's sake; it is of little conceptual consequence to afford a swimming body some mass of its own. Since there exists no mechanism for the creation of vorticity in an inviscid fluid, the flow around the surface will remain irrotational and acyclic. The spatial velocity field $u$ will therefore constitute the gradient of a time-varying potential function $\phi$. The motion of the fluid must be determined uniquely by the motion of the surface. If $r(t) \in M$ denotes the shape of the surface at any point in time and $g(t) \in SE(3)$ its position and orientation, we may write

$$\phi = \phi\,(r, \dot{r}, g, \dot{g}).$$

The potential function $\phi$ must satisfy Laplace's equation together with two boundary conditions. The first, imposed by the impenetrability of the surface, requires agreement of the velocity of the fluid normal to the surface with that of the surface itself where they meet. The second, a consequence of the finite energy introduced to the fluid by the swimming surface, requires that the fluid remain at rest infinitely far away. The linearity of Laplace's equation allows us to superpose solutions to satisfy Neumann boundary conditions. The distribution of velocity on a swimming surface constitutes the sum of its deformation velocity and the velocities

of its displacement. It follows that

$$\phi = \phi_d(r, \dot{r}) + \phi_i(r) \left(g^{-1}\dot{g}\right)^i,$$

where $g^{-1}\dot{g}$ is the velocity of displacement in a body-fixed frame. The function $\phi_d$ is called the *deformation potential* and the functions $\phi_i$ the *Kirchhoff potentials.*

The total kinetic energy

$$\mathrm{KE} = \frac{1}{2}\rho \int_{\mathrm{F}} \nabla\phi\left(r, \dot{r}, g^{-1}\dot{g}\right) \cdot \nabla\phi\left(r, \dot{r}, g^{-1}\dot{g}\right) dx$$

determines a function $L : TQ \to \mathbb{R}$, where $Q = M \times SE(3)$, which is invariant with respect to left translation in $SE(3)$. The Kelvin impulse and impulse couple comprise the components of the corresponding momentum map, which takes values in $\mathfrak{se}(3)^* \approx \mathbb{R}^6$. Their conservation is thus a consequence of Noether's theorem. The locked inertia tensor represents the *virtual inertia* of the swimming surface. Were the surface replaced by a body with nonzero inertia of its own, this inertia would combine with its virtual counterpart to constitute the body's *apparent inertia.*

The connection

$$\Gamma_{\mathrm{mech}} = \mathbb{I}^{-1} I$$

is a true mechanical connection since it is derived from the total kinetic energy. In considering the swimming of a body with nonzero mass, however, one must take care not to confuse the mechanical connection obtained from the total kinetic energy with that obtained from the kinetic energy of the body alone. It is the latter which arose in the control analysis of the vehicle in Section 5.3.2. When there is danger of confusion, we refer to the former as the *hydromechanical connection.*

## 7.2 Creeping flow and the Stokes connection

### 7.2.1 Stokes flow

The evolution of an incompressible, viscous fluid is governed by the *Navier-Stokes equations*

$$\frac{\partial u}{\partial t} + u \cdot \nabla u + \frac{1}{\rho}\nabla p - \nu \nabla^2 u = 0, \qquad \nabla \cdot u = 0, \tag{7.9}$$

which are derived in [68] and elsewhere. The *absolute viscosity* of the fluid is given by $\mu = \rho\nu$, where $\nu$ denotes its *kinematic viscosity* and $\rho$ its density. The vector Laplacian is given by

$$\nabla^2 u = \nabla(\nabla \cdot u) - \nabla \times (\nabla \times u).$$

Energy is dissipated from the flow of a viscous fluid in a domain F at a rate

$$R = \frac{1}{2}\mu \int_{\mathrm{F}} \Phi \, dx, \tag{7.10}$$

where the quantity

$$\Phi = (\nabla \times u) \cdot (\nabla \times u) + 2\nabla \cdot \left(\frac{1}{2}\nabla |u|^2 - u \times \nabla \times u\right)$$

is integrated over the entire fluid. We restrict a viscous fluid in contact with a solid boundary to move with the boundary tangentially as well as normally. In general, *Navier slip boundary conditions* [21] permit some tangential motion between a viscous fluid and a solid boundary. We adopt the most common, "no slip" convention.

If we allow $\nu \to 0$ in (7.9), we recover Euler's equations. If, instead, we multiply (7.9) by $\rho$ and neglect inertial terms, we obtain Stokes' equations

$$\nabla p = \mu \nabla^2 u, \qquad \nabla \cdot u = 0 \tag{7.11}$$

for creeping flow. This simplification is equivalent to nondimensionalizing (7.9) and

taking the formal limit as $\mathrm{Re} \to 0$, where the Reynolds number $\mathrm{Re} = UL/\nu$ is defined in terms of a characteristic velocity $U$ and length $L$ [15]. The left-hand equality in (7.11) represents the balance of pressure forces and viscous forces on every fluid element. Note that (7.11) imply that

$$\nabla^2 p = 0;$$

the distribution of pressure in an inertialess flow is harmonic. Like potential flow, Stokes flow is characterized by the instantaneous diffusion of momentum [15]. The applicability of Stokesian analysis to the swimming of aquatic microorganisms is demonstrated in [53].

We often consider problems in which creeping flows exhibit one-dimensional symmetries. A problem in which no more than two spatial variables are needed to describe the velocity field can be solved using an appropriate *stream function* [19]. For planar flow, we introduce the Lagrange stream function $\psi(t)$ such that (in polar coordinates)

$$u_r = -\frac{1}{r}\frac{\partial \psi}{\partial \theta}, \qquad u_\theta = \frac{\partial \psi}{\partial r}.$$

This velocity field will correspond to a solution of Stokes' equations provided

$$\nabla^4 \psi = 0. \tag{7.12}$$

For axisymmetric flow, we introduce the Stokes stream function $\Psi(t)$ such that (in cylindrical coordinates, where the $z$ axis is the axis of symmetry)

$$u_r = \frac{1}{r}\frac{\partial \Psi}{\partial z}, \qquad u_z = -\frac{1}{r}\frac{\partial \Psi}{\partial r}.$$

This flow field will satisfy Stokes' equations provided

$$E^4 \Psi = 0,$$

where

$$E^4 = \left( \frac{\partial^2}{\partial r^2} - \frac{1}{r}\frac{\partial}{\partial r} + \frac{\partial^2}{\partial z^2} \right)^2 .$$

We note that not all solutions to Stokes' equations may be obtained from stream functions [15]. We note, also, that these equations represent only the simplest model for real creeping flow. A good discussion of Oseen's improvement to this model, itself fettered by some practical shortcomings, appears in [48].

### 7.2.2 The Stokes connection

Just as the flow around a surface in an irrotational fluid is determined uniquely by the deformation and displacement of the surface, so too is the Stokes flow around such a surface recaptured by (7.11). If $r \in M$ again denotes the shape of the surface and $g \in SE(3)$ its position and orientation, the dissipation function defined by (7.10) may be written as

$$R(r, \dot{r}, g, \dot{g}) = \frac{1}{2}\mu \int_{\mathrm{F}} \Phi(r, \dot{r}, g^{-1}\dot{g})\, dx.$$

The fiber-preserving map $F = \mathbb{F}(-R) : TQ \to T^*Q$, where $Q = M \times SE(3)$, is a force field in the sense of Section 3.1.3. In the Stokesian limit, the absence of inertial effects requires the net fiberwise drag on a deforming surface to remain zero at every instant.

In two dimensions, we encounter some difficulty related to *Stokes' paradox*, the nonexistence of a planar Stokes flow about a translating body which tends to zero at infinity. In attempting to compute the drag on such a body, we consider the drag per unit length on a long cylinder translating perpendicular to its axis through a three-dimensional medium. While this result is not well defined as the cylinder's length becomes infinite, we find it to remain linear through successive approximations in the fluid velocity persistant infinitely far away [48, 53]. When studying the Stokesian swimming of a surface in the plane, we therefore assume $F : TQ \to T^*Q$ to take the

form

$$F_i(q, \dot{q}) = C_{ij}(r)\, U^j_\infty,$$

where $U_\infty(r, \dot{r}, g^{-1}\dot{g})$ is the fluid velocity at infinity resulting from the body's motion.

## 7.3 Squirming circles

We illustrate the hydromechanical and Stokes connections with a pair of related examples. Consider the infinitely long, approximately circular cylinder whose time-varying cross-section is given in polar coordinates by

$$r(t, \theta) = 1 + \epsilon \left(k^1(t) \cos 2\theta + k^2(t) \cos 3\theta\right),$$

where $\epsilon$ is a small parameter. We imagine this cylinder to "float" freely in an infinite fluid medium with constant density $\rho = 1$. We may regard the flow in the periphractic region around such a cylinder as two-dimensional, and study its evolution in any plane perpendicular to the cylinder's longitudinal axis. We assume the interior of the cylinder to be massless, and consider the self-propulsion of the cylinder due to appropriate time-variations in $k^1$ and $k^2$.

It is clear from the bilateral symmetry of the problem that any such swimming motion will be rectilinear and parallel (or antiparallel) to the ray $\theta = 0$. We define the coordinate $x$ to measure the displacement in this direction of the $(r, \theta)$-origin, as shown in Figure 7.2. We regard the configuration $(k^1, k^2, x)$ of the system at any moment as a point in the trivial principal bundle $Q = M \times (\mathbb{R}, +)$, where $M$ is the submanifold of $\mathbb{R}^2$ corresponding to physically reasonable pairs $(k^1, k^2)$.

Suppose the cylinder to move with velocity $\dot{x}$ through an incompressible, inviscid fluid. This velocity is determined by the mechanical connection on the bundle $Q$ derived from the total kinetic energy of the fluid. We approximate this connection

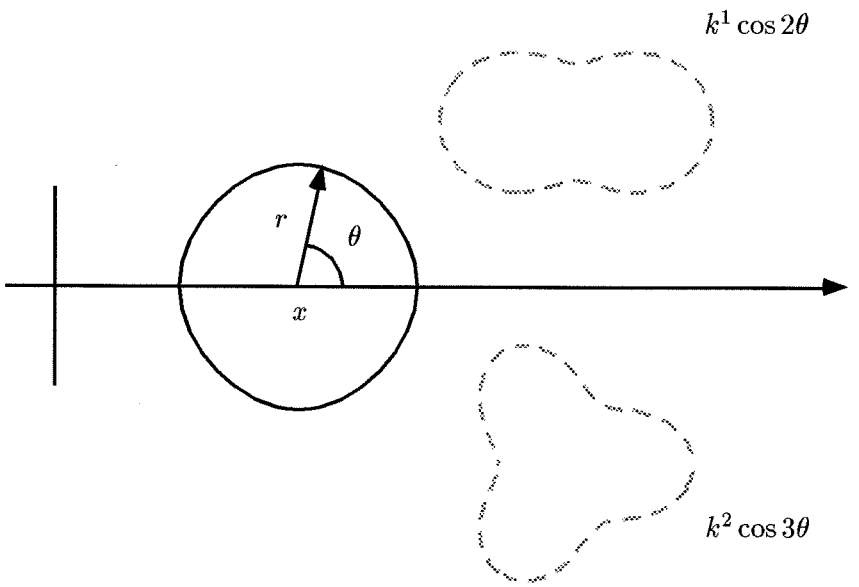


**Figure 7.2** A squirming circle.

using regular perturbation theory, seeking a solution of the form

$$\phi = \phi_0 + \epsilon\phi_1 + \epsilon^2\phi_2 + \dots$$

to the Neumann problem

$$\nabla^2\phi = 0,$$
$$\left.\frac{\partial\phi}{\partial n}\right|_{r=R} = (\dot{x}\cos\theta, -\dot{x}\sin\theta)\cdot n + \left(\epsilon\dot{k}^1\cos 2\theta + \epsilon\dot{k}^2\cos 3\theta, 0\right)\cdot n.$$

We obtain

$$\phi = \phi_0 + \epsilon\phi_1 + \epsilon^2\phi_2 + O\left(\epsilon^3\right),$$

where

$$\phi_0 = -\dot{x} r^{-1} \cos\theta,$$

$$\phi_1 = k^1 \dot{x} r^{-1} \cos\theta + \frac{1}{2}\left(2k^2\dot{x} - \dot{k}^1\right) r^{-2}\cos 2\theta - \frac{1}{3}\left(3k^1\dot{x} + \dot{k}^2\right) r^{-3}\cos 3\theta$$

$$- k^2 \dot{x} r^{-4} \cos 4\theta,$$

$$\phi_2 = c_0 \log r - c_1 r^{-1}\cos\theta - \cdots - \frac{c_7}{7} r^{-7}\cos 7\theta,$$

$$c_0 = \frac{k^1\dot{k}^1}{2} + \frac{k^2\dot{k}^2}{2},$$

$$c_1 = k^1\dot{k}^2 + \frac{3k^1k^1\dot{x}}{2} + \frac{5k^2k^2\dot{x}}{2},$$

$$c_2 = 4k^1k^2\dot{x},$$

$$c_3 = -\frac{3k^1k^1\dot{x}}{4},$$

$$c_4 = \frac{5k^1\dot{k}^1}{2} - 4k^1k^2\dot{x},$$

$$c_5 = 3\dot{k}^1k^2 + 3k^1\dot{k}^2 + \frac{25k^1k^1\dot{x}}{4} - \frac{15k^2k^2\dot{x}}{4},$$

$$c_6 = \frac{7k^2\dot{k}^2}{2} + 18k^1k^2\dot{x},$$

$$c_7 = \frac{49k^2k^2\dot{x}}{4}.$$

The total kinetic energy is therefore given by

$$\begin{aligned} L &= \frac{1}{2}\int_0^{2\pi}\int_r^{\infty} |\nabla\phi|^2\, r\, dr\, d\theta \\ &= \frac{1}{2}\pi\dot{x}^2 - \epsilon\pi k^1\dot{x}^2 \\ &\quad + \epsilon^2\pi\left(\frac{\dot{k}^1\dot{k}^1}{4} + \frac{\dot{k}^2\dot{k}^2}{6} + \dot{x}\left(k^1\dot{k}^2 - k^2\dot{k}^1\right) + \frac{\dot{x}^2}{4}\left(5k^1k^1 + 9k^2k^2\right)\right) + O(\epsilon^3), \end{aligned}$$

and is unchanged by displacement of the cylinder along its axis of propulsion. The momentum map $J : TQ \to \mathbb{R}$ and the locked inertia tensor $\mathbb{I} : \mathbb{R} \to \mathbb{R}$ are given by

$$J = \pi\dot{x} - 2\epsilon\pi k^1\dot{x} + \epsilon^2\pi\left(k^1\dot{k}^2 - k^2\dot{k}^1 + \frac{\dot{x}}{2}\left(5k^1k^1 + 9k^2k^2\right)\right) + O\left(\epsilon^3\right)$$

and

$$\mathbb{I}\left(k^1, k^2\right) : \xi \mapsto \pi\xi\left(1 - 2\epsilon k^1 + \frac{\epsilon^2}{2}\left(5k^1k^1 + 9k^2k^2\right)\right) + O\left(\epsilon^3\right),$$

and the connection $\Gamma_{\text{mech}} : TQ \to \mathbb{R}$ by

$$\Gamma_{\text{mech}} = \mathbb{I}^{-1}J = dx + \epsilon^2\left(k^1\, dk^2 - k^2\, dk^1\right) + O\left(\epsilon^3\right).$$

Self-propulsion of the cylinder is governed by the requirement that its velocity on configuration space remain horizontal with respect to this connection. Thus

$$\dot{x} = \epsilon^2\left(k^2\dot{k}^1 - k^1\dot{k}^2\right) + O\left(\epsilon^3\right).$$

We compute the $x$ component of the Kelvin impulse to be

$$\int_{\mathcal{S}} \phi\, n_x\, dS = -\pi\dot{x} + 2\epsilon\pi k^1\dot{x} - \epsilon^2\pi\left(k^1\dot{k}^2 - k^2\dot{k}^1 + \frac{\dot{x}}{2}\left(5k^1k^1 + 9k^2k^2\right)\right) + O(\epsilon^3).$$

This quantity differs from the momentum $J$ in sign only.

We now replace the assumption of potential flow with the assumption of Stokes flow. The velocity field $u$ and pressure $p$ must satisfy (7.11) together with the no-slip condition on the cylinder's surface. We therefore seek $u = \nabla \times \psi$, where

$$\begin{aligned} \nabla^4 \psi &= 0, \\ u|_{r=R} &= (u_r, u_\theta) = \left(\epsilon \dot{k}^1 \cos 2\theta + \epsilon \dot{k}^2 \cos 3\theta, 0\right). \end{aligned}$$

The solution to this Neumann problem is given to $O\left(\epsilon^2\right)$ by the biharmonic function

$$\psi = \psi_0 + \epsilon \psi_1 + \epsilon^2 \psi_2 + O\left(\epsilon^3\right),$$

where

$$\psi_0 = 0,$$

$$\psi_1 = \frac{1}{2}\dot{k}^1 \sin 2\theta + \dot{k}^2 \left(\frac{1}{2} r^{-1} - \frac{1}{6} r^{-3}\right) \sin 3\theta,$$

$$\psi_2 = c_0 \theta \left(r^2 - 2 \log r\right) + \left(c_1 r^{-1} + c_2 r\right) \sin \theta + \left(c_3 r^{-2} + c_4 r^{-4}\right) \sin 4\theta$$

$$+ \left(c_5 r^{-3} + c_6 r^{-5}\right) \sin 5\theta + \left(c_7 r^{-4} + c_8 r^{-6}\right) \sin 6\theta,$$

$$c_0 = \frac{k^1 \dot{k}^1}{2} + \frac{k^2 \dot{k}^2}{2},$$

$$c_1 = \frac{\dot{k}^1 k^2}{4},$$

$$c_2 = \frac{\dot{k}^1 k^2}{4} + \frac{k^1 \dot{k}^2}{2},$$

$$c_4 = -\frac{k^1 \dot{k}^1}{8},$$

$$c_3 = \frac{k^1 \dot{k}^1}{4},$$

$$c_6 = -\frac{3\dot{k}^1 k^2}{20} - \frac{2k^1 \dot{k}^2}{5},$$

$$c_8 = -\frac{5k^2 \dot{k}^2}{12},$$

$$c_7 = \frac{k^2 \dot{k}^2}{2},$$

$$c_5 = \frac{\dot{k}^1 k^2}{4} + \frac{k^1 \dot{k}^2}{2}.$$

As $r \to \infty$, the velocity field approaches

$$\begin{aligned}(u_r, u_\theta)|_{r\to\infty} &= \left(\frac{1}{r}\frac{\partial \psi}{\partial \theta}, -\frac{\partial \psi}{\partial r}\right)\Bigg|_{r\to\infty} \\ &= \epsilon^2 \left(U\cos\theta, -U\sin\theta\right) + O\left(\epsilon^3\right),\end{aligned}$$

where

$$U = \frac{1}{4}k^2 \dot{k}^1 + \frac{1}{2}k^1 \dot{k}^2.$$

These are the polar components of a uniform flow with speed $\epsilon^2 U + O\left(\epsilon^3\right)$ in the positive $x$ $(\theta = 0)$ direction. If the cylinder translates with velocity $\dot{x}$, then $K$ :

$TQ \to \mathbb{R}$ and $\mathbb{V} : \mathbb{R} \to \mathbb{R}$ are given by

$$\begin{aligned} K\left(k^1, k^2, \dot{k}^1, \dot{k}^2, \dot{x}\right) &= C\left(k^1, k^2\right) U_\infty \\ &= C\left(k^1, k^2\right)\left(\dot{x} + \epsilon^2\left(\frac{1}{4}k^2\dot{k}^1 + \frac{1}{2}k^1\dot{k}^2\right)\right) + O\left(\epsilon^3\right) \end{aligned}$$

and

$$\mathbb{V}\left(k^1, k^2\right) = C\left(k^1, k^2\right).$$

The Stokes connection $\Gamma_{\text{Stokes}} : TQ \to \mathbb{R}$ is then given by

$$\Gamma_{\text{Stokes}} = dx + \epsilon^2\left(\frac{1}{4}k^2\, dk^1 + \frac{1}{2}k^1\, dk^2\right) + O\left(\epsilon^3\right).$$

Along a trajectory in configuration space which remains horizontal with respect to this connection,

$$\dot{x} = -\epsilon^2\left(\frac{1}{4}k^2\dot{k}^1 + \frac{1}{2}k^1\dot{k}^2\right) + O\left(\epsilon^3\right).$$

Figure 7.3 illustrates the difference between $\Gamma_{\text{mech}}$ and $\Gamma_{\text{Stokes}}$ for the gait

$$\left(k^1, k^2\right) = (1 - \cos t, \sin t)$$

with $\epsilon = 0.1$.

We conclude this discussion with a comment on "conveyor-belt" locomotion at low Reynolds number. The example above illustrates the self-propulsion of a surface undergoing radial deformation only. Tangential surface velocities play no role in self-propulsion through inviscid media, but the stricter boundary conditions imposed upon creeping flow allow a cylinder to propel itself while remaining circular

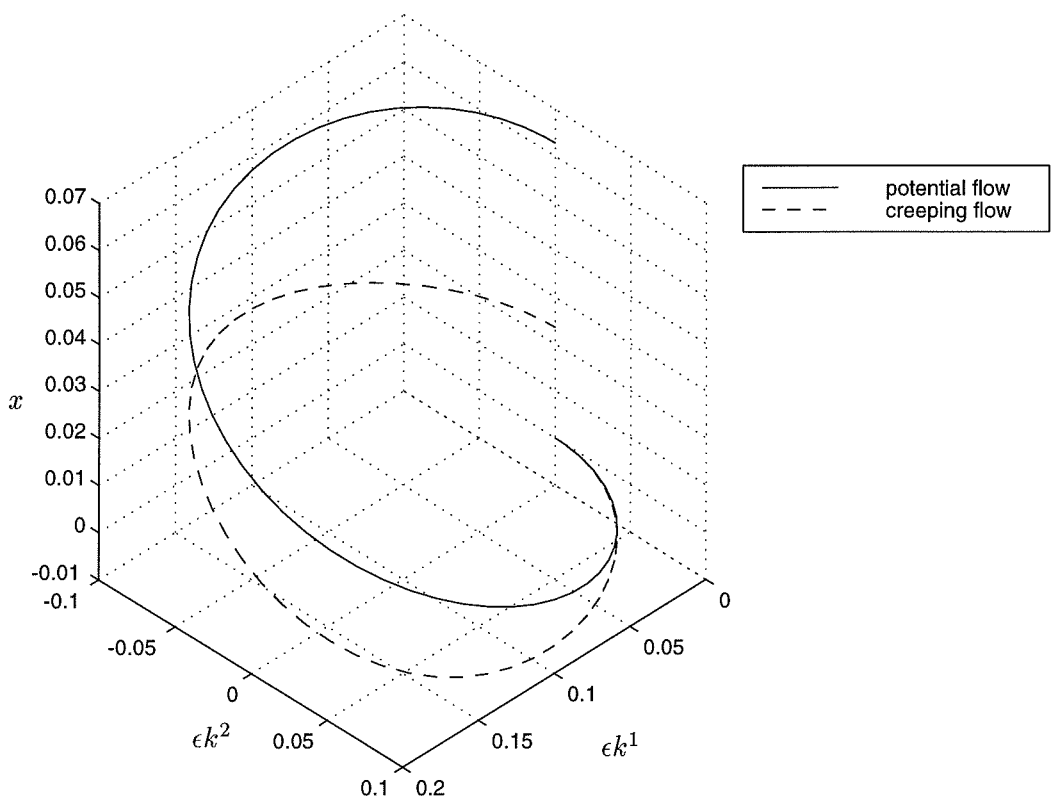


**Figure 7.3** Geometric phase for a particular gait.

in cross section. A tangential surface velocity

$$v_\theta|_{r=1} = \epsilon k\,(t) \sin\theta,$$

for example, produces the connection

$$\Gamma_{\text{Stokes}} = dx - \frac{\epsilon}{2} dk.$$

A cylinder which can effect such a surface velocity will move along the ray $\theta = 0$ with velocity

$$\dot{x}\,(t) = \frac{\epsilon}{2} k\,(t)\,.$$

Tangential deformation will always prove $O\,(1/\epsilon)$ more efficient than radial deformation at low Reynolds number. There is evidence that a swimming amoeba converts fluid endoplasm to jellylike ectoplasm at its forward end, reabsorbing ectoplasm at its rear [3].

# Chapter 8

# Rigid Bodies in Fluids

## 8.1 Modelling assumptions

We develop our model for carangiform locomotion in this chapter and the next. We begin by deriving the reduced Euler-Lagrange equations (3.3) for the interaction of the rigid body of a carangiform swimmer with an infinite surrounding fluid. This derivation parallels the realization of unreduced Euler-Lagrange equations in [81] for a fluid-filled spacecraft. We assume the densities of the body and fluid to be constant and equal, both to simplify our development and to obviate the consideration of buoyancy forces. It is straightforward to relax this assumption. A biological carangid can regulate its buoyancy, and will remain approximately neutrally buoyant when swimming in a plane perpendicular to the direction of gravity. We also assume the fluid to be inviscid. The role of water's viscosity in real carangiform swimming is twofold. Clearly, it accounts for the dissipation of energy introduced to the fluid by an undulating swimmer. More subtly, however, it enforces the Kutta condition which prompts vortex shedding from the trailing edge of the swimmer's caudal fin. We take these effects to be independent and disregard the former. The predominant localization of vortex shedding to the caudal fin is a signature of carangiform locomotion. We note that the flow around a streamlined aquatic vehicle is often assumed to be inviscid [50, 51]. This assumption is consistent, in the large, with boundary layer theory [68].

In the fluid's absence, we specify the position and orientation of a rigid body

relative to a fixed frame of reference with an element $Y$ of $SE(3)$. We specify the configuration of a surrounding fluid relative to an initial state with an element of the group of volume-preserving diffeomorphisms $\mathrm{Diff}_{\mathrm{vol}}(\mathrm{F})$ of the region F occupied by the fluid in the body frame. Each configuration of the body-fluid system, then, corresponds to an element of the Cartesian product $SE(3) \times \mathrm{Diff}_{\mathrm{vol}}(\mathrm{F})$.

In Section 8.2, we demonstrate that the kinetic energy of the body and fluid together exhibits the symmetry called for by Proposition 3.4. Specifically, we show that we can write the total kinetic energy in terms of the body velocity $\xi = Y^{-1}\dot{Y}$ and the spatial fluid velocity field $u = \dot{\eta} \circ \eta^{-1}$ in the body frame.

## 8.2 The reduced Lagrangian

We use the symbol $X$ to label material particles in the reference configuration of the body-fluid system. The total kinetic energy is given by

$$\begin{aligned} L\left(Y, \dot{Y}, \eta, \dot{\eta}\right) &= \frac{1}{2} \int_{\text{body + fluid}} \rho\left(\eta(X)\right) \left\| \frac{d}{dt}\left(Y\eta\right) \right\|^2 dX \\ &= \frac{\rho}{2} \int_{\text{body + fluid}} \left\| \frac{d}{dt}\left(Y\eta\right) \right\|^2 dX, \end{aligned}$$

or

$$\begin{aligned} \tilde{L}\left(R, \dot{R}, p, \dot{p}, \eta, \dot{\eta}\right) &= \frac{\rho}{2} \int_{\text{body + fluid}} \left\| \frac{d}{dt}\left( \begin{bmatrix} R & p \\ 0 & 1 \end{bmatrix} \begin{bmatrix} \eta(X) \\ 1 \end{bmatrix} \right) \right\|^2 dX \\ &= \frac{\rho}{2} \int_{\text{body + fluid}} \Big( \eta^T \dot{R}^T \dot{R} \eta + \eta^T \dot{R}^T \dot{p} + \dot{p}^T \dot{R} \eta + \dot{p}^T \dot{p} + \eta^T \dot{R}^T R \dot{\eta} \\ &\qquad + \dot{p}^T R \dot{\eta} + \dot{\eta}^T R^T \dot{R} \eta + \dot{\eta}^T R^T \dot{p} + \dot{\eta}^T R^T R \dot{\eta} \Big) \, dX \\ &= \frac{\rho}{2} \int_{\text{body + fluid}} \left( \eta^T \hat{\omega}^T \hat{\omega} \eta + \eta^T \hat{\omega}^T v + v^T \hat{\omega} \eta + v^T v + \eta^T \hat{\omega}^T \dot{\eta} \right. \\ &\qquad \left. + v^T \dot{\eta} + \dot{\eta}^T \hat{\omega} \eta + \dot{\eta}^T v + \dot{\eta}^T \dot{\eta} \right) dX, \end{aligned}$$

where $v$ and $\omega$ satisfy

$$v = R^{-1}\dot{p} \qquad \text{and} \qquad \hat{\omega} = R^{-1}\dot{R}.$$

Defining

$$x = \eta(X) \qquad \text{and} \qquad u(x) = \dot{x},$$

we may rewrite this integral in a body-fixed frame as

$$\begin{aligned}\tilde{l}(v,\omega,u(x)) &= \frac{\rho}{2}\int_{\mathbb{R}^3}\left(x^T\hat{\omega}^T\hat{\omega}x + x^T\hat{\omega}^Tv + v^T\hat{\omega}x + v^Tv + x^T\hat{\omega}^Tu(x)\right.\\ &\qquad\left. + v^Tu(x) + u^T(x)\hat{\omega}x + u^T(x)v + u^T(x)u(x)\right)dx\\ &= \frac{\rho}{2}\int_{\mathbb{R}^3}\left(x^T\hat{\omega}^T\hat{\omega}x + 2x^T\hat{\omega}^T(u+v) + (u+v)^T(u+v)\right)dx.\end{aligned}$$

The quantity $u(x)$ represents the spatial velocity of particles with respect to the body frame; $u = 0$ within the body. In terms of the body velocity $\xi \in \mathfrak{se}(3)$, where

$$\hat{\xi} = \begin{bmatrix}\hat{\omega} & v\\ 0 & 0\end{bmatrix},$$

the reduced Lagrangian is thus

$$\begin{aligned}&l(\xi,u(x))\\ &= \frac{\rho}{2}\int_{\mathbb{R}^3}\left(\begin{bmatrix}x^T & 1\end{bmatrix}\hat{\xi}^T\hat{\xi}\begin{bmatrix}x\\1\end{bmatrix} + 2\begin{bmatrix}x^T & 1\end{bmatrix}\hat{\xi}^T\begin{bmatrix}u(x)\\0\end{bmatrix} + \begin{bmatrix}u^T(x) & 0\end{bmatrix}\begin{bmatrix}u(x)\\0\end{bmatrix}\right)dx.\end{aligned}$$

## 8.3 The reduced equations

We now obtain the reduced Euler-Lagrange equations explicitly, beginning with the equation

$$\frac{d}{dt}\frac{\partial l}{\partial u} = \mathrm{ad}^*_u \frac{\partial l}{\partial u}. \tag{8.1}$$

We will summarize our results at the end of this section. For notational convenience, we introduce the $L^2$ inner product of vector fields on $\mathbb{R}^3$ defined by

$$\langle\!\langle a, b \rangle\!\rangle = \int_{\mathbb{R}^3} \rho \langle a(x), b(x) \rangle dx = \rho \int_{\mathbb{R}^3} a(x) \cdot b(x)\, dx.$$

We may then write the kinetic energy as

$$\begin{aligned}\tilde{l}(v, \omega, u(x)) = \frac{1}{2}\langle\!\langle \hat{\omega}x, \hat{\omega}x \rangle\!\rangle + \langle\!\langle \hat{\omega}x, v \rangle\!\rangle + \frac{1}{2}\langle\!\langle v, v \rangle\!\rangle + \langle\!\langle \hat{\omega}x, u \rangle\!\rangle \\ + \langle\!\langle v, u \rangle\!\rangle + \frac{1}{2}\langle\!\langle u, u \rangle\!\rangle.\end{aligned}$$

Let $z$ be a vector field on $\mathbb{R}^3$ such that

$$z = 0 \text{ in } \mathrm{B} = \mathbb{R}^3 - \mathrm{F}, \quad z || \partial \mathrm{F}, \quad \text{and} \quad \nabla \cdot z = 0, \tag{8.2}$$

where the second expression of the three indicates that $z$ is tangent to the boundary between the body and fluid along that boundary. Then

$$\begin{aligned}\left\langle \frac{\partial l}{\partial u}, z \right\rangle &= \left\langle \frac{\partial \tilde{l}}{\partial u}, z \right\rangle \\ &= \left\langle \frac{\partial}{\partial u}\left( \langle\!\langle \hat{\omega}x, u \rangle\!\rangle + \langle\!\langle v, u \rangle\!\rangle + \frac{1}{2}\langle\!\langle u, u \rangle\!\rangle \right), z \right\rangle \\ &= \left.\frac{d}{d\epsilon}\right|_{\epsilon=0} \left( \langle\!\langle \hat{\omega}x, u + \epsilon z \rangle\!\rangle + \langle\!\langle v, u + \epsilon z \rangle\!\rangle + \frac{1}{2}\langle\!\langle u + \epsilon z, u + \epsilon z \rangle\!\rangle \right) \\ &= \langle\!\langle \hat{\omega}x, z \rangle\!\rangle + \langle\!\langle v, z \rangle\!\rangle + \langle\!\langle u, z \rangle\!\rangle \\ &= \int_{\mathbb{R}^3} \rho \langle (\hat{\omega}x + v + u), z \rangle dx.\end{aligned}$$

Similarly

$$\left\langle \frac{d}{dt}\frac{\partial l}{\partial u}, z \right\rangle = \int_{\mathbb{R}^3} \rho \left\langle \frac{\partial}{\partial t}\left(\hat{\omega}x + v + u\right), z \right\rangle dx$$

and

$$\begin{aligned}\left\langle \mathrm{ad}^*_u \frac{\partial l}{\partial u}, z \right\rangle &= \left\langle \frac{\partial l}{\partial u}, \mathrm{ad}_u\, z \right\rangle \\ &= \langle \hat{\omega}x + v + u, [u, z] \rangle \\ &= \int_{\mathbb{R}^3} \rho \langle \hat{\omega}x + v + u, [u, z] \rangle\, dx \\ &= \int_{\mathbb{R}^3} \rho \langle \hat{\omega}x + v + u, u \cdot \nabla z - z \cdot \nabla u \rangle\, dx.\end{aligned}$$

Thus (8.1) becomes

$$\int_{\mathbb{R}^3} \left( \frac{\partial}{\partial t}\left(\omega \times x + v + u\right) \cdot z - \left(\omega \times x + v + u\right) \cdot \left(u \cdot \nabla z - z \cdot \nabla u\right) \right) dx = 0.$$

We now consider the second component of this integral term by term. We make repeated use of of the identity from vector calculus

$$\int_D \nabla \cdot (\phi H)\, dV = \int_D \phi \nabla \cdot H dV + \int_D H \cdot \nabla \phi\, dV = \int_{\partial D} \phi H \cdot n\, dS,$$

where $H$ and $\phi$ are vector-valued and scalar-valued functions, respectively. We note, furthermore, that since $z = 0$ in B, we need only integrate each term over the region F occupied by the fluid.

First of all,

$$\begin{aligned}\int_{\mathrm{F}} (\omega \times x) \cdot (u \cdot \nabla z)\, dx &= \int_{\mathrm{F}} \delta_{ik}\epsilon^i_{lm}\omega^l x^m u^j \frac{\partial z^k}{\partial x^j} dx \\ &= \int_{\mathrm{F}} \left( \frac{\partial}{\partial x^j} \left( \delta_{ik}\epsilon^i_{lm}\omega^l x^m z^k \right) u_j - \delta_{ik}\epsilon^i_{lm}\omega^l \frac{\partial x^m}{\partial x^j} z^k u^j \right) dx \\ &= -\int_{\mathrm{F}} \delta_{ik}\epsilon^i_{lm}\omega^l \frac{\partial x^m}{\partial x^j} z^k u^j dx \\ &= -\int_{\mathrm{F}} \delta_{ik}\delta^m_j \epsilon^i_{lm}\omega^l z^k u^j dx \\ &= -\int_{\mathrm{F}} \delta_{ik}\epsilon^i_{lj}\omega^l z^k u^j dx \\ &= -\int_{\mathrm{F}} (\omega \times u) \cdot z dx.\end{aligned}$$

Similarly,

$$\begin{aligned}\int_{\mathrm{F}} v \cdot (u \cdot \nabla z)\, dx &= \int_{\mathrm{F}} \delta_{ik} v^i u^j \frac{\partial z^k}{\partial x^j} dx \\ &= \int_{\mathrm{F}} \frac{\partial}{\partial x^j} \left( \delta_{ik} v^i z^k \right) u^j dx \\ &= 0,\end{aligned}$$

$$\begin{aligned}\int_{\mathrm{F}} v \cdot (z \cdot \nabla u)\, dx &= \int_{\mathrm{F}} \delta_{ik} v^i z^j \frac{\partial u^k}{\partial x^j} dx \\ &= \int_{\mathrm{F}} \frac{\partial}{\partial x^j} \left( \delta_{ik} v^i u^k \right) z^j dx \\ &= 0,\end{aligned}$$

and

$$\begin{aligned}\int_{\mathrm{F}} (\omega \times x) \cdot (z \cdot \nabla u)\, dx &= \int_{\mathrm{F}} \delta_{ik}\epsilon^i_{lm}\omega^l x^m z^j \frac{\partial u^k}{\partial x^j} dx \\ &= \int_{\mathrm{F}} \left( \frac{\partial}{\partial x^j}\left(\delta_{ik}\epsilon^i_{lm}\omega^l x^m u^k\right) z_j - \delta_{ik}\epsilon^i_{lm}\omega^l \frac{\partial x^m}{\partial x^j} u^k z^j \right) dx \\ &= -\int_{\mathrm{F}} \delta_{ik}\delta^m_j \epsilon^i_{lm}\omega^l z^j u^k dx \\ &= -\int_{\mathrm{F}} \delta_{ik}\epsilon^i_{lj}\omega^l z^j u^k dx \\ &= -\int_{\mathrm{F}} \delta_{ki}\epsilon^i_{lj}\omega^l z^j u^k dx \\ &= -\int_{\mathrm{F}} \delta_{ji}\epsilon^i_{kl}\omega^l z^j u^k dx \\ &= -\int_{\mathrm{F}} (u \times \omega) \cdot z dx.\end{aligned}$$

The fact that $\delta_{ki}\epsilon^i_{lj} = \delta_{ji}\epsilon^i_{kl}$ follows from the invariance of the vector triple product with respect to even permutations. Finally

$$\begin{aligned}\int_{\mathrm{F}} u \cdot (u \cdot \nabla z)\, dx &= \int_{\mathrm{F}} \delta_{ik} u^i u^j \frac{\partial z^k}{\partial x^j} dx \\ &= \int_{\mathrm{F}} \left( \frac{\partial}{\partial x^j}\left(\delta_{ik} u^i z^k\right) u^j - \delta ik \frac{\partial u^i}{\partial x^j} z^k u^j \right) dx \\ &= -\int_{\mathrm{F}} \delta_{ik} \frac{\partial u^i}{\partial x^j} u^j z^k dx \\ &= \int_{\mathrm{F}} (u \cdot \nabla u) \cdot z dx\end{aligned}$$

and

$$\begin{aligned}\int_{\mathrm{F}} u \cdot (z \cdot \nabla u)\, dx &= \int_{\mathrm{F}} \delta_{ik} u^i z^j \frac{\partial u^k}{\partial x^j} dx \\ &= \frac{1}{2}\int_{\mathrm{F}} \frac{\partial}{\partial x^j}\left(\delta_{ik} u^i u^k\right) z^j dx \\ &= 0.\end{aligned}$$

Gathering terms, we are left with

$$\int_{\mathrm{F}} (\dot{\omega} \times x + \dot{u} + \dot{v} + u \cdot \nabla u + 2\omega \times u) \cdot z \, dx = 0.$$

We now invoke the following result, which is proven in [17].

**Theorem 8.1 (Helmholtz-Hodge)** *A vector field $w$ on $F$ has a unique decomposition*

$$w = w_G + w_S,$$

*where $w_G$ is the gradient of a function on $F$ and $w_S$ is solenoidal and parallel to $\partial F$ on $\partial F$.*

Thus $z = z_S + z_G = z_S$ and

$$\int_{\mathrm{F}} ((\dot{\omega} \times x)_S + \dot{u}_S + \dot{v}_S + (u \cdot \nabla u)_S + 2\,(\omega \times u)_S) \cdot z \, dx =$$
$$\int_{\mathrm{F}} (\dot{\omega} \times x + \dot{u} + \dot{v} + (u \cdot \nabla u)_S + 2\,(\omega \times u)_S) \cdot z \, dx = 0,$$

or, since $z$ is otherwise arbitrary,

$$\dot{\omega} \times x + \dot{u} + \dot{v} + u \cdot \nabla u + 2\omega \times u = (u \cdot \nabla u + 2\omega \times u)_G \,. \tag{8.3}$$

We define the *pressure gradient*

$$\nabla p = (-\rho\,(u \cdot \nabla u + 2\omega \times u))_G = -\rho\,(u \cdot \nabla u + 2\omega \times u)_G$$

and, following [81], the *gauge gradient*

$$\nabla s = \nabla p + \nabla \left( \frac{1}{2} \rho u^T u \right);$$

then (8.3) may be written as

$$\rho\left(\dot{\omega}\times x+\dot{u}+\dot{v}+u\cdot\nabla u+2\omega\times u\right)=\nabla\left(\frac{1}{2}\rho u^{T}u\right)-\nabla s. \tag{8.4}$$

We now turn to the equation

$$\frac{d}{dt}\frac{\partial l}{\partial\hat{\xi}}=\mathrm{ad}^{*}_{\hat{\xi}}\frac{\partial l}{\partial\hat{\xi}}. \tag{8.5}$$

We rewrite the kinetic energy as

$$l\left(\hat{\xi},u\left(x\right)\right)=\frac{1}{2}\left\langle\left\langle\hat{\xi}\bar{x},\hat{\xi}\bar{x}\right\rangle\right\rangle+\left\langle\left\langle\hat{\xi}\bar{x},\tilde{u}\right\rangle\right\rangle+\frac{1}{2}\left\langle\left\langle\tilde{u},\tilde{u}\right\rangle\right\rangle,$$

where

$$\bar{x}=\begin{bmatrix}x\\1\end{bmatrix}\quad\text{and}\quad\tilde{u}=\begin{bmatrix}u\left(x\right)\\0\end{bmatrix}.$$

Let $\nu$ be an element of $\mathfrak{se}(3)$, such that

$$\hat{\nu}=\begin{bmatrix}\hat{\gamma}&\lambda\\0&0\end{bmatrix}$$

for some skew-symmetric $3\times3$ matrix $\hat{\gamma}$ and some column vector $\lambda$. Then

$$\begin{aligned}\left\langle\frac{\partial l}{\partial\hat{\xi}},\hat{\nu}\right\rangle&=\left\langle\frac{\partial}{\partial\hat{\xi}}\left(\frac{1}{2}\left\langle\left\langle\hat{\xi}\bar{x},\hat{\xi}\bar{x}\right\rangle\right\rangle+\left\langle\left\langle\hat{\xi}\bar{x},\tilde{u}\right\rangle\right\rangle\right),\hat{\nu}\right\rangle\\&=\left.\frac{d}{d\epsilon}\right|_{\epsilon=0}\left(\frac{1}{2}\left\langle\left\langle\left(\hat{\xi}+\epsilon\hat{\nu}\right)\bar{x},\left(\hat{\xi}+\epsilon\hat{\nu}\right)\bar{x}\right\rangle\right\rangle+\left\langle\left\langle\left(\hat{\xi}+\epsilon\hat{\nu}\right)\bar{x},\tilde{u}\right\rangle\right\rangle\right)\\&=\left\langle\left\langle\hat{\xi}\bar{x},\hat{\nu}\bar{x}\right\rangle\right\rangle+\left\langle\left\langle\hat{\nu}\bar{x},\tilde{u}\right\rangle\right\rangle\\&=\int_{\mathbb{R}^{3}}\rho\left(\hat{\xi}\bar{x}+\tilde{u}\right)\cdot\left(\hat{\nu}\bar{x}\right)dx.\end{aligned}$$

Similarly,

$$\left\langle\frac{d}{dt}\frac{\partial l}{\partial\hat{\xi}},\hat{\nu}\right\rangle=\int_{\mathbb{R}^{3}}\rho\frac{\partial}{\partial t}\left(\hat{\xi}\bar{x}+\tilde{u}\right)\cdot\left(\hat{\nu}\bar{x}\right)dx$$

and

$$\begin{aligned}\left\langle \mathrm{ad}^*_{\hat{\xi}} \frac{\partial l}{\partial \hat{\xi}}, \hat{\nu} \right\rangle &= \left\langle \frac{\partial l}{\partial \hat{\xi}}, \mathrm{ad}_{\hat{\xi}} \hat{\nu} \right\rangle \\ &= \left\langle \hat{\xi}\bar{x} + \tilde{u}, [\hat{\xi}, \hat{\nu}]\bar{x} \right\rangle \\ &= \int_{\mathbb{R}^3} \left(\hat{\xi} + \tilde{u}\right) \cdot \left(\hat{\xi}\hat{\nu} - \hat{\nu}\hat{\xi}\right) \bar{x} dx.\end{aligned}$$

Thus (8.5) becomes

$$\int_{\mathbb{R}^3} \left( \frac{\partial}{\partial t} \left(\hat{\xi}\bar{x} + \tilde{u}\right) \cdot \hat{\nu}\bar{x} - \left(\hat{\xi} + \tilde{u}\right) \cdot \left(\hat{\xi}\hat{\nu} - \hat{\nu}\hat{\xi}\right) \bar{x} \right) dx = 0,$$

or

$$\begin{aligned}\int_{\mathbb{R}^3} \Big( & x^T\hat{\gamma}^T\dot{\hat{\omega}}x + x^T\hat{\gamma}^T\dot{u} + x^T\hat{\gamma}^T\dot{v} - x^T\hat{\gamma}^T\hat{\omega}^T\hat{\omega}x + x^T\hat{\omega}^T\hat{\gamma}^T\hat{\omega}x + v^T\hat{\gamma}^T\hat{\omega}x \\ & - x^T\hat{\gamma}^T\hat{\omega}^Tv + x^T\hat{\omega}^T\hat{\gamma}^Tv + v^T\hat{\gamma}^Tv - x^T\hat{\gamma}^T\hat{\omega}^Tu + x^T\hat{\omega}^T\hat{\gamma}^Tu + v^T\hat{\gamma}^Tu \\ & + \left(x^T\dot{\hat{\omega}}^T + \dot{u}^T + \dot{v}^T - x^T\hat{\omega}^T\hat{\omega} - v^T\hat{\omega} - u^T\hat{\omega}\right)\lambda \Big) dx = 0.\end{aligned}$$

Because of the independence of $\gamma \in \mathfrak{so}(3)$ and $\lambda \in \mathbb{R}^3$, (8.5) is therefore equivalent to the independent equations

$$\begin{aligned}\int_{\mathbb{R}^3} \Big( & x^T\hat{\gamma}^T\dot{\hat{\omega}}x + x^T\hat{\gamma}^T\dot{u} + x^T\hat{\gamma}^T\dot{v} - x^T\hat{\gamma}^T\hat{\omega}^T\hat{\omega}x + x^T\hat{\omega}^T\hat{\gamma}^T\hat{\omega}x + v^T\hat{\gamma}^T\hat{\omega}x \\ & - x^T\hat{\gamma}^T\hat{\omega}^Tv + x^T\hat{\omega}^T\hat{\gamma}^Tv + v^T\hat{\gamma}^Tv - x^T\hat{\gamma}^T\hat{\omega}^Tu + x^T\hat{\omega}^T\hat{\gamma}^Tu + v^T\hat{\gamma}^Tu \Big) dx = 0\end{aligned} \tag{8.6}$$

and

$$\int_{\mathbb{R}^3} \lambda^T \left(\dot{\hat{\omega}}x + \dot{u} + \dot{v} + \hat{\omega}^2x + \hat{\omega}u + \hat{\omega}v\right) dx = 0. \tag{8.7}$$

We simplify the former of these equalities with the assistance of the following result, easily obtained by direct calculation.

**Lemma 8.2** *Let $a(x), b(x), c(x)$, and $d(x)$ be vector fields on $\mathbb{R}^3$. Then*

$$\int_{\mathbb{R}^3} \left(a^T \hat{\gamma}^T b + c^T \hat{\gamma}^T d\right) dx = 0$$

*for all skew-symmetric $3 \times 3$ matrices $\hat{\gamma}$ if and only if*

$$\int_{\mathbb{R}^3} \left(\left(ba^T\right)_A + \left(dc^T\right)_A\right) dx = 0,$$

*where the subscript A denotes projection onto the skew (anti-) symmetric component of its argument.*

It follows that (8.6) is equivalent to

$$\begin{aligned}\int_{\mathbb{R}^3} \Big(\left(\dot{\hat{\omega}} x x^T\right)_A + \left(\left(\dot{u} + \dot{v}\right) x^T\right)_A + \left(\hat{\omega}^2 x x^T\right)_A + \left(\hat{\omega}\left(u + v\right) x^T\right)_A \\ + \left(\left(u + v\right) x^T \hat{\omega}^T\right)_A + \left(\hat{\omega} x v^T\right)_A + \left(u v^T\right)_A\Big) dx = 0.\end{aligned} \tag{8.8}$$

Since the terms appearing in the integrand are all skew-symmetric $3 \times 3$ matrices, we may rewrite (8.8) in terms of the integral of a vector quantity. Up to a multiplicative constant, (8.8) is identically

$$\int_{\mathbb{R}^3} \Big(I\omega \times \omega - I\dot{\omega} + b \times \omega - \dot{b} + u \times v - v \times \left(\omega \times x\right)\Big) = 0, \tag{8.9}$$

where

$$I = \left(\operatorname{trace} x x^T\right) \operatorname{id} - x x^T$$

and

$$b = x \times \left(u + v\right).$$

Since $\lambda$ is arbitrary, (8.7) is equivalent to

$$\int_{\mathbb{R}^3} \left(\dot{\omega} \times x + \left(\dot{u} + \dot{v}\right) + \omega \times \left(\omega \times x\right) + \omega \times \left(u + v\right)\right) dx = 0. \tag{8.10}$$

Equations (8.9), (8.10), and

$$\rho\left(\dot{\omega}\times x+\dot{u}+\dot{v}+u\cdot\nabla u+2\omega\times u\right)=\nabla\left(\frac{1}{2}\rho u^{T}u\right)-\nabla s \tag{8.11}$$

completely describe the interaction of a homogeneous rigid body and a surrounding fluid of equal density.

## 8.4 Special cases

We can readily verify the equations derived in Section 8.3 for certain limiting cases. Suppose that the rigid body in question were not surrounded by a fluid at all. Then (8.9) would be replaced by

$$\int_{\mathrm{B}}\left(I\omega\times\omega-I\dot{\omega}+b\times\omega-\dot{b}-v\times(\omega\times x)\right)dx=0, \tag{8.12}$$

where $b=x\times v$, and (8.10) by

$$\int_{\mathrm{B}}\left(\dot{\omega}\times x+\dot{v}+\omega\times(\omega\times x)+\omega\times v\right)dx=0. \tag{8.13}$$

If we set $v=0$ identically, we recover Euler's equation

$$\int_{\mathrm{B}}\left(I\omega\times\omega-I\dot{\omega}\right)dx=0 \tag{8.14}$$

for the motion of a free rigid body from (8.12). Similarly, the assumption that $\omega=0$ returns Newton's second law. In [39], we represent (8.9) and (8.10) as the traditional rigid body equations amended by the forces and moments due to the distribution of fluid pressure on the body's surface.

In a fixed frame (for which $\omega=v=0$ identically), (8.11) is equivalent to Euler's equation (7.3) for the motion of an incompressible fluid. Taking the curl of (8.11) and noting the identities

$$\nabla\times(a\times b)=a\left(\nabla\cdot b\right)-b\left(\nabla\cdot a\right)+\left(b\cdot\nabla\right)a-\left(a\cdot\nabla\right)b$$

and

$$u \cdot \nabla u = (\nabla \times u) \times u + \nabla \left( \frac{1}{2} u^T u \right),$$

we obtain

$$\dot{\zeta} + u \cdot \nabla \zeta = \zeta \cdot \nabla u + 2 (\omega \cdot \nabla u - \dot{\omega}), \tag{8.15}$$

where $\zeta = \nabla \times u$ is the *vorticity*. In the absence of the terms involving $\omega$, this is Helmholtz's vorticity equation for an incompressible fluid [68].

# Chapter 9

# Planar Carangiform Locomotion

## 9.1 The unforced equations

We espouse a planar model for carangiform locomotion. If we restrict ourselves to the case $x^3 = 0$, (8.9), (8.10) and (8.11) become

$$\int_{\mathbb{R}^3} \left(-\dot{\omega}^3 \left(x^1 x^1 + x^2 x^2\right) - x^1 \left(\dot{u}^2 + \dot{v}^2\right) - x^2 \left(\dot{u}^1 + \dot{v}^1\right) + u^1 v^2 - u^2 v^1 - \omega^3 \left(x^1 v^1 + x^2 v^2\right)\right) dx = 0, \quad (9.1)$$

$$\int_{\mathbb{R}^3} \begin{bmatrix} -x^2\dot{\omega}^3 + \dot{u}^1 + \dot{v}^1 - x^1\omega^3\omega^3 - \left(u^2 + v^2\right)\omega^3 \\ \\ x^1\dot{\omega}^3 + \dot{u}^2 + \dot{v}^2 + x^2\omega^3\omega^3 + \left(u^1 + v^1\right)\omega^3 \end{bmatrix} dx = 0, \quad (9.2)$$

and

$$\rho \begin{bmatrix} -x^2\dot{\omega}^3 + \dot{u}^1 + \dot{v}^1 + u^1\frac{\partial u^1}{\partial x^1} + u^2\frac{\partial u^1}{\partial x^2} - 2u^2\omega^3 \\ \\ x^1\dot{\omega}^3 + \dot{u}^2 + \dot{v}^2 + u^1\frac{\partial u^2}{\partial x^1} + u^2\frac{\partial u^2}{\partial x^2} + 2u^1\omega^3 \end{bmatrix} = \begin{bmatrix} \frac{\rho}{2}\frac{\partial}{\partial x^1}\left(u^1u^1 + u^2u^2\right) - \frac{\partial s}{\partial x^1} \\ \\ \frac{\rho}{2}\frac{\partial}{\partial x^2}\left(u^1u^1 + u^2u^2\right) - \frac{\partial s}{\partial x^2} \end{bmatrix}, \quad (9.3)$$

respectively.

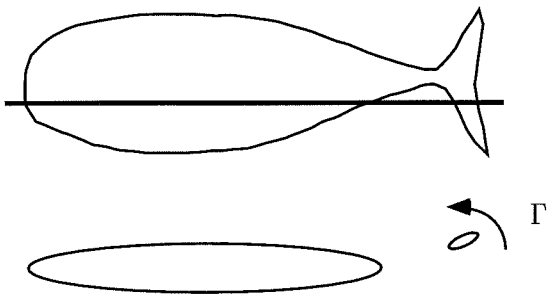


**Figure 9.1** Silhouette and cross section of a louvar.

## 9.2 The substitution vortex model

Figure 9.1 depicts a horizontal cross section of a louvar, a typical carangiform swimmer. Away from the midline of the fish, the body and caudal fin are disjoint. The force developed on a representative section of the caudal fin is transmitted to the body of the swimmer, but the caudal peduncle which couples them has no hydrodynamic impact.

The symbol $\Gamma$ in Figure 9.1 represents the circulation about the caudal fin, which we regard as a hydrofoil. As the velocity and effective angle of attack of the caudal fin vary, vorticity is shed from its trailing edge, changing the circulation $\Gamma$. The lift on the fin, which is proportional in magnitude to $\Gamma$ and directed according to the flow experienced by the fin, is transmitted to the body of the swimmer as thrust.

Because the caudal section is small compared with the body and separated from the body by a distance greater than one chord length, it is reasonable to approximate its hydrodynamic effect on the body as that of a single point vortex of appropriate strength. We will justify this notion of a *substitution vortex* rigorously in Section 9.6, following our overview in Section 9.5.1 of the role of complex variables in hydrofoil theory. At the most abstract level, then, we model a carangiform swimmer as a planar rigid body coupled to a controlled vortex.

We assume that a carangid's authority over the position and shape of its caudal fin afford effective control of the position $x_v$ of the substitution vortex and the circulation $\Gamma$ around it. Equations (9.1), (9.2), and (9.3) describe the drift behavior

of the paired body and fluid. The controlled substitution vortex completes our model for planar swimming.

As it moves through the fluid, the substitution vortex experiences a flow with relative velocity $u_{v\,\mathrm{eff}} = u(x_v) - \dot{x}_v$. We will see in Section 9.5.1 that, as a result, it transmits to the body a thrust equal in magnitude to $\rho u_{v\,\mathrm{eff}}\Gamma$. In the absence of the drift associated with equations (9.1), (9.2), and (9.3), we can write the remaining dynamics as the control affine system

$$\begin{aligned}
\frac{d}{dt}\begin{bmatrix} x_v^1 \\ x_v^2 \\ \Gamma \\ v^1 \\ v^2 \\ \omega^3 \\ u^1 \\ u^2 \end{bmatrix} &= \begin{bmatrix} 0 \\ 0 \\ 0 \\ \frac{\rho}{m}\Gamma u^2(x_v) \\ -\frac{\rho}{m}\Gamma u^1(x_v) \\ -\frac{\rho}{\mathbb{I}}\Gamma\Big(x_v^1 u^1(x_v) + x_v^2 u^2(x_v)\Big) \\ 0 \\ 0 \end{bmatrix} \\
&\quad + \begin{bmatrix} 1 \\ 0 \\ 0 \\ 0 \\ \frac{\rho}{m}\Gamma \\ \frac{\rho}{\mathbb{I}}\Gamma x_v^1 \\ 0 \\ 0 \end{bmatrix} \tau^1 + \begin{bmatrix} 0 \\ 1 \\ 0 \\ -\frac{\rho}{m}\Gamma \\ 0 \\ \frac{\rho}{\mathbb{I}}\Gamma x_v^2 \\ 0 \\ 0 \end{bmatrix} \tau^2 + \begin{bmatrix} 0 \\ 0 \\ 1 \\ 0 \\ 0 \\ 0 \\ * \\ * \end{bmatrix} \tau^3 \qquad (9.4) \\
&= f(q) + h_1(q)\tau^1 + h_2(q)\tau^2 + h_3(q)\tau^3.
\end{aligned}$$

Here

$$m = \int_{\mathrm{B}} \rho \, dx$$

is the mass of the body,

$$\mathbb{I} = \int_{\mathrm{B}} \rho I dx$$

its moment of inertia, and

$$\tau^1 = \dot{x}_v^1, \qquad \tau^2 = \dot{x}_v^2, \qquad \text{and} \qquad \tau^3 = \dot{\Gamma}$$

the control inputs.

The asterisks in $h_3$ represent the effects of changes in $\Gamma$ on the flow field $u(x,t)$; we do not specify them in this form here. Since changes in $\Gamma$ are most directly related to the shedding of vorticity, it makes some sense to replace the velocity field in our state vector with the vorticity field $\zeta(x,t)$. The unforced evolution of the vorticity is determined by the planar version of (8.15); in the presence of the substitution vortex we have

$$\dot{\zeta} + u \cdot \nabla\zeta = \zeta \cdot \nabla u + 2(\omega \cdot \nabla u - \dot{\omega}) = \dot{\Gamma}\delta(x_v).$$

In taking the curl of (9.3), however, we lose information about the gradient component of $u$. The unforced gradient projection of (9.3) then completes the forced fluid system. We explore this perspective in [39].

## 9.3 Planar carangiform accessibility

We resume the discussion of gaits from Chapter 6 by interpreting the partial construction of the accessibilty algebra associated with (9.4). We recognize that this is only one component of the model we advance for carangiform locomotion. We assume that the drift associated with with the phenomena addressed in Section 8.3 combines with the drift represented by the vector $f(q)$ in Section 9.2 without interfering, qualitatively, with with the input vector fields $\{h_1, h_2, h_3\}$. Note that we are not concerned, in practice, with accessibility in the fluid velocity $u$.

We compute, for example,

$$[h_2, h_3] = \begin{bmatrix} 0 \\ 0 \\ 0 \\ -\frac{\rho}{m} \\ 0 \\ \frac{\rho}{\mathbb{I}} x_v^2 \\ * \\ * \end{bmatrix}.$$

We infer that cyclic variations in the heave of the caudal fin and the circulation about it, properly phased, will rotate the body and propel it forward. The circulation about the caudal fin, we recall, depends upon its effective angle of attack as well as its velocity. The rotation term is proportional to the lateral displacement $x_v^2$ of the susbstitution vortex; small excursions of a caudal fin extended straight back do not generate rotation. Furthermore,

$$[h_1, h_3] = \begin{bmatrix} 0 \\ 0 \\ 0 \\ 0 \\ \frac{\rho}{m} \\ \frac{\rho}{\mathbb{I}} x_v^1 \\ * \\ * \end{bmatrix};$$

we infer that appropriate cyclic variations in the longitudinal extension of the caudal fin and its effective angle of attack afford rotation and lateral motion in the body

frame. Finally

$$[h_1, h_2] = 0.$$

Infinitesimal cyclic variations in the thrust which involve no changes in $\Gamma$ provide, to our approximation, zero propulsive effect. This result is reminiscent of the observation that a gliding kestral, maintaining constant circulation about its wings, must alter their geometry to effect a change in course [92].

## 9.4 The experiment

The substitution vortex model supposes a carangiform swimmer to control the position of its caudal fin and the circulation about it. In actuality, the swimmer controls the fin's position and orientation; the circulation depends upon the velocity and inclination of the fin relative to the fluid through which it moves. We now examine the development of hydrodynamic lift quantitatively, comparing the numerical predictions of a mathematical model with the actual behavior of a robotic propulsor.

The fluid component of the substitution vortex model is influenced by the motion of the propulsor's body as well as the evolution of the vortex itself. We wish to isolate the interaction of the fin and fluid. It is an advantage rather than a compromise, then, that our experimental fin propels a constant load with no hydrodynamic impact. Indeed, the propulsive mechanism detailed below need not drive a carangiform body; its adaptability to different marine vehicle architectures remains to explore.

Figures 9.2 and 9.3 depict the main component of our experimental apparatus from the top and side schematically. Figures 9.4 and 9.5 provide photographic contrast. The actuated mechanism is intended to exemplify the tail of a carangiform swimmer with a fin of constant section, and is suspended from a carriage which is free to translate along the length of either of two laboratory water tanks. Figures 9.2 and 9.3 depict a two meter tank, over which the carriage slides on pillow block bearings. Figures 9.4 and 9.5 depict a seven meter tank, over which the carriage slides

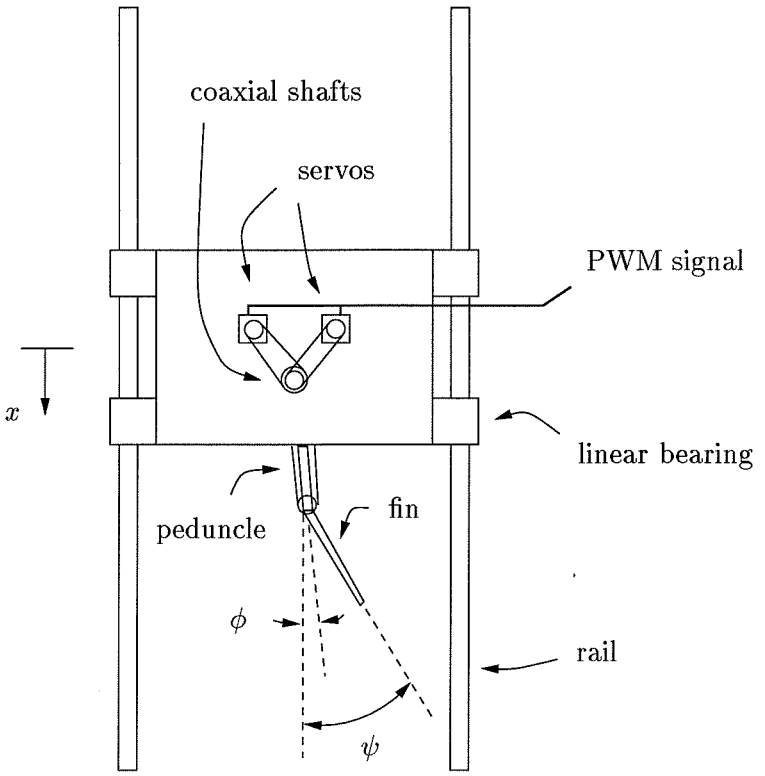


**Figure 9.2** The apparatus from above.

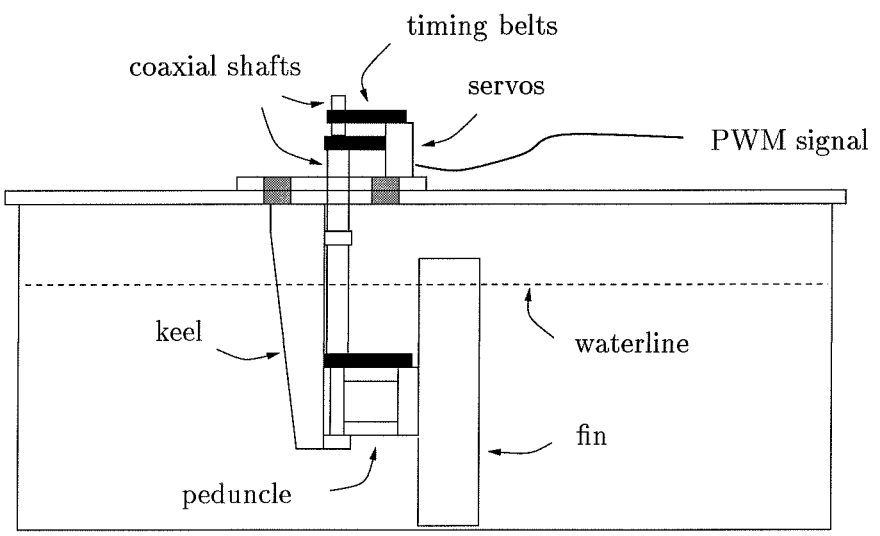


**Figure 9.3** The apparatus from the side.

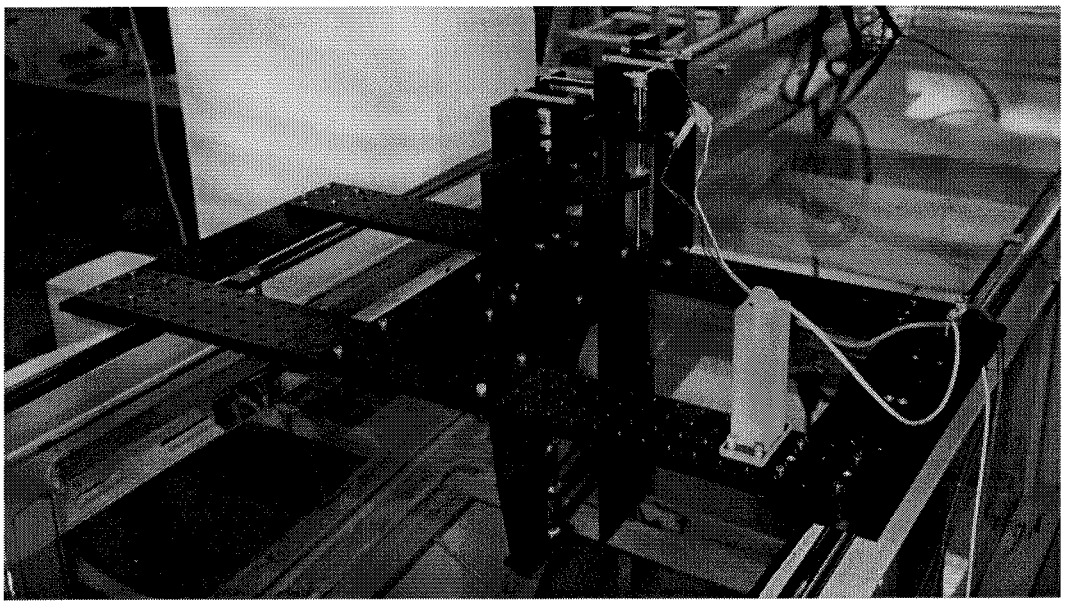

**Figure 9.4** The apparatus from forward and above.

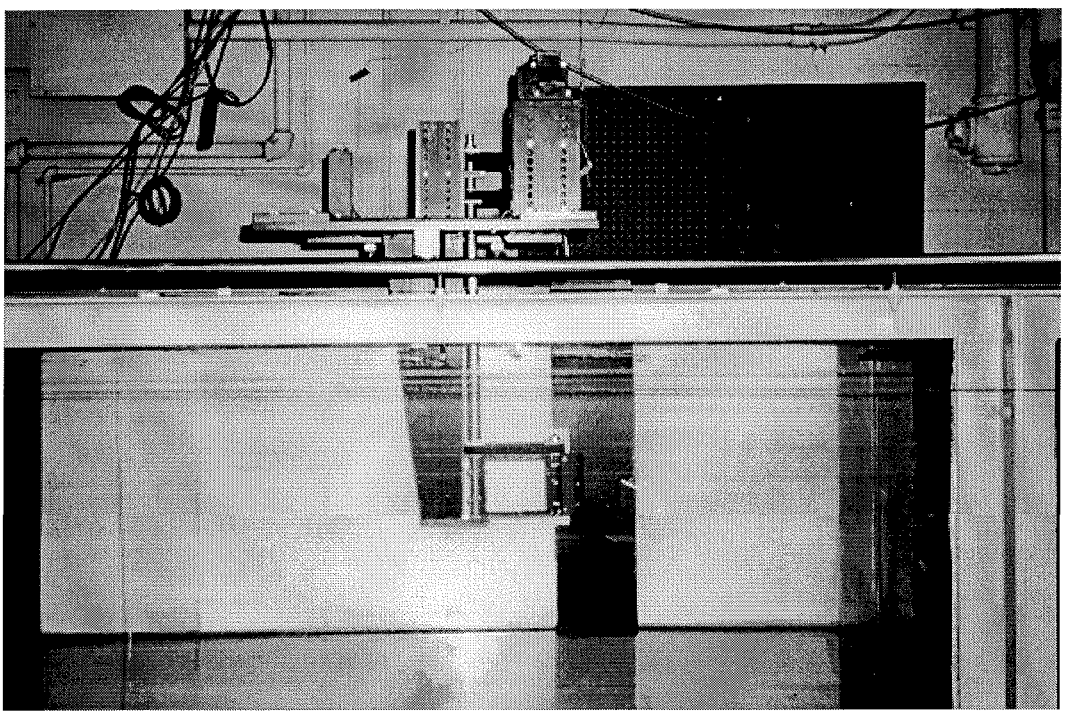

**Figure 9.5** The apparatus from the side.

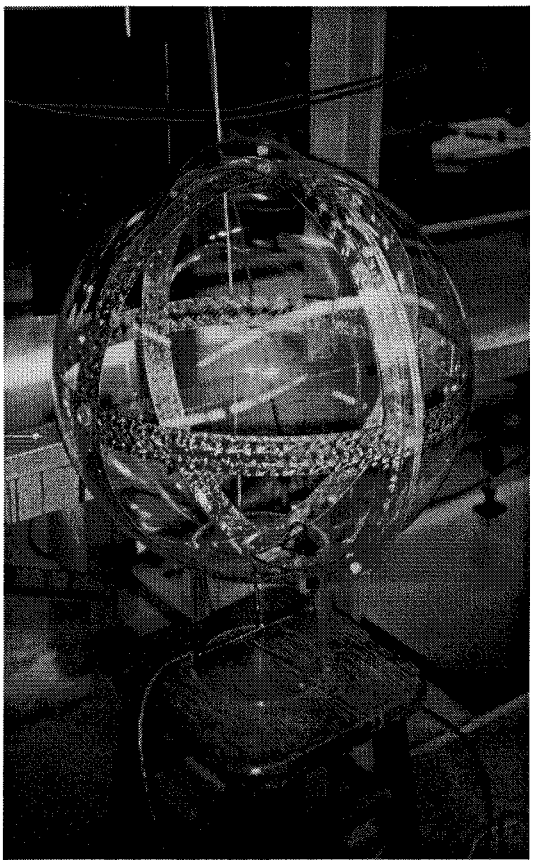

**Figure 9.6** The Polhemus transmitter.

on wheels. The peduncle and fin, each .125 m in length, are submerged to a depth of .50 m in either tank. The tank in which we collect our numerical data is .76 m wide.

The apparatus permits independent, software-based control of the horizontal angles $\phi$ and $\psi$ between the direction of translation, the peduncle, and the fin. The peduncle and fin are driven by PWM servomotors, while a Polhemus receiver mounted on the carriage measures its displacement based on the low-frequency magnetic field created by the stationary transmitter shown in Figure 9.6.

Figure 9.7 shows the measured displacement versus time corresponding to a

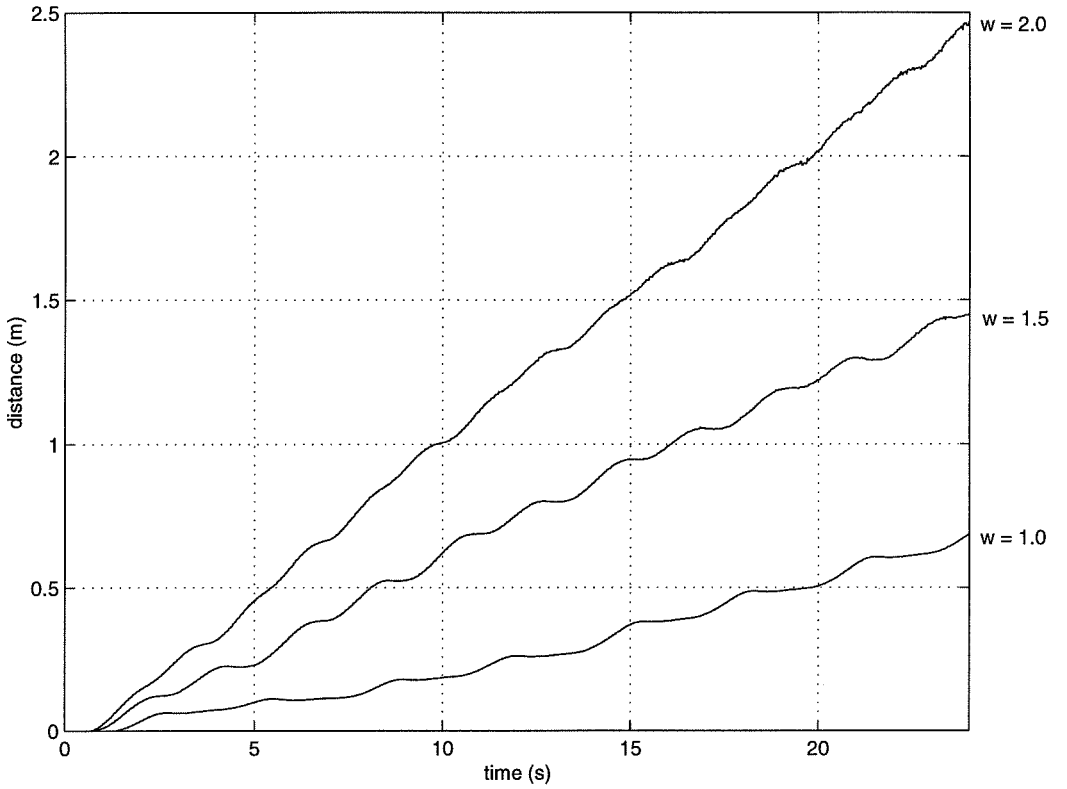


**Figure 9.7** Displacement with the peduncle and fin in phase.

family of fin oscillations of the form

$$\begin{aligned} \phi(t) &= \cos \omega t \\ \psi(t) &= \phi(t) + \cos \omega t. \end{aligned} \tag{9.5}$$

The apparatus begins at rest at $t = 0$. At lower frequencies, the plot clearly shows the cyclic acceleration and deceleration of the carriage. The fin acts as a brake as it swings toward each extreme of its motion, assuming the role of a thruster only as it swings back toward the midline of the tank. As the frequency $\omega$ increases, the increased forward momentum of the carriage attenuates this effect. In every case, the motion of the carriage settles quickly about a steady mean velocity; this mean velocity increases with $\omega$.

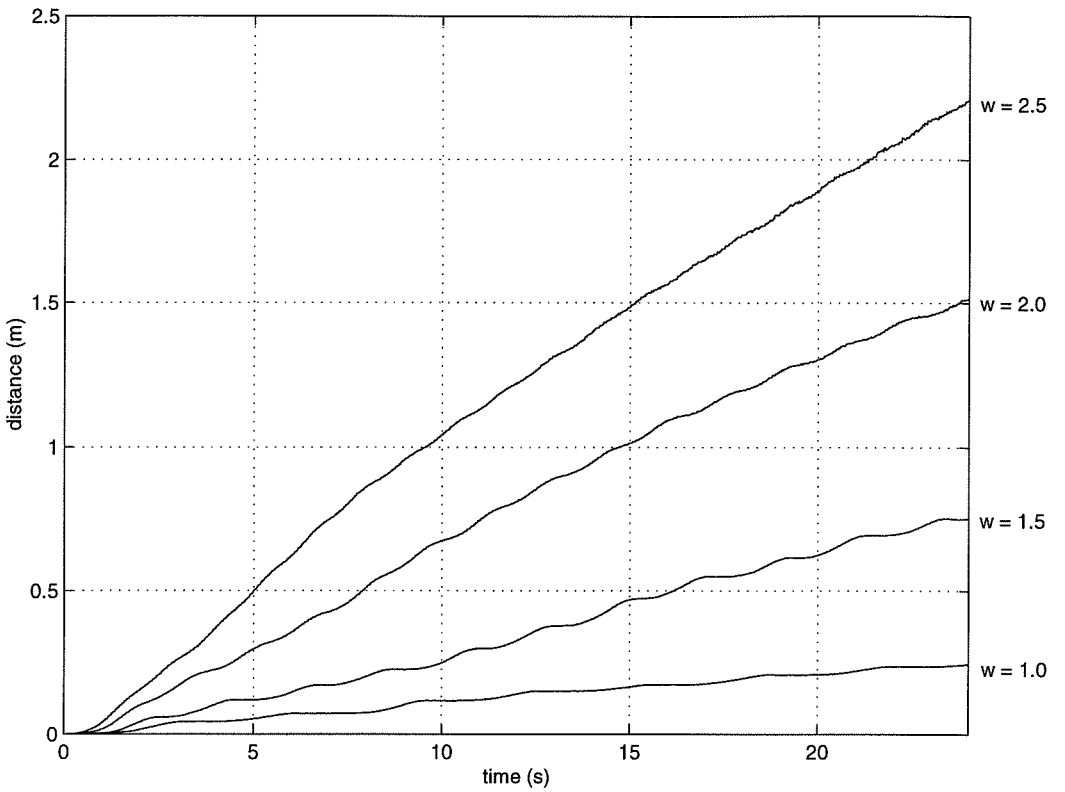


**Figure 9.8** Displacement with the peduncle and fin out of phase.

Figure 9.8 depicts oscillations of the form

$$\begin{aligned} \phi(t) &= \cos \omega t \\ \psi(t) &= \phi(t) + \sin \omega t \end{aligned} \tag{9.6}$$

at four frequencies $\omega$. At a given frequency, the gait given by (9.5) generates greater mean thrust than that given by (9.6). We take care not to infer the superiority of gaits in which the peduncle and fin oscillate in phase, however. The tip of the fin enjoys a greater maximum excursion according to (9.5) than according to (9.6). Indeed, the peduncle of the Pacific Whitesided Dolphin—an efficient carangiform swimmer—precedes its caudal fin by approximately $\pi/2$ radians [99]. Overall, the out-of-phase gaits shown in Figure 9.8 propel the platform more smoothly than the in-phase gaits shown in Figure 9.7. The smoothness of out-of-phase gaits may

contribute to their prevalence in nature. We omit the gait corresponding to $\omega = 2.5$ from Figure 9.7 because it exceeds the capacity of our servomotors.

In Section 9.5, we will assess our theoretical model for the experimental apparatus by its ability to reproduce Figures 9.7 and 9.8. Although they illustrate only seven gaits in all, these span the range of available frequencies at the extremes of practical phasing.

## 9.5 Modelling and simulation

### 9.5.1 The steady flow model

The flow around the oscillating caudal fin of a carangiform propulsor is essentially unsteady. In modelling the hydrodynamic forces acting upon our robotic fin, however, we seek the simplest theory with which to explain our data. We therefore advance a model based on the assumption of steady flow.

We regard the thrust developed by a moving fin as a hydrodynamic lift. A hydrofoil subject to a steady ambient flow experiences both a lift and a pitching moment. The lift may be considered to act at the *center of pressure* of the foil, about which the pitching moment is zero. The forces acting upon certain planar hydrofoils are readily determined using complex analysis; we follow [67] in our exposition of this approach and omit computational proofs contained therein.

Continuity of two-dimensional incompressible flow in the $(x, y)$ plane requires that

$$\frac{\partial u_x}{\partial x} + \frac{\partial u_y}{\partial y} = 0;$$

we define a continuous stream function $\psi$ such that

$$u_x = \frac{\partial \psi}{\partial y} \qquad \text{and} \qquad u_y = -\frac{\partial \psi}{\partial x}. \tag{9.7}$$

Note that (7.5) and (9.7) imply that the potential function $\phi$ and the stream function

$\psi$ satisfy the Cauchy-Riemann equations

$$\frac{\partial \phi}{\partial x} = \frac{\partial \psi}{\partial y} \qquad \text{and} \qquad \frac{\partial \phi}{\partial y} = -\frac{\partial \psi}{\partial x}.$$

If $\phi(z)$ and $\psi(z)$ denote the velocity potential and stream function corresponding to steady irrotational flow about a cylinder with contour $C$ in the complex $z$ plane, we refer to the function $w(z) = \phi(z) + i\psi(z)$ as the corresponding *complex potential* and apply the following result.

**Theorem 9.1 (Blausius)** *If $z = x + iy$, then the forces $X$ and $Y$ acting upon the cylinder in the $x$ and $y$ directions are given by*

$$X - iY = \frac{1}{2} i\rho \int_C \left(\frac{dw}{dz}\right)^2 dz$$

*and the pitching moment about the origin $z = 0$ by*

$$M = \textit{real part of } -\frac{1}{2} i\rho \int_C z \left(\frac{dw}{dz}\right)^2 dz.$$

The quantity

$$u - iv = -\frac{dw}{dz}$$

is called the *complex velocity* corresponding to the complex potential $w(z)$. If a hydrofoil (about which there may be circulation) is placed at an angle $\alpha$ to a uniform flow with speed $U$, we may expand the complex velocity for large $|z|$ in the form

$$-\frac{dw}{dz} = -U\mathrm{e}^{i\alpha} + \frac{A}{z} + \frac{B}{z^2} + \ldots.$$

The complex potential is then

$$w = U\mathrm{e}^{i\alpha} z - A \log z + \frac{B}{z} + \ldots$$

and the circulation $\Gamma$ must satisfy

$$-A = \frac{i\Gamma}{2\pi}.$$

Choosing our contour of integration $C$ to be a circle of sufficiently large radius, we apply Blausius' theorem to obtain

$$X - iY = \rho U \Gamma \mathrm{e}^{i\left(\frac{3\pi}{2}+\alpha\right)}$$

and

$$M = \text{real part of } 2\pi i \rho B U \mathrm{e}^{i\alpha}.$$

The first of these equations suggests the following result, discovered by its two namesakes independently.

**Theorem 9.2 (Kutta-Joukowski)** *A hydrofoil subject to the uniform relative flow of a fluid with density $\rho$ and speed $U$ experiences a lift*

$$L = \rho U \Gamma$$

*perpendicular to the direction of flow. A vector in the direction of the lift is obtained by rotating a vector in the direction of the flow through a right angle opposite the sense of the circulation.*

The net absence of drag in two-dimensional inviscid flow is termed *d'Alembert's paradox.*

Suppose that the complex potential $w = f(z)$ corresponds to the planar flow of an inviscid fluid in the absence of rigid boundaries. The *first circle theorem* [68] states that the introduction of the cylinder with impenetrable contour $|z| = a$ alters the flow to that with complex potential

$$w = f(z) + \bar{f}\left(\frac{a^2}{z}\right).$$

The complex potential corresponding to a uniform flow in the $x$ direction takes the form $w = Uz$. The complex potential corresponding to the flow around the contour $|z| = a$ with added circulation $\Gamma$ is therefore

$$w = Uz + U\frac{a^2}{z} + \frac{i\Gamma}{2\pi}\log z. \tag{9.8}$$

Suppose that the exterior of a circle centered at the origin in the $\zeta$ plane is mapped conformally to the exterior of a hydrofoil in the $z$ plane. Then we can determine the complex potential corresponding to flow about the hydrofoil from (9.8) and the form of the conformal map. A variety of practical hydrodynamic profiles may be realized in this way. *Kármán-Trefftz profiles* are determined by conformal maps which satisfy

$$\frac{z - kl}{z + kl} = \frac{(\zeta - l)^k}{(\zeta + l)^k},$$

where $k \geq 2$. Kármán-Trefftz profiles for which $k = 2$ are called *Joukowski profiles*; the Joukowski transformation is more frequently written as

$$z = \zeta + \frac{l^2}{\zeta}.$$

Kármán-Trefftz profiles belong to the more general class of *von Mises profiles*, all of which feature cusps at their trailing points. Cuspless profiles, such as the *Carafoli profiles*, may also be obtained by conformal mapping [67].

Suppose that we wish to construct the complex potential corresponding to the flow about a Joukowski profile with a given angle of attack relative to a given uniform incident flow. It remains for us to specify the circulation $\Gamma$ about the profile. *Joukowski's hypothesis* restricts the flow speed at a foil's trailing point to remain finite, effectively requiring the circulation about the foil to adjust so that the fluid stagnates there.

Since an inviscid fluid can exert no tangential force upon a solid surface element, one might expect the net force on a flat plate with nonzero angle of attack to act in

a direction perpendicular to the plate. According to the Kutta-Joukowski theorem, however, the lift upon a flat plate must act in a direction perpendicular to the ambient fluid flow. The drag on the plate, which acts parallel to the ambient flow, is cancelled by a *leading edge suction* which results from the vanishing radius of the plate's forward edge.

We obtain the flow around a flat Joukowski profile of length $F$ from the flow around a circle of radius $a = F/4$ using the transformation

$$z = \zeta + \frac{a^2}{\zeta}.$$

It is shown in [38] that the circulation about the profile is given, consequently, by

$$\Gamma = \pi F U \sin \alpha,$$

and the lift by

$$L = \pi \rho F U^2 \sin \alpha.$$

The lift experienced by a moving plate depends upon the relative velocity of fluid incident to the plate. We assume the fin which propels our experimental apparatus to encounter only quiescent fluid; disturbances due to the fin's excursion remain largely downstream. The torso of a biological carangid precedes its caudal fin as it swims; the flow incident to the caudal fin may incorporate vorticity shed from the pectoral fins and other physical structures upstream. The role of the caudal fin in this context is to modify nonzero incident flow to effect propulsion. This point of view is addressed in [93].

As our experimental fin translates and rotates, different points along its length describe different velocities relative to the laboratory frame. In computing the lift developed on the fin, we assign to every point along its length the instantaneous velocity of the quarter-chord point. Were we so inclined, we might instead compute an effective camber from the distribution of velocities along the fin's length.

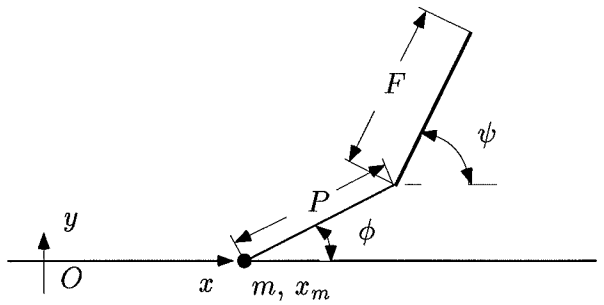


**Figure 9.9** The simulated experiment.

We simulate the motion of the system depicted in Figure 9.9. The position of the quarter-chord point relative to the origin $O$ is

$$(x_{\mathrm{QC}}, y_{\mathrm{QC}}) = \left( x_m + P\cos\phi + \frac{F}{4}\cos\psi, P\sin\phi + \frac{F}{4}\sin\psi \right)$$

and its velocity

$$v_{\mathrm{QC}} = -U = \left( \dot{x}_m - P\sin\phi\dot{\phi} - \frac{F}{4}\sin\psi\dot{\psi}, P\cos\phi\dot{\phi} + \frac{F}{4}\cos\psi\dot{\psi} \right).$$

The leading edge of the fin points in the direction

$$le = -(\cos\psi, \sin\psi).$$

We denote with an overbar the inclusion of planar vectors into $\mathbb{R}^3$, so that

$$\bar{v}_{\mathrm{QC}} = (v_{\mathrm{QC}}, 0), \quad \bar{le} = (le, 0) \quad \in \mathbb{R}^3.$$

As long as the fin's angle of attack $\alpha$ remains in the interval $[3\pi/2, \pi/2]$, in order that the leading edge and trailing edge remain as such, the lift developed on the fin is given by

$$\bar{L}_{\alpha\,\mathrm{small}} = \pi\rho F\left(\bar{v}_{\mathrm{QC}} \times \bar{le}\right) \times \bar{v}_{\mathrm{QC}}.$$

If the angle of attack lies in the interval $(\pi/2, 3\pi/2)$, the fin's leading edge and

trailing edge reverse roles. We therefore compute the lift in general to be

$$L = \operatorname{sgn}\left(\cos\left(\operatorname{atan2} le - \operatorname{atan2} v_{\mathrm{QC}}\right)\right) \pi \rho F \left(\bar{v}_{\mathrm{QC}} \times \bar{le}\right) \times \bar{v}_{\mathrm{QC}},$$

where $\operatorname{atan2}(\cdot)$ denotes the four-quadrant inverse tangent of its argument.

Since the system is constrained to translate in the $x$ direction, we are concerned only with the corresponding component $L_x$ of the lift. The equations we simulate, then, are

$$m\ddot{x}_m = L_x\left(\phi, \psi, \dot{\phi}, \dot{\psi}, \dot{x}_m\right).$$

### 9.5.2 Simulation and validation

In the theoretical absence of dissipative effects, our simulation overestimates the acceleration of the platform. We attentuate the predicted thrust developed by the fin with a viscous drag term [86], tuning a single gain until our numerical and experimental data agree over the range of gaits considered.

Figures 9.10 and 9.11 reproduce Figures 9.7 and 9.8 from the model developed in Section 9.5.1. The apparent mean curvature of the experimental trajectories corresponding to faster gaits may reflect some imperfection of the rails along which our platform translates. The model predicts the mean velocity of the platform consistently over the range of gaits considered, but does not reflect the smoothing effect of higher speeds.

## 9.6 The substitution vortex revisited

In Section 9.5.1, we outlined the construction of the flow around different hyrofoils in the complex $z$ plane from the flow around the contour $|\zeta| = a$ using transformations of the form

$$z = \zeta + \frac{a_1}{\zeta} + \frac{a_2}{\zeta^2} + \ldots. \tag{9.9}$$

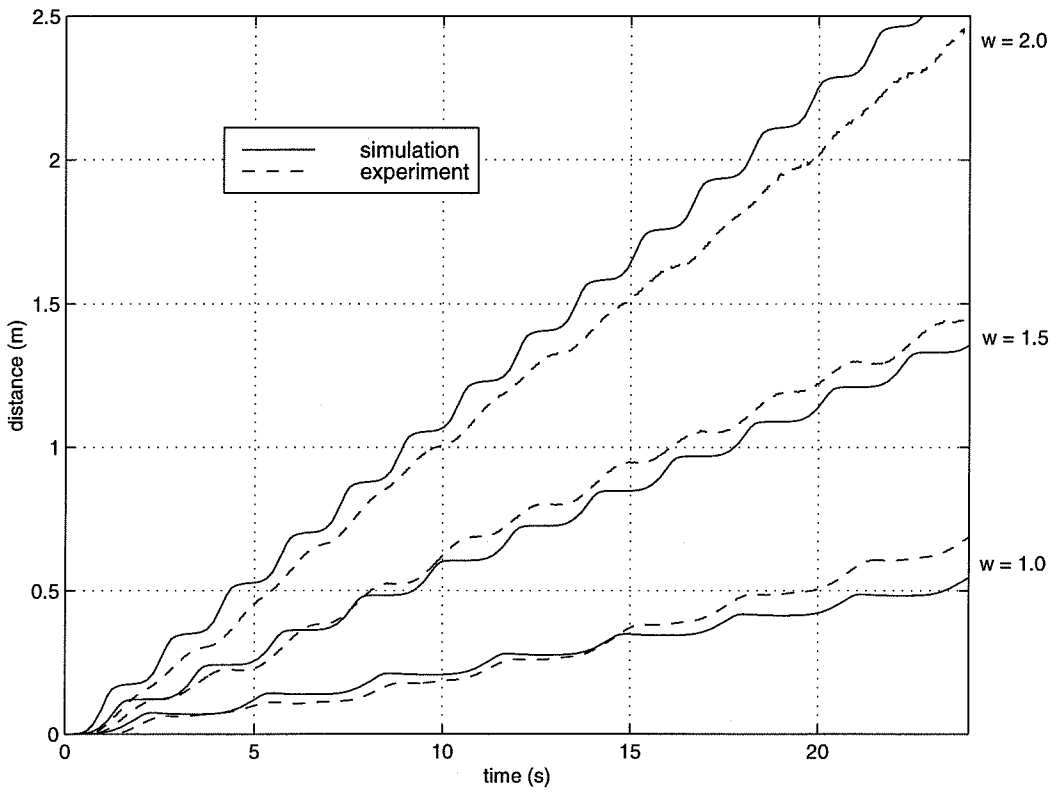


**Figure 9.10** Steady flow model for in-phase gaits.

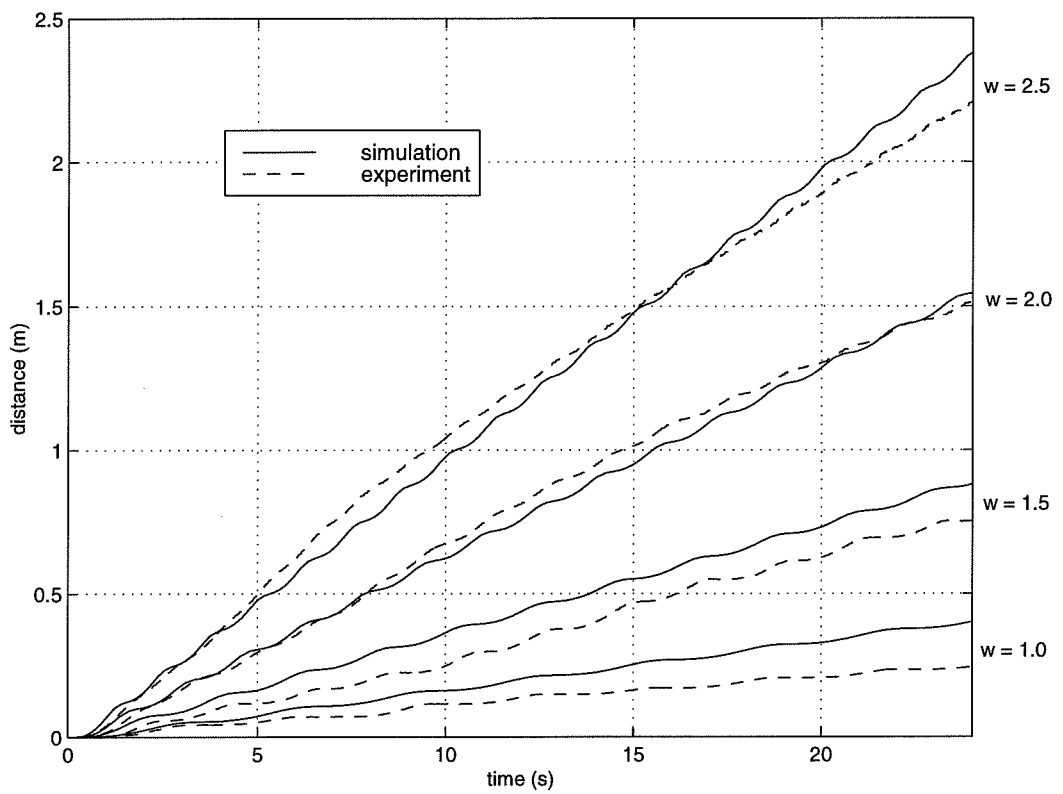


**Figure 9.11** Steady flow model for out-of-phase gaits.

For sufficiently large $|\zeta|$, such transformations leave $z \sim \zeta$, so that streamlines far enough from the origin approximate concentric circles. Suppose, for example, that

$$a_1 = a^2 = \frac{F^2}{16} \qquad \text{and} \qquad a_2 = a_3 = \cdots = 0,$$

as for a flat plate. Then

$$\begin{aligned} \frac{|z-\zeta|}{|z|} &= \frac{|\frac{a^2}{\zeta}|}{|z|} \\ &= \frac{|\frac{F^2}{16\zeta}|}{|z|} \\ &= \frac{F^2}{16}\frac{1}{|z||\zeta|}. \end{aligned}$$

If $z = Re^{i\theta}$, then

$$\zeta = \frac{R}{2}e^{i\theta} + \sqrt{\frac{R^2}{4}e^{2i\theta} - \frac{F^2}{16}}$$

and

$$\begin{aligned} \frac{1}{|z||\zeta|} &= \frac{2}{R\left|Re^{i\theta} + \sqrt{R^2e^{2i\theta} - \frac{F^2}{4}}\right|} \\ &= \frac{2}{R^2\left|e^{i\theta} + \sqrt{e^{2i\theta} - \frac{F^2}{4R^2}}\right|}, \end{aligned}$$

so that

$$\begin{aligned} \frac{|z-\zeta|}{|z|} &= \frac{F^2}{8R^2}\frac{1}{|e^{i\theta} + \sqrt{e^{2i\theta} - \frac{F^2}{4R^2}}|} \\ &\leq \frac{F^2}{8R^2}\frac{1}{1+\sqrt{1+\frac{F^2}{4R^2}}}. \end{aligned}$$

If $R > F$, then

$$\frac{|z-\zeta|}{|z|} < \frac{1}{8}\frac{1}{1+\sqrt{1+\frac{1}{4}}}$$
$$< \frac{1}{16}.$$

Thus, at distances greater than one chord length $F$ from a flat plate, our error in treating the flow as that around a point vortex amounts to less than one part in sixteen. Figure 9.12 depicts the deformation of circles in the $z$ plane by the transformation

$$z \mapsto z + \frac{1}{z}.$$

The complex potential for a vortex of strength $\kappa$ at the point $z_0$ subject to a uniform flow with angle of incidence $\alpha$ may be written as

$$\begin{aligned} w &= U\mathrm{e}^{i\alpha}z + \frac{i\Gamma}{2\pi}\log(z-z_0) \\ &= U\mathrm{e}^{i\alpha}z + \frac{i\Gamma}{2\pi}\log z + \frac{i\Gamma}{2\pi}\log\left(1-\frac{z_0}{z}\right) \\ &= U\mathrm{e}^{i\alpha}z + \frac{i\Gamma}{2\pi}\log z + O\left(\frac{z_0^2}{z^2}\right). \end{aligned}$$

The complex potential for the flow around a hydrofoil is given (as for $\alpha = 0$ in (9.8)) by

$$w = U\mathrm{e}^{i\alpha}\zeta + U\mathrm{e}^{-i\alpha}\frac{a^2}{\zeta} + \frac{i\Gamma}{2\pi}\log\zeta,$$

where $\zeta$ may be obtained from $z$ by reversing (9.9) to yield

$$\zeta = z\left(1 - \frac{a_1}{z^2} - \ldots\right).$$

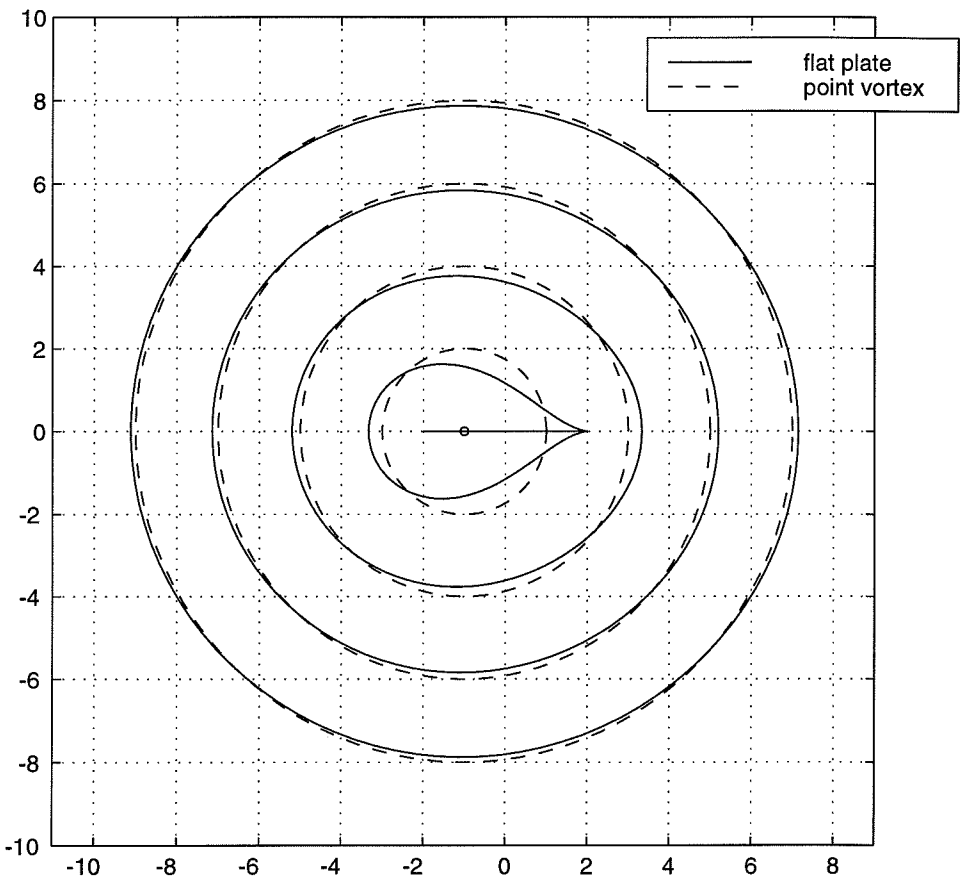


**Figure 9.12** Flow around a flat plate with circulation.

Thus

$$z_0 = \frac{2\pi i}{\Gamma} U \left( a^2 \mathrm{e}^{-i\alpha} - a_1 \mathrm{e}^{i\alpha} \right) + O\left(\frac{1}{z^2}\right)$$

provides the position of the substitution vortex.

For a flat plate with chord length $F$, $a = F/4$ and $a_1 = F^2/16$ so that

$$\begin{aligned} z_0 &= \frac{2\pi i}{\Gamma} U \left( \frac{F^2}{16} \mathrm{e}^{-i\alpha} - \frac{F^2}{16} \mathrm{e}^{i\alpha} \right) \\ &= \frac{\pi}{4\Gamma} U F^2 \sin\alpha \end{aligned}$$

up to $O\left(\frac{1}{z^2}\right)$. Since Joukowski's hypothesis requires that

$$\Gamma = \pi F U \sin\alpha$$

for a flat plate, the corresponding substitution vortex is situated at the quarter chord point

$$z_0 = \frac{F}{4}.$$

## 9.7 Flow visualization

Commercially available Kalliroscope fluid is a colloidal suspension of reflective, oblong guanine platelets which, when added to an aqueous flow, align with instantaneous streamlines. A 0.2% solution provides opacity and reflectivity to the water in our smaller tank, allowing us to photograph flow patterns with ordinary cameras and lighting. Figure 9.13 (best viewed at arm's length) depicts the inverted Kármán vortex street left behind by our robotic fin. Figure 9.14 depicts the vortex pair shed by an abrupt quarter-stroke.

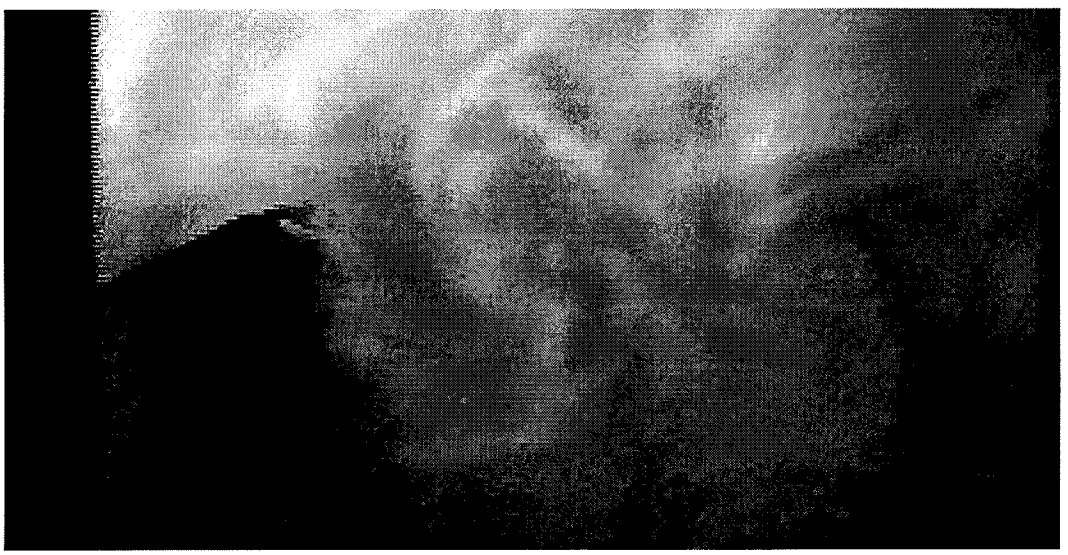

**Figure 9.13** The characteristic carangiform wake.

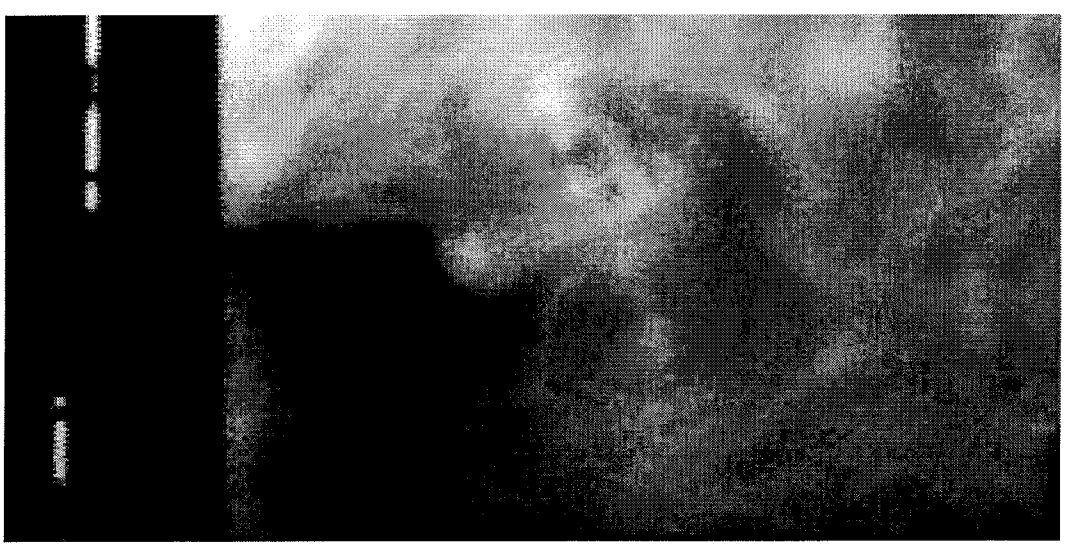

**Figure 9.14** A counter-rotating vortex pair.

## 9.8 Carangiform gaits

Unlike the propulsors addressed in Chapter 6, a carangiform swimmer describes gaits which are sensitive in their efficacy to time reparametrization. A variety of dimensionless parameters are used to index the similitude of viscous fluid flows; we have already encountered the Reynolds number $\mathrm{Re} = UL/\nu$. The two degrees of internal freedom enjoyed by our experimental propulsor afford us two frequencies with which to characterize gaits, the phase between them a third.

A single caudal frequency $\omega$ (in rad/s) is typically ascribed to the swimming of a biological carangid [53], combining with the body length $L_{\mathrm{body}}$ and characteristic swimming velocity $U$ to provide the *reduced frequency*

$$\sigma = \omega L_{\mathrm{body}}/U.$$

A related parameter is the *Strouhal number*

$$\mathrm{St} = \omega \mathrm{E}/U,$$

where E denotes the width of the caudal fin's excursion. Species as diverse as the goldfish, dace, trout, and bream beat their caudal fins such that $E \approx 0.2 L_{\mathrm{body}}$ [53]. The efficient swimming of marine animals is characterized by Strouhal numbers between 1.5 and 2.2 [96]. We note that the Strouhal number is sometimes defined in terms of the frequency $f = \omega/2\pi$ in Hertz.

The single-frequency gaits depicted in Chapter 9 represent Strouhal numbers between 9.5 and 15.0. We are limited by the speed at which the motors driving our experimental fin can respond; an increase in $\omega$ forces a decrease in E. Because we command the positions of the motors directly, however, we do not observe the presumed inefficiency of these gaits.

Our experiments focus on forward motion because the platform which supports our experimental fin can move only longitudinally. The model developed in Section 9.5, however, is readily adjusted to accommodate full planar motion. Consider

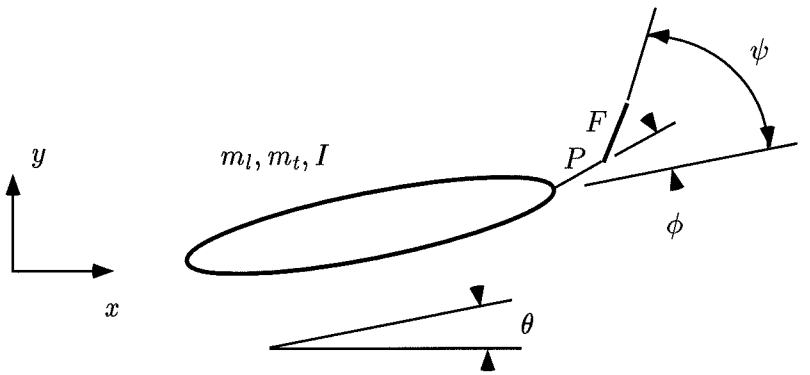


**Figure 9.15** A planar carangiform robot.

the aquatic robot shown in Figure 9.15. We ascribe to the body apparent masses $(m_l, m_t)$ corresponding to longitudinal and transverse motion and an apparent inertia $I$. For an ellipse with semimajor axes $a$ and $b$, where $a > b$,

$$m_l = \pi\rho\, a^2, \qquad m_t = \pi\rho\, b^2, \qquad \text{and} \qquad I = \frac{1}{8}\pi\rho\,(a^2 - b^2)^2$$

per unit depth [68]. Since $P = F = .125$ m for our experimental apparatus, we simulate a robot with these parameters and an elliptical body measuring $2a = .750$ m by $2b = .125$ m in water with planar density $\rho = 1000\,\mathrm{Kg/m^2}$.

Figure 9.16 depicts several snapshots of the robot as it executes the gait

$$\phi(t) = \cos 2t$$
$$\psi(t) = \phi(t) + \sin 2t.$$

The Jacobi-Lie brackets computed in Section 9.3 suggest that a gait of the form

$$\phi(t) = \phi_0 + \cos\omega t$$
$$\psi(t) = \phi(t) + \sin\omega t$$

will, for $\phi_0 \neq 0$, rotate and advance the robot simultaneously. Figure 9.17 depicts

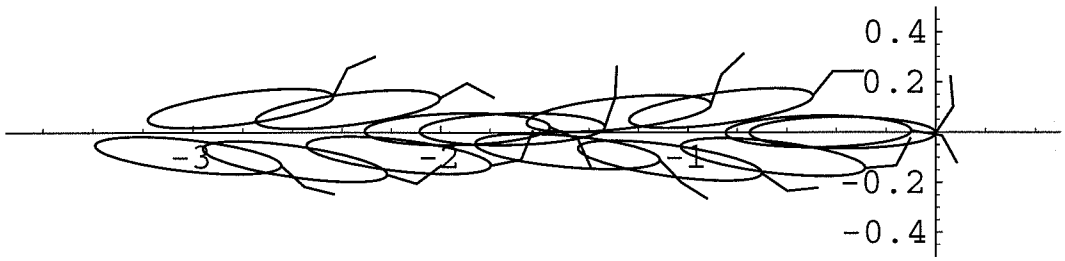


**Figure 9.16** An out-of-phase drive gait.

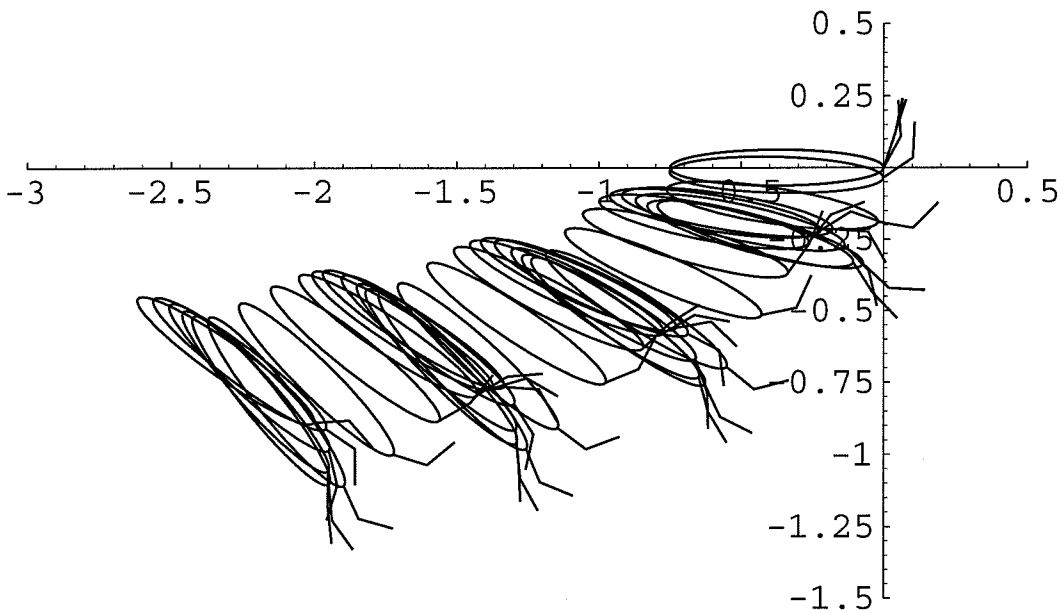


**Figure 9.17** An out-of-phase drive-and-rotate gait

the gait

$$\phi(t) = .25 + \cos 2t$$

$$\psi(t) = \phi(t) + \sin 2t.$$

# Chapter 10

# Future Work

The preceding pages suggest a great many topics for future investigation; we acknowledge only a few of these here.

The fluid mechanics providing for the connections in Section 7.3 were distilled from the Navier-Stokes equations by physical assumption. A comprehensive theory of the swimming of deformable bodies should encompass the idiosyncrasies of ideal flow and creeping flow mathematically. The momentum map corresponding to the particle relabelling symmetry of an ideal fluid in a domain F takes values in the space dual to the Lie algebra of vector fields on F which are solenoidal and parallel to $\partial$F on $\partial$F. If F is the periphractic region complemeting a body about which the flow is acyclic, this space is naturally identified with the space of vorticity fields on F [61]. The assumption of irrotational flow therefore corresponds to restriction to the preimage of a momentum level set. This restriction, together with reduction, should recapture the Kirchhoff potentials from the Euler-Lagrange equations. This remains to be shown explicitly.

In order to simultaneously realize Stokes' equations via reduction, we must begin with a geometric model for viscous flow. Parametric dependence of an accompanying Navier slip boundary condition upon fluid viscosity and Reynolds number is only one apparent requirement of a pandectic formulation.

The end product of the Lagrangian analysis of Chapter 8 was a set of equations indicating the overall conservation of certain quantities shared by a rigid body and

a surrounding fluid. The nonholonomic connection governing the motion of certain terrestrial vehicles [80, 13] speaks to dynamics which are essentially nonconservative, their symmetry broken by equations of constraint. Considered together, however, a vehicle and the Earth to which it is coupled may be modelled a conservative system. Symmetry is lost when the Earth's large inertial reservoir is assumed to be infinite. A similar assumption regarding an infinite fluid's capacity to absorb the vorticity shed from a natant surface may allow us to synthesize a structure like the nonholonomic connection. We anticipate a complete theory of *composite* Lagrangian systems which will unify conceptually the swimming of undulating surfaces and the negotiation of large inertial bodies by wheeled mobile robots. Specialization of results like Noether's theorem to such systems should guide the development of the general theory.

Indeed, the implicit nature of the drift derived in Chapter 8 has prevented us, thusfar, from interleaving the pieces of the model we proposed in Chapters 8 and 9 for carangiform swimming. Our cursory assessment of controllability drew conclusions from a fragment of this model; proper control analysis will follow our realization of its complete form.

From a Hamiltonian point of view, the conservative interconnection of mechanical systems may be studied in the context of Dirac structures [97]. We note only the availability of this formalism, citing an assessment of its utility as an objective for the future.

The experimental apparatus detailed in Chapter 9 is constrained to translate rectilinearly. Its displacement reflects one component of the lift developed by the caudal fin, but neither the other nor the yawing moment to which a real carangid is subject. Subsequent generations of the experiment will provide full $SE(2)$ mobility to the peduncle and fin, replacing the lateral reistance of the bearings on the rails with the apparent load of a submerged body.

The longitudinal translation of an elliptical body in an irrotational flow is unstable [68]. A fish, however, will coast forward with apparent stability after ceasing to generate thrust with its tail. This stability may be the result of a continued but

subtle control effort on the fish's part, or a consequence of the damping inherent to real hydrodynamic systems. The cross-sectional signature of rectilinear carangiform swimming is a wake resembling an inverted Kármán vortex street. The notion of image vorticity permits extension of the Hamiltonian theory of planar vortices to the advection of free surfaces by vortex systems. This context could illuminate stabilizing properties of conservative wakes, particularly if physical maneuvers of interest were to correspond to relative equilibria of constrained vortex systems. Were this the case, a technique like the energy-momentum method [56] could be applied to evaluate the stability of these relative equilibria. Models for the interaction of vortex patches [91] may also prove adaptable to the interaction of rigid bodies and structured vortex wakes.

The autonomy of piscimimetic vehicles requires the integration of appropriate sensors and feedback laws. The nature of the lateral line sensor common to many fish is the subject of ongoing biological research. Results from that field could motivate artificial sensor design; an understanding of the data needed to negotiate a fluid environment could guide the zoological community in its efforts.

Efficient numerical schemes which allow vortex shedding to be decoupled from other viscous phenomena can validate theoretical results more adaptably than any experimental platform. Modifications of Chorin's method, which supposes a discrete distribution of vorticity, are particularly suited to abstractions of carangiform swimming based on the substitution vortex. Ready simulation will speed the assessment of gaits for hyperarticulated marine propulsors.

The classification of nonlinear control systems according to their feedback equivalence to certain canonical systems is tantamount to the identification of pertinent invariant differential forms. Locomotion systems are, compatibly, distinguished by adherent connections, curvatures, and related forms. It remains to develop a taxonomy of locomotion systems based on equivalence under feedback transformations. Cartan's method of equivalence [26, 79] may provide the tools to geometrize feedback design for locomotion.

# Bibliography

[1] R. Abraham and J. E. Marsden. *Foundations of Mechanics.* Addison-Wesley, third edition, 1978.

[2] B. Ahlborn, D. G. Harper, R. W. Blake, D. Ahlborn, and M. Cam. Fish Without Footprints. *Journal of Theoretical Biology*, 148:521–533, 1991.

[3] R. M. Alexander. *Exploring Biomechanics.* Scientific American Library, 1992.

[4] H. Andreas. Underwater Locomotion Using Swimming Cylinders. Master's thesis, California Institute of Technology, 1997.

[5] H. Aref. On the Equilibrium and Stability of a Row of Point Vortices. *Journal of Fluid Mechanics*, 290:167–181, 1995.

[6] V. Arnol'd. Sur la Géometrie Differentielle des Groupes de Lie de Dimension Infinie et ses Applications a l'Hydrodynamique des Fluids Parfaits. *Annales de l'Institute Fourier, Grenoble*, 16(1):319–361, 1966.

[7] V. I. Arnol'd and Boris A. Khesin. *Topological Methods in Hydrodynamics.* Springer-Verlag, 1998.

[8] T. B. Benjamin. Hamiltonian Theory for Motions of Bubbles in an Infinite Liquid. *Journal of Fluid Mechanics*, 181:349–379, 1987.

[9] T. B. Benjamin and A. T. Ellis. The Collapse of Cavitation Bubbles and the Pressure Thereby Produced Against Solid Boundaries. *Philosophical Transactions of the Royal Society of London A*, 260:221–240, 1966.

[10] T. B. Benjamin and A. T. Ellis. Self-Propulsion of Asymmetrically Vibrating Bubbles. *Journal of Fluid Mechanics*, 212:65–80, 1990.

[11] J. R. Blake. A Spherical Envelope Approach to Ciliary Propulsion. *Journal of Fluid Mechanics*, 46:199–208, 1971.

[12] J. R. Blake. Self Propulsion due to Oscillations on the Surface of a Cylinder at low Reynolds Number. *Bulletin of the Australian Mathematical Society*, 5:255–264, 1971.

[13] A. M. Bloch, P. S. Krishnaprasad, J. E. Marsden, and R. M. Murray. Nonholonomic Mechanical Systems with Symmetry. *Archive for Rational Mechanics and Analysis*, 136:21–99, 1996.

[14] C. M. Breder. The Locomotion of Fishes. *Zoologica*, 4:159–297, 1926.

[15] S. Childress. *Mechanics of Swimming and Flying.* Cambridge University Press, 1981.

[16] G. S. Chirikjian and J. W. Burdick. The Kinematics of Hyper-Redundant Robot Locomotion. *IEEE Transactions on Robotics and Automation*, 11:781–793, 1995.

[17] A. J. Chorin and J. E. Marsden. *A Mathematical Introduction to Fluid Mechanics.* Springer-Verlag, third edition, 1993.

[18] W-L. Chow. Über Systeme von Linearen Partiellen Differentialgleichungen Erster Ordnung. *Mathematische Annalen*, 117:98–105, 1941.

[19] S. W. Churchill. *Viscous Flows: The Practical Use of Theory.* Butterworth Publishers, 1988.

[20] J. J. Collins and I. Stewart. Hexapod Gaits and Coupled Nonlinear Oscillator Models. *Biological Cybernetics*, 68:287–298, 1993.

[21] J-M. Coron. On the Controllability of the 2-D Incompressible Navier-Stokes Equations with the Navier Slip Boundary Conditions. *ESAIM: Control, Optimisation, and Calculus of Variations*, 1:35–75, 1996.

[22] D. G. Ebin and J. E. Marsden. Groups of Diffeomorphisms and the Motion of an Incompressible Fluid. *Annals of Mathematics*, 92:102–163, 1970.

[23] K. M. Ehlers. *The Geometry of Swimming and Pumping at Low Reynolds Number.* Ph.D. thesis, University of California at Santa Cruz, 1995.

[24] M. J. Enos, editor. *Dynamics and Control of Mechanical Systems*, 1993. Proceedings of the Fields Institute Workshop on The Falling Cat and Related Problems.

[25] T. Fukuda, A. Kawamoto, F. Arai, and H. Matsuura. Mechanism and Swimming Experiment of Micro Mobile Robot in Water. In *Proceedings of the IEEE International Conference on Robotics and Automation*, pages 814–819, 1994.

[26] R. B. Gardner. *The Method of Equivalence and its Applications.* SIAM, 1989.

[27] Sir J. Gray. *Animal Locomotion.* Weidenfeld & Nicolson, 1968.

[28] Twelve Killed when Tank of Molasses Explodes. *New York Times*, page 4, January 16, 1919.

[29] K. A. Harper. Modeling the Dynamics of Carangiform Swimming for Application to Underwater Robot Locomotion. Master's thesis, Boston University, 1997.

[30] K. A. Harper, M. D. Berkemeier, and S. Grace. Modeling the Dynamics of Spring-Driven, Oscillating-Foil Propulsion. 1997. To appear, *IEEE Journal of Oceanic Engineering.*

[31] M. Hausner and J. T. Schwartz. *Lie Groups; Lie Algebras.* Gordon and Breach, 1968.

[32] M. Hildebrand. Symmetrical Gaits of Horses. *Science*, 150:701–709, 1967.

[33] S. Hirose and Y. Umetani. Kinematic Control of an Active Cord Mechanism with Tactile Sensors. In *2nd CISM-IFToMM Symposium on the Theory & Practice of Robots & Manipulators*, pages 241–252, 1977.

[34] S. Hirose, Y. Umetani, and S. Oda. An Active Cord Mechanism with Oblique Swivel Joints, and its Control. In *4th CISM-IFToMM Symposium on the Theory & Practice of Robots & Manipulators*, pages 327–340, 1983.

[35] A. C. Hutchinson. Machines Can Walk. *The Chartered Mechanical Engineer*, 1967.

[36] T. R. Kane and M. P. Scher. A Dynamical Explanation of the Falling Cat Phenomenon. *International Journal of Structures and Solids*, 5:663–670, 1969.

[37] G. Karpouzian, G. Spedding, and H. K. Cheng. Lunate-Tail Swimming Propulsion. Part 2. Performance Analysis. *Journal of Fluid Mechanics*, 210:329–351, 1990.

[38] J. Katz and A. Plotkin. *Low Speed Aerodynamics: From Wing Theory to Panel Methods.* McGraw-Hill, 1991.

[39] S. D. Kelly, R. J. Mason, C. T. Anhalt, R. M. Murray, and J. W. Burdick. Modelling and Experimental Investigation of Carangiform Locomotion for Control. To appear, *1998 American Control Conference.*

[40] S. D. Kelly and R. M. Murray. Lagrangian Mechanics and Carangiform Locomotion. To appear, *4th IFAC Nonlinear Control Systems Design Symposium.*

[41] S. D. Kelly and R. M. Murray. Geometric Phases and Robotic Locomotion. *Journal of Robotic Systems*, 12:417–431, 1995. Extended version available online via http://avalon.caltech.edu/cds/reports.

[42] S. D. Kelly and R. M. Murray. The Geometry and Control of Dissipative Systems. In *Proceedings of the IEEE Control and Decision Conference*, 1996.

[43] Lord Kelvin. On Vortex Motion. *Transactions of the Royal Society of Edinburgh*, 25:217–260, 1868.

[44] S. Kobayashi and K. Nomizu. *Foundations of Differential Geometry*, volume 1. Interscience Publishers, 1963.

[45] J. Koiller. Note on Coupled Motion of Vortices and Rigid Bodies. *Physics Letters A*, 120:391–395, 1987.

[46] J. Koiller, K. Ehlers, and R. Montgomery. Problems and Progress in Microswimming. *Journal of Nonlinear Science*, 6:507–541, 1996.

[47] P. S. Krishnaprasad and D. P. Tsakiris. $G$-Snakes: Nonholonomic Kinematic Chains on Lie Groups. In *Proceedings of the 33rd IEEE Conference on Decision and Control*, 1994.

[48] Sir H. Lamb. *Hydrodynamics.* Dover, 1945.

[49] W. F. Langford and K. Zhan. Dynamics of Strong 1:1 Resonance in Vortex-Induced Vibration. In *Fundamental Aspects of Fluid-Structure Interactions.* ASME, 1992.

[50] N. E. Leonard. Control Synthesis and Adaptation for an Underactuated Autonomous Underwater Vehicle. *IEEE Journal of Ocean Engineering*, 20(3), 1995.

[51] N. E. Leonard and J. E. Marsden. Stability and Drift of Underwater Vehicle Dynamics: Mechanical Systems with Rigid Motion Symmetry. *Physica D*, 105:130–162, 1996.

[52] D. Lewis, J. Marsden, R. Montgomery, and T. Ratiu. The Hamiltonian Structure for Dynamic Free Boundary Problems. *Physica D*, 18:391–404, 1986.

[53] Sir J. Lighthill. *Mathematical Biofluiddynamics.* SIAM, 1975.

[54] W. Magnus. On the Exponential Solutions of Differential Equations for a Linear Operator. *Communications on Pure and Applied Mathematics*, VII:649–673, 1954.

[55] A. Mahalov and S. Nikitin. Position Controllability of a Deformable Body in Ideal Fluid. *Mathematical Models & Methods in Applied Sciences*, 7:139–149, 1997.

[56] J. E. Marsden. *Lectures on Mechanics.* Cambridge University Press, 1992.

[57] J. E. Marsden, R. Montgomery, and T. S. Ratiu. Reduction, Symmetry, and Phases in Mechanics. *Memoirs of the American Mathematical Society*, 436, 1990.

[58] J. E. Marsden and T. S. Ratiu. *Introduction to Mechanics and Symmetry.* Springer-Verlag, 1994.

[59] J. E. Marsden and J. Scheurle. Lagrangian Reduction and the Double Spherical Pendulum. *Zeitschrift fur angewandte Mathematik und Physik*, 44:17–43, 1993.

[60] J. E. Marsden and J. Scheurle. The Reduced Euler-Lagrange Equations. *Fields Institute Communications*, 1:139–164, 1993.

[61] J. E. Marsden and A. Weinstein. Coadjoint Orbits, Vortices, and Clebsch Variables for Incompressible Fluids. *Physica 7D*, pages 305–323, 1983.

[62] D. Martin. *Manifold Theory.* Ellis Horwood Limited, 1991.

[63] L-F. Martins and A. F. Ghoniem. Vortex Simulation of the Intake Flow in a Planar Piston-Chamber Device. *International Journal for Numerical Methods in Fluids*, 12:237–260, 1991.

[64] R. J. Mason. Notes on a Planar Amoeba Swimming in an Inviscid Fluid. 1997. Unpublished.

[65] T. McGeer. Dynamics and Control of Bipedal Locomotion. *Journal of Theoretical Biology*, 163:277–314, 1993.

[66] R.B. McGhee. Some Finite State Aspects of Legged Locomotion. *Mathematical Biosciences*, 2:67–84, 1968.

[67] L. M. Milne-Thomson. *Theoretical Aerodynamics.* Dover, 1973.

[68] L. M. Milne-Thomson. *Theoretical Hydrodynamics.* Dover, 1996.

[69] T. Miloh and A. Galper. Self-Propulsion of General Deformable Shapes in a Perfect Fluid. *Proceedings of the Royal Society of London A*, 442:273–299, 1993.

[70] R. Montgomery. Isoholonomic Problems and Some Applications. *Communications in Mathematical Physics*, 128:565–592, 1990.

[71] R. S. Mosher. Test and Evaluation of a Versatile Walking Truck. In *Proceedings of Off-Road Mobility Research Symposium*, pages 359–379, 1968. International Society for Terrain Vehicle Systems.

[72] R. M. Murray, Z. Li, and S. S. Sastry. *A Mathematical Introduction to Robotic Manipulation.* CRC Press, 1994.

[73] R. M. Murray and S. S. Sastry. Nonholonomic Motion Planning: Steering Using Sinusoids. *IEEE Transactions on Automatic Control*, 38:700–716, 1993.

[74] E. Muybridge. *The Human Figure in Motion.* Dover, 1955. First published in 1901.

[75] E. Muybridge. *Animals in Motion.* Dover, 1958. First published in 1899.

[76] J. N. Newman and T. Y. Wu. Hydromechanical Aspects of Fish Swimming. In T. Wu, C. J. Brokaw, and C. Brennen, editors, *Swimming and Flying in Nature*, pages 615–634, 1974.

[77] H. Nijmeijer and A. J. van der Schaft. *Nonlinear Dynamical Control Systems.* Springer-Verlag, 1990.

[78] Confraternity of Christian Doctrine. *The New American Bible.* Catholic Book Publishing Company, 1987.

[79] P. J. Olver. *Equivalence, Invariants, and Symmetry.* Cambridge University Press, 1995.

[80] J. P. Ostrowski. *The Mechanics and Control of Undulatory Robotic Locomotion.* Ph.D. thesis, California Institute of Technology, 1995.

[81] Y. Özcazanç. *Dynamics and Stability of Spacecraft with Fluid-Filled Containers.* Ph.D. thesis, University of Maryland, 1994.

[82] E. Purcell. Life at Low Reynolds Number. *American Journal of Physics*, 45:3–11, 1977.

[83] J. E. Radford and J. W. Burdick. Local Motion Planning for Nonholonomic Control Systems Evolving on Principal Bundles. 1998. Unpublished.

[84] M. H. Raibert. *Legged Robots that Balance.* MIT Press, 1986.

[85] M. H. Raibert and I. E. Sutherland. Machines that Walk. *Scientific American*, 248:44–53, 1983.

[86] S. S. Rao. *Mechanical Vibrations.* Addison-Wesley, 1990.

[87] P. G. Saffman. The Self-Propulsion of a Deformable Body in a Perfect Fluid. *Journal of Fluid Mechanics*, 28:385–389, 1967.

[88] P. G. Saffman. *Vortex Dynamics.* Cambridge University Press, 1992.

[89] A. Shapere and F. Wilczek. Efficiencies of Self-Propulsion at Low Reynolds Number. *Journal of Fluid Mechanics*, 198:587–599, 1989.

[90] A. Shapere and F. Wilczek. Geometry of Self-Propulsion at Low Reynolds Number. *Journal of Fluid Mechanics*, 198:557–585, 1989.

[91] B. N. Shashikanth and P. K. Newton. The Geometric Phase in the Second Order Melander-Zabusky-Styczek Vortex Patch Model. 1998. Unpublished.

[92] G. R. Spedding. The Aerodynamics of Flight. In *Advances in Comparative and Environmental Physiology*, volume II. Springer-Verlag, 1992.

[93] K. Streitlien, G. S. Triantafyllou, and M. S. Triantafyllou. Efficient Foil Propulsion Through Vortex Control. *AIAA Journal*, 34:2315–2319, 1996.

[94] *Tenth International Symposium on Unmanned Untethered Submersible Technology*, 1997. Proceedings of the Special Session on Bio-Engineering Research Related to Autonomous Underwater Vehicles.

[95] R. Tomovic and W. J. Karplus. Land Locomotion Simulation and Control. In *Proceedings of the Third International Analogue Computation Meeting*, pages 385–390, 1961.

[96] M. S. Triantafyllou and G. S. Triantafyllou. An Efficient Swimming Machine. *Scientific American*, 272:64–70, 1995.

[97] A. J. van der Schaft and B. M. Maschke. Interconnected Mechanical Systems, part I: Geometry of Interconnection and Implicit Hamiltonian Systems. In *Modelling and Control of Mechanical Systems*. Imperial College Press, 1997.

[98] F. W. Warner. *Foundations of Differentiable Manifolds and Lie Groups*. Springer-Verlag, 1983.

[99] T. Wu. Hydrodynamics of Swimming of Fishes and Cetaceans. In *Advances in Applied Mechanics*, volume II. Academic Press, 1971.